1 Introduction

1.1. An experiment

Take a shallow dish and pour in salty water to a depth of 1 cm. Make a model wing with a length and span of 2 cm or so, ensuring that it has a sharp trailing edge. (One method is to cut the wing out of an india rubber with a knife.) Dip the wing vertically in the water and turn it to make a small angle of attack α with the direction in which it is to be moved. Put a blob of ink or food colouring around the trailing edge; a thin layer of this should then float on the salt water.

Now move the wing across the dish, giving it a clean, sudden start. If α is not too large there should be a strong anticlockwise vortex left behind at the point where the trailing edge started, as in Fig. 1.1.

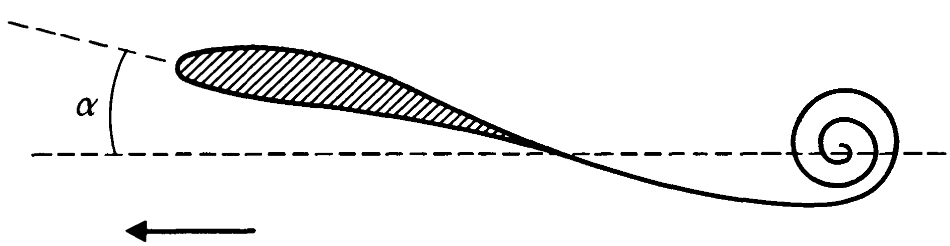

Fig. 1.1. The starting vortex.

A 'starting vortex' of this kind forms a crucial part of the mechanism by which an aircraft obtains lift, and we shall use aerodynamics in this chapter as a means of introducing some fundamental concepts of fluid flow.

Aerodynamics is, arguably, well suited to this purpose, but it goes without saying that the theory of fluid motion finds application in a wide variety of different fields. Within this book alone we may point to waves on a pond (§3.1), the instability of flow down a pipe (§9.1), the hydraulic jump in a kitchen sink

(§3.10), the interaction of two smoke rings (§5.4), the jet stream in the atmosphere (§9.8), the motion of quantum vortices in liquid helium (§5.8), the flow of volcanic lava (§7.9), the swimming of biological micro-organisms (§7.5), and the spin-down of a stirred cup of tea (§8.5) as examples of the breadth and diversity of the subject.

1.2. Some preliminary ideas

The usual way of describing a fluid flow is by means of an expression

$$\boldsymbol{u} = \boldsymbol{u}(\boldsymbol{x}, t) \tag{1.1}$$

for the flow velocity $\boldsymbol{u}$ at any point $\boldsymbol{x}$ and at any time t. This tells us what all elements of the fluid are doing at any time; finding eqn (1.1) is usually the main task.

In general we must expect this task to be quite difficult. Let us take Cartesian coordinates, for example, and denote the three components of $\boldsymbol{u}$ by u, v, and w. Then eqn (1.1) is a convenient shorthand for

$$u = u(x, y, z, t), \qquad v = v(x, y, z, t), \qquad w = w(x, y, z, t).$$

There are, however, special classes of flow which have simplifying features.

A *steady* flow is one for which

$$\frac{\partial \boldsymbol{u}}{\partial t} = 0, \tag{1.2}$$

so that $\boldsymbol{u}$ depends on $\boldsymbol{x}$ alone. At any fixed point in space the speed and direction of flow are both constant.

A *two-dimensional* (2-D) *flow* is of the form

$$\boldsymbol{u} = [u(x, y, t), v(x, y, t), 0], \tag{1.3}$$

so that $\boldsymbol{u}$ is independent of one spatial coordinate (here selected to be z) and has no component in that direction.

A *two-dimensional steady flow* is thus of the form

$$\boldsymbol{u} = [u(x, y), v(x, y), 0]. \tag{1.4}$$

These are idealizations. No real flow can be exactly two-dimensional, but in the case of flow past a fixed wing of long span and uniform cross-section we might reasonably expect a close approximation to 2-D flow, except near the wing-tips.

Before exploring such a flow more closely it is useful to introduce the concept of a *streamline*. This is, at any particular time t, a curve which has the same direction as $\boldsymbol{u}(\boldsymbol{x}, t)$ at each point. Mathematically, then, a streamline $x = x(s)$, $y = y(s)$, $z = z(s)$ is obtained by solving

$$\frac{\mathrm{d}x/\mathrm{d}s}{u} = \frac{\mathrm{d}y/\mathrm{d}s}{v} = \frac{\mathrm{d}z/\mathrm{d}s}{w} \tag{1.5}$$

at a particular time t.

To imagine streamlines it can be convenient to consider a widely used experimental technique which involves putting tiny, neutrally buoyant polystyrene beads into the fluid. One particular plane of the fluid region is then illuminated by a collimated light beam, and the beads reflect this light to the camera, thus appearing as tiny pin-pricks of light if they are stationary. When the fluid is moving, however, the beads get carried around with it, so that a short-exposure-time photograph consists of short streaks, the length and direction of each one giving a measure of the fluid velocity at that particular point in space. As an example, we show in Fig. 1.2 a streak photograph for the flow (with uniform velocity at infinity) past a fixed wing. Because this is a steady flow the streamline pattern is the same at all times, and a fluid particle started on some streamline will travel along that

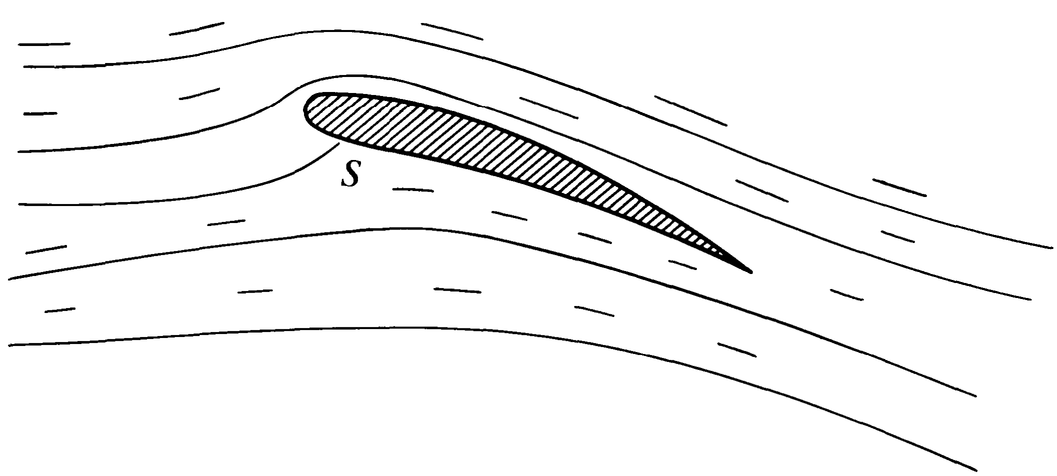

Fig. 1.2. Streamlines for steady flow past a fixed wing, as inferred from a streak photograph.

streamline as time proceeds. (In an unsteady flow, on the other hand, streamlines and particle paths are usually quite different; see Exercise 1.8.)

It is evident from Fig. 1.2 that even though the flow is steady, so that $\boldsymbol{u}$ is constant at a point fixed in space, $\boldsymbol{u}$ changes *as we follow any particular fluid element.* In particular—changes in direction of flow aside—an element riding over the top of the wing first speeds up and then slows down again.

Rate of change 'following the fluid'

This notion is of fundamental importance in fluid dynamics.

Let $f(x, y, z, t)$ denote some quantity of interest in the fluid motion. It could, for example, be one component of the velocity $\boldsymbol{u}$, or it could be the density ρ. Note first that $\partial f/\partial t$ means the rate of change of f at fixed x, y, and z, i.e. at a fixed position in space.

In contrast, the rate of change of f 'following the fluid', which we denote by $\mathrm{D}f/\mathrm{D}t$, is

$$\frac{\mathrm{D}f}{\mathrm{D}t} = \frac{\mathrm{d}}{\mathrm{d}t} f[x(t), y(t), z(t), t],$$

where $x(t)$, $y(t)$, and $z(t)$ are understood to change with time at the local flow velocity $\boldsymbol{u}$:

$$\mathrm{d}x/\mathrm{d}t = u, \qquad \mathrm{d}y/\mathrm{d}t = v, \qquad \mathrm{d}z/\mathrm{d}t = w,$$

so as to 'follow the fluid'. A simple application of the chain rule gives

$$\frac{\mathrm{D}f}{\mathrm{D}t} = \frac{\partial f}{\partial x}\frac{\mathrm{d}x}{\mathrm{d}t} + \frac{\partial f}{\partial y}\frac{\mathrm{d}y}{\mathrm{d}t} + \frac{\partial f}{\partial z}\frac{\mathrm{d}z}{\mathrm{d}t} + \frac{\partial f}{\partial t},$$

whence

$$\frac{\mathrm{D}f}{\mathrm{D}t} = \frac{\partial f}{\partial t} + u\frac{\partial f}{\partial x} + v\frac{\partial f}{\partial y} + w\frac{\partial f}{\partial z},$$

i.e.

$$\frac{\mathrm{D}f}{\mathrm{D}t} = \frac{\partial f}{\partial t} + (\boldsymbol{u} \cdot \nabla)f. \tag{1.6}$$

By applying eqn (1.6) to the velocity components u, v, and w in turn it follows, in particular, that the *acceleration* of the fluid element at $\boldsymbol{x}$ is

$$\frac{\mathrm{D}\boldsymbol{u}}{\mathrm{D}t}=\frac{\partial \boldsymbol{u}}{\partial t}+(\boldsymbol{u}\cdot\nabla)\boldsymbol{u}. \tag{1.7}$$

As an immediate check on eqn (1.7) consider fluid in uniform rotation with angular velocity Ω, so that

$$u=-\Omega y, \qquad v=\Omega x, \qquad w=0.$$

Now $\partial \boldsymbol{u}/\partial t$ is zero, because the flow is steady, but

$$\begin{aligned}(\boldsymbol{u}\cdot\nabla)\boldsymbol{u}&=\left(-\Omega y\frac{\partial}{\partial x}+\Omega x\frac{\partial}{\partial y}\right)(-\Omega y, \Omega x, 0)\\ &=-\Omega^2(x, y, 0).\end{aligned}$$

This is just as expected; it represents the familiar centrifugal acceleration $\Omega^2 r$ towards the rotation axis.

According to eqn (1.6) in any *steady* flow the rate of change of f following a fluid element is $(\boldsymbol{u}\cdot\nabla)f$, and it is quite easy to see why this should be so. Let $\boldsymbol{e}_s$ denote a unit vector which is always parallel to the streamlines and in the same sense as the flow. Then

$$\boldsymbol{u}\cdot\nabla f=|\boldsymbol{u}|\,\boldsymbol{e}_s\cdot\nabla f=|\boldsymbol{u}|\frac{\partial f}{\partial s},$$

where s denotes distance along a streamline. Now, $\partial f/\partial s$ is the rate of change of f with distance along a streamline, so multiplying it by the flow speed $|\boldsymbol{u}|$ evidently gives the rate of change with time as we follow a fluid element along that streamline.

The equation

$$(\boldsymbol{u}\cdot\nabla)f=0, \tag{1.8}$$

which arises at some important stages in the following theory, thus implies that f is constant *along a streamline*. It should be emphasized that eqn (1.8) offers no information at all about whether f might be a different constant on different streamlines. Suppose, for instance, that the flow is everywhere in the x-direction, so that eqn (1.8) reduces to $\partial f/\partial x=0$. This equation says that f is independent of x, but it contains no implication about how f might depend on y, z, or t.

Likewise, the equation

$$\frac{Df}{Dt} = 0, \tag{1.9}$$

which also arises in the following theory, implies that f is a constant *for a particular fluid element*, and this follows directly from the definition of Df/Dt above. It does not preclude different elements having different values of f; it just implies that each such element will retain whatever value of f it started with.

Finally, it is worth remarking that there will be occasions on which we wish to follow not just an infinitesimal fluid element but a finite blob consisting always of the same fluid particles. Such a blob, which will of course deform as it moves about, is typically called a 'material' volume in the literature, but we shall freely describe it instead as 'dyed', with the understanding, of course, that no diffusion of this imaginary dye is envisaged. Such terminology can become rather colourful, but if it evokes a sharp mental picture of a moving and deforming blob of fluid, as opposed to some region fixed in space, it serves its purpose.

1.3. Equations of motion for an ideal fluid

In this text we define an *ideal fluid* as one with the following properties:

(i) It is *incompressible*, so that no 'dyed' blob of fluid can change in volume as it moves.

(ii) The density ρ (i.e. the mass per unit volume) is a constant, the same for all fluid elements and for all time t.

(iii) The force exerted across a geometrical surface element $\boldsymbol{n}\,\delta S$ within the fluid is

$$p\boldsymbol{n}\,\delta S, \tag{1.10}$$

where $p(x, y, z, t)$ is a scalar function, independent of the normal $\boldsymbol{n}$, called the *pressure*. (To be more precise, eqn (1.10) is the force exerted *on* the fluid into which $\boldsymbol{n}$ is pointing *by* the fluid on the other side of δS.)

There is, of course, no such thing in practice as an ideal fluid. All fluids are to some extent compressible, and all fluids are to some extent *viscous*, so that adjacent fluid elements exert both normal and tangential forces on one another across their common interface. For the time being, however, we explore some consequences of the assumptions (i)–(iii).

To examine the implications of (i), consider a fixed closed surface S drawn in the fluid, with unit outward normal $\boldsymbol{n}$. Fluid will be entering the enclosed region V at some places on S, and leaving it at others. The velocity component along the outward normal is $\boldsymbol{u} \cdot \boldsymbol{n}$, so the volume of fluid leaving through a small surface element δS in unit time is $\boldsymbol{u} \cdot \boldsymbol{n}\, \delta S$. The net volume rate at which fluid is leaving V is therefore

$$\int_S \boldsymbol{u} \cdot \boldsymbol{n}\, \mathrm{d}S.$$

But this must plainly be zero for an incompressible fluid, and on using the divergence theorem we find that

$$\int_V \nabla \cdot \boldsymbol{u}\, \mathrm{d}V = 0.$$

Now, this must be true for all regions V within the fluid. Suppose, then, that $\nabla \cdot \boldsymbol{u}$ is greater than zero at some point in the fluid. Assuming that it is continuous, $\nabla \cdot \boldsymbol{u}$ will be greater than zero in some small sphere around that point, and by taking V to be such a sphere we violate the above equation. The same applies if $\nabla \cdot \boldsymbol{u}$ is negative at some point. We thus conclude that

$$\nabla \cdot \boldsymbol{u} = 0 \tag{1.11}$$

everywhere in the fluid.

This *incompressibility condition* is an important constraint on the velocity field $\boldsymbol{u}$ in virtually the whole of this book.†

To examine the implications of (iii) consider a surface S enclosing a 'dyed' blob of fluid. The force exerted by the surrounding fluid across any surface element δS is, by hypothesis, given by eqn (1.10), so that the net force exerted on the dyed blob is

$$-\int_S p\boldsymbol{n}\, \mathrm{d}S = -\int_V \nabla p\, \mathrm{d}V,$$

† Air is, of course, highly compressible, but it can behave like an incompressible fluid if the flow speed is much smaller than the speed of sound (see p. 58).

where we have used the identity (A.14)—see the Appendix (the negative sign arises because $\boldsymbol{n}$ points out of S). Now, provided that ∇p is continuous it will be almost constant over a *small* blob of fluid of volume δV. The net force on such a small blob due to the pressure of the surrounding fluid will therefore be $-\nabla p\, \delta V$.

Euler's equations of motion

We are now in a position to apply the principle of linear momentum to a small 'dyed' blob of fluid of volume δV. Allowing for the presence of a gravitational body force per unit mass $\boldsymbol{g}$, the total force on the blob is

$$(-\nabla p + \rho \boldsymbol{g})\, \delta V.$$

This force must be equal to the product of the blob's mass (which is conserved) and its acceleration, i.e. to

$$\rho\, \delta V \frac{\mathrm{D}\boldsymbol{u}}{\mathrm{D}t}.$$

We thus obtain

$$\frac{\mathrm{D}\boldsymbol{u}}{\mathrm{D}t} = -\frac{1}{\rho}\nabla p + \boldsymbol{g}, \qquad (1.12)$$

$$\nabla \cdot \boldsymbol{u} = 0,$$

as the basic equations of motion for an ideal fluid. They are known as *Euler's equations,* and written out in full they become

$$\frac{\partial u}{\partial t} + u\frac{\partial u}{\partial x} + v\frac{\partial u}{\partial y} + w\frac{\partial u}{\partial z} = -\frac{1}{\rho}\frac{\partial p}{\partial x},$$

$$\frac{\partial v}{\partial t} + u\frac{\partial v}{\partial x} + v\frac{\partial v}{\partial y} + w\frac{\partial v}{\partial z} = -\frac{1}{\rho}\frac{\partial p}{\partial y},$$

$$\frac{\partial w}{\partial t} + u\frac{\partial w}{\partial x} + v\frac{\partial w}{\partial y} + w\frac{\partial w}{\partial z} = -\frac{1}{\rho}\frac{\partial p}{\partial z} - g,$$

$$\frac{\partial u}{\partial x} + \frac{\partial v}{\partial y} + \frac{\partial w}{\partial z} = 0,$$

i.e. four scalar equations for four unknowns: u, v, w, and p. In dealing with the gravitational term we have momentarily taken the z-axis vertically upward, setting $\boldsymbol{g} = (0, 0, -g)$.

Now, the gravitational force, being conservative, can be written as the gradient of a potential:

$$\boldsymbol{g} = -\nabla\chi. \tag{1.13}$$

(In the above case, $\chi = gz$.) Using the expression (1.7) for the fluid acceleration we may rewrite eqn (1.12) in the form†

$$\frac{\partial \boldsymbol{u}}{\partial t} + (\boldsymbol{u} \cdot \nabla)\boldsymbol{u} = -\nabla\left(\frac{p}{\rho} + \chi\right),$$

where we have used the assumption that ρ is constant. Furthermore, it can be helpful to use the identity

$$(\boldsymbol{u} \cdot \nabla)\boldsymbol{u} = (\nabla \wedge \boldsymbol{u}) \wedge \boldsymbol{u} + \nabla(\tfrac{1}{2}\boldsymbol{u}^2)$$

to cast the momentum equation into the form

$$\frac{\partial \boldsymbol{u}}{\partial t} + (\nabla \wedge \boldsymbol{u}) \wedge \boldsymbol{u} = -\nabla\left(\frac{p}{\rho} + \tfrac{1}{2}\boldsymbol{u}^2 + \chi\right). \tag{1.14}$$

The Bernoulli streamline theorem

If the flow is steady, eqn (1.14) reduces to

$$(\nabla \wedge \boldsymbol{u}) \wedge \boldsymbol{u} = -\nabla H,$$

where

$$H = \frac{p}{\rho} + \tfrac{1}{2}\boldsymbol{u}^2 + \chi. \tag{1.15}$$

On taking the dot product with $\boldsymbol{u}$ we obtain

$$(\boldsymbol{u} \cdot \nabla)H = 0, \tag{1.16}$$

† The way in which $p/\rho + \chi$ appears as a combination is significant; there will be many circumstances in this book in which gravity simply modifies the pressure distribution in the fluid and does nothing to change the velocity $\boldsymbol{u}$. Thus when we speak occasionally of 'ignoring' gravity, or of gravitational body forces being 'absent', what we often mean is that separate allowance may be made for gravity simply by subtracting $\rho\chi$ from the pressure field. This is emphatically not the case, however, if there is a free surface—as with water waves in Chapter 3—or if ρ is not constant—as in §3.8 and §9.3.

so

If an ideal fluid is in steady flow,
then H is constant along a streamline.

In the absence of gravity it follows that $p + \frac{1}{2}\rho \boldsymbol{u}^2$ is constant along a streamline in steady flow.

The above theorem says nothing about H being the same constant on different streamlines, only that it remains constant along each one. There is, however, one important circumstance in which H is constant throughout the whole flow field, and this now follows.

DEFINITION. An *irrotational* flow is one for which

$$\nabla \wedge \boldsymbol{u} = 0. \tag{1.17}$$

The Bernoulli theorem for irrotational flow

If the flow is steady and irrotational, then eqn (1.14) reduces to $\nabla H = 0$, so H is independent of x, y, and z, as well as t. Thus

If an ideal fluid is in steady irrotational flow,
then H is constant throughout the whole flow field.

Whether this result is of any value rests, evidently, on whether irrotational flows are of any real interest in practice. We address this matter in the next section.

1.4. Vorticity: irrotational flow

The *vorticity* $\boldsymbol{\omega}$ is defined as

$$\boldsymbol{\omega} = \nabla \wedge \boldsymbol{u}, \tag{1.18}$$

and it is a concept of central importance in fluid dynamics. The vorticity is, by definition, zero for an *irrotational* flow.

We consider vorticity first in the context of two-dimensional flow, for if

$$\boldsymbol{u} = [u(x, y, t), v(x, y, t), 0]$$

then $\boldsymbol{\omega}$ is $(0, 0, \omega)$, where

$$\omega = \frac{\partial v}{\partial x} - \frac{\partial u}{\partial y}. \tag{1.19}$$

Interpretation of vorticity in 2-D flow

Consider two short fluid line elements AB and AC *which are perpendicular at a certain instant,* as in Fig. 1.3. Note that the y-component of velocity at B exceeds that at A by

$$v(x+\delta x, y, t) - v(x, y, t) \doteqdot \frac{\partial v}{\partial x}\,\delta x,$$

so that $\partial v/\partial x$ represents the instantaneous angular velocity of the fluid line element AB. Likewise, $\partial u/\partial y$ represents the instantaneous angular velocity (in the opposite sense) of the line element AC. Thus at any point of the flow field

$$\tfrac{1}{2}\omega = \tfrac{1}{2}\left(\frac{\partial v}{\partial x} - \frac{\partial u}{\partial y}\right)$$

represents the average angular velocity of two short fluid line elements that happen, at that instant, to be mutually perpendicular. In this precise sense the vorticity ω acts as a measure of the *local* rotation, or spin, of fluid elements.

We emphasize that vorticity has nothing directly to do with any global rotation of the fluid. Take, for example, the shear flow of

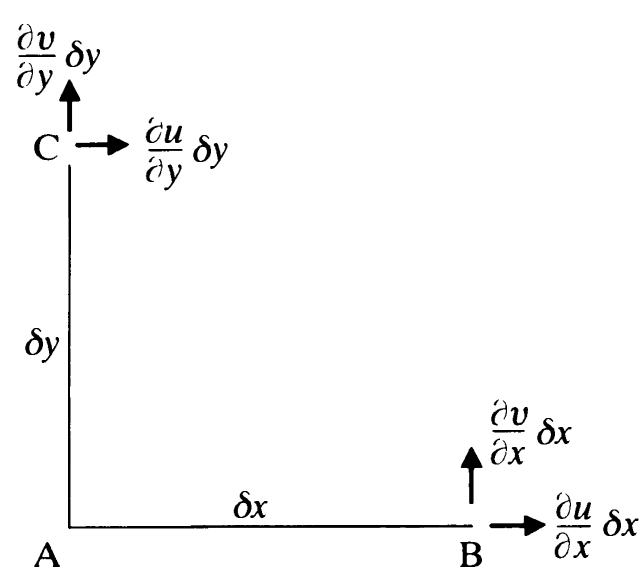

Fig. 1.3. Sketch for the interpretation of vorticity in 2-D flow. The velocity components shown are relative to the fluid particle at A.

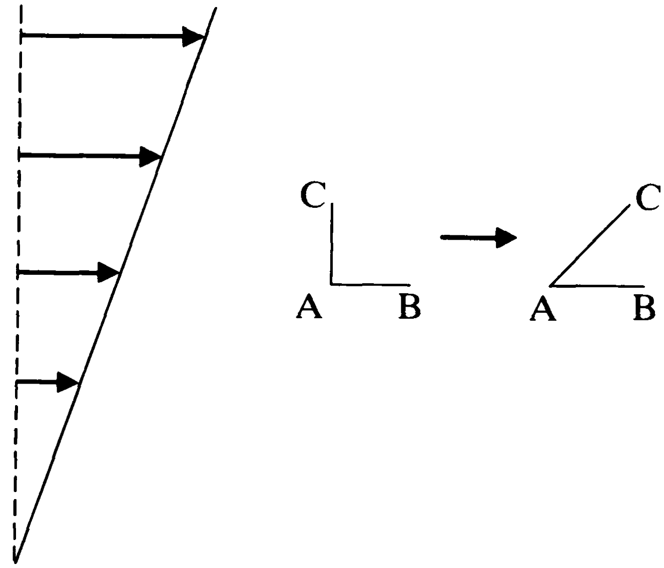

Fig. 1.4. Deformation of two short, momentarily perpendicular fluid line elements in a shear flow.

Fig. 1.4, in which

$$\boldsymbol{u} = (\beta y, 0, 0), \tag{1.20}$$

where β is a constant. The fluid is certainly not rotating globally in any sense, but it has vorticity:

$$\omega = \frac{\partial v}{\partial x} - \frac{\partial u}{\partial y} = -\beta;$$

and two momentarily perpendicular line elements, AB and AC, orientated as shown plainly have an average angular velocity (in fact, of $-\frac{1}{2}\beta$), because while that of AB is zero that of AC is not.

A more colourful example of the distinction between vorticity and global rotation of the fluid is provided by the so-called *line vortex* flow given in cylindrical polar coordinates (r, θ, z) by

$$\boldsymbol{u} = \frac{k}{r}\boldsymbol{e}_\theta, \tag{1.21}$$

where k is a constant. To find the vorticity of this flow we need the expression (A.32) for $\nabla \wedge \boldsymbol{u}$ in cylindrical polar coordinates:

$$\nabla \wedge \boldsymbol{u} = \frac{1}{r}\begin{vmatrix} \boldsymbol{e}_r & r\boldsymbol{e}_\theta & \boldsymbol{e}_z \\ \dfrac{\partial}{\partial r} & \dfrac{\partial}{\partial \theta} & \dfrac{\partial}{\partial z} \\ u_r & ru_\theta & u_z \end{vmatrix}.$$

Plainly, then, the vorticity is zero except at $r = 0$, where neither $\boldsymbol{u}$ nor $\nabla \wedge \boldsymbol{u}$ is defined. Thus although the fluid is clearly rotating in a global sense the flow is in fact *irrotational*, since $\nabla \wedge \boldsymbol{u} = 0$, except on the axis. This is quite understandable if we consider two momentarily perpendicular fluid line elements, AB and AC, at $\theta = 0$ in Fig. 1.5. Clearly AC is rotating in an anticlockwise sense, because it will continue to lie along the circular streamline as time proceeds, but AB is rotating clockwise because of the decrease of u_θ with r in eqn (1.21). This particular fall-off of u_θ with r is, apparently, just the correct one—neither too slow nor too rapid—to ensure that AB has an equal and opposite angular velocity to AC at the instant they are perpendicular, so that their average angular velocity is zero.

We keep emphasizing the instantaneous nature of this conclusion about zero average angular velocity because two fluid line elements such as AB and AC in Fig. 1.5 will not remain perpendicular as they get carried about by the flow, and as soon as this happens we have no cause to conclude from the irrotationality of the flow that their average angular velocity should any longer be zero.

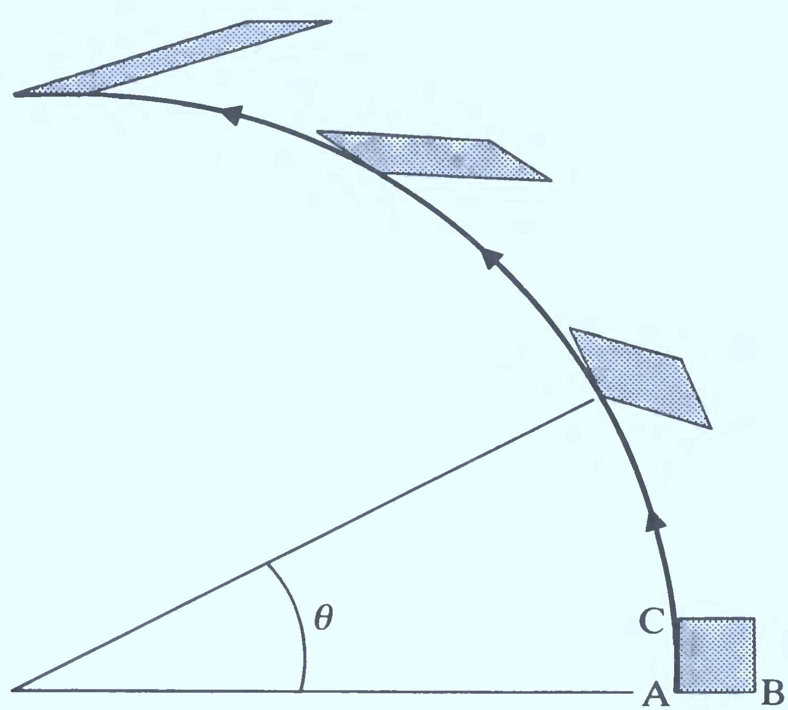

Fig. 1.5. The fate of a small square fluid element in a line vortex flow. The size of the element has been greatly exaggerated for the sake of clarity; an unfortunate consequence is that B does not look as if it is following a circular path.

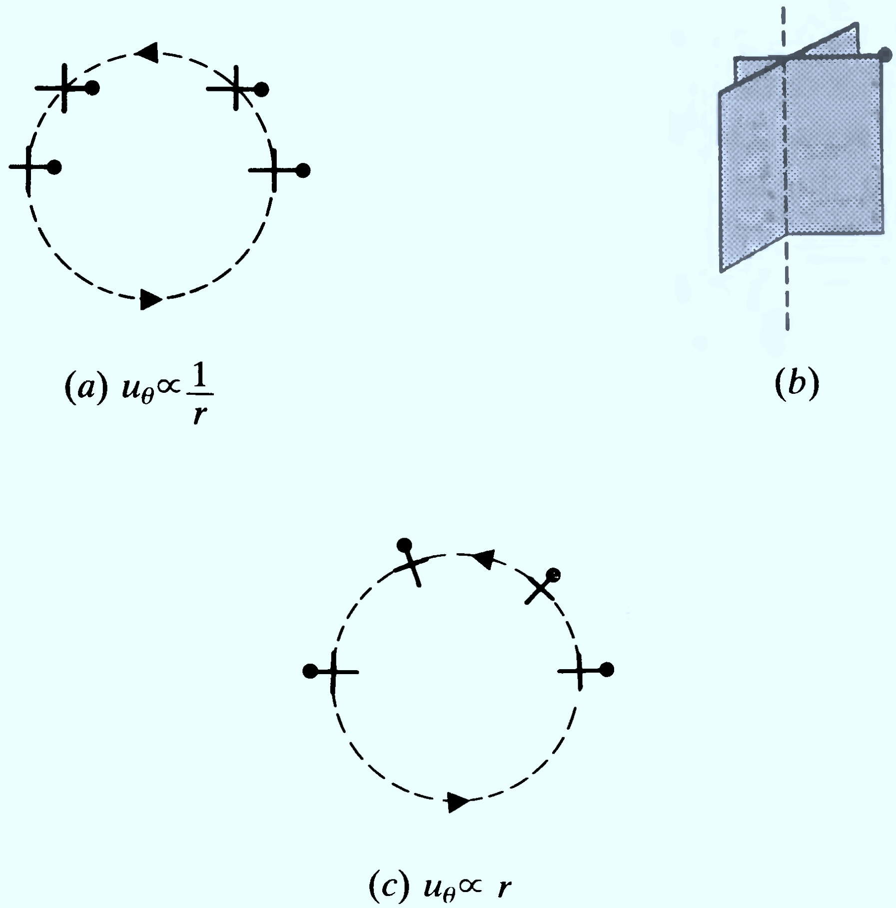

Fig. 1.6. A crude 'vorticity meter' (*b*), and its behaviour when immersed in a line vortex flow (*a*) and a uniformly rotating flow (*c*).

What we have sketched in Fig. 1.6(*a*), then, is not what happens to two momentarily dyed fluid elements, AB and AC, as they get swept round but what would happen if we were to immerse in the fluid a small 'vorticity meter' consisting of two short, rigid vanes fixed at right angles to each other, as in Fig. 1.6(*b*). We have marked one tip of one of the vanes, and in Fig. 1.6(*a*) we see that this device would not rotate in this particular (line vortex) flow, even though its axis would of course get swept round on a circular streamline. This behaviour may be seen in the bath by observing closely the strong vortex that may occur as the water goes down the plug-hole. The azimuthal velocity u_θ varies roughly as r^{-1} over a fair distance from the axis, and a crude but simple vorticity meter which serves the purpose consists of a pair of short wooden line elements shaved off a matchstick, sellotaped together at right angles and floated on the surface.

However, if such a vorticity meter were to be inserted in the flow

$$\boldsymbol{u} = \Omega r \boldsymbol{e}_\theta, \tag{1.22}$$

Ω being a constant, the result would of course be as in Fig. 1.6(*c*), because the device would get carried around just as if it were embedded in a rigid body. Its angular velocity would evidently be Ω, the same as the uniform angular velocity of the fluid as a whole, and the vorticity of the flow is therefore $(0, 0, 2\Omega)$, as may be confirmed by direct calculation of $\nabla \wedge \boldsymbol{u}$.

By putting the two flows in Fig. 1.6 together in the following way:

$$u_\theta = \begin{cases} \Omega r, & r < a, \\ \dfrac{\Omega a^2}{r}, & r > a, \end{cases}$$

$$u_r = u_z = 0, \tag{1.23}$$

we obtain a so-called 'Rankine vortex', which serves as a simple model for a real vortex such as that in Fig. 1.1. Real vortices are typically characterized by fairly small vortex 'cores' in which, by definition, the vorticity is concentrated, while outside the core the flow is essentially irrotational. The core is not usually exactly circular, of course; nor is the vorticity usually uniform within it. In these two respects the Rankine vortex of Fig. 1.7 is only an idealized model.

We have now said a fair amount about vorticity, albeit strictly

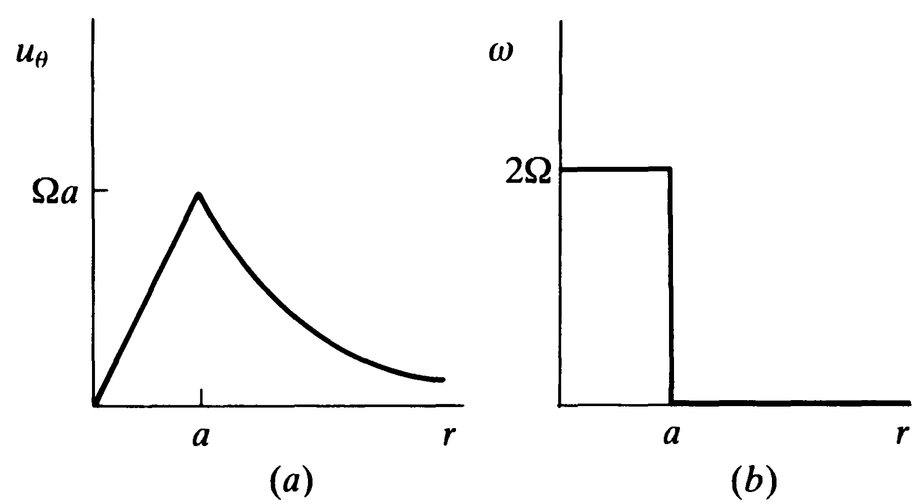

Fig. 1.7. Distribution of (*a*) azimuthal velocity u_θ and (*b*) vorticity ω in a Rankine vortex.

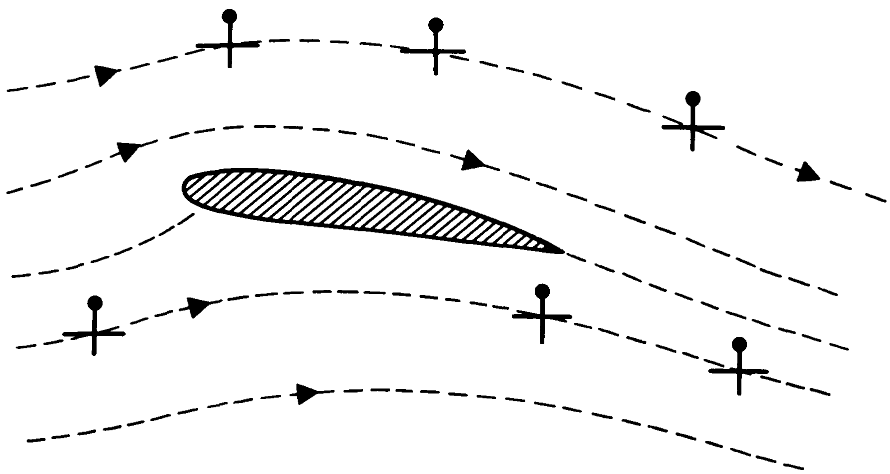

Fig. 1.8. The behaviour of a small 'vorticity meter' placed in the steady flow past a fixed wing at small angle of attack. The flow is clearly irrotational.

in the context of two-dimensional flow. We have discussed in particular detail the absence of vorticity, i.e. irrotational flow. At this stage, before the development seems to be getting rather a long way from our starting point (the experiment in §1.1), we should say that steady flow past a wing at small angles of incidence α *is* typically irrotational, as indicated in Fig. 1.8.

Why this should be so emerges from the Euler equations in a very elegant manner, as we now see.

1.5. The vorticity equation

In its form (1.14), Euler's equation may be written

$$\frac{\partial \boldsymbol{u}}{\partial t} + \boldsymbol{\omega} \wedge \boldsymbol{u} = -\nabla H,$$

and on taking the curl we obtain

$$\frac{\partial \boldsymbol{\omega}}{\partial t} + \nabla \wedge (\boldsymbol{\omega} \wedge \boldsymbol{u}) = 0. \tag{1.24}$$

Using the vector identity (A.6) this becomes

$$\frac{\partial \boldsymbol{\omega}}{\partial t} + (\boldsymbol{u} \cdot \nabla)\boldsymbol{\omega} - (\boldsymbol{\omega} \cdot \nabla)\boldsymbol{u} + \boldsymbol{\omega}\nabla \cdot \boldsymbol{u} - \boldsymbol{u}\nabla \cdot \boldsymbol{\omega} = 0.$$

Now the fourth term vanishes because the fluid is incompressible, while the fifth term vanishes because div curl $= 0$. We therefore have

$$\frac{\partial \boldsymbol{\omega}}{\partial t} + (\boldsymbol{u} \cdot \nabla)\boldsymbol{\omega} = (\boldsymbol{\omega} \cdot \nabla)\boldsymbol{u},$$

or, alternatively,

$$\frac{\mathrm{D}\boldsymbol{\omega}}{\mathrm{D}t} = (\boldsymbol{\omega} \cdot \nabla)\boldsymbol{u}. \tag{1.25}$$

This *vorticity equation* is extremely valuable. Note that the pressure has been eliminated; eqn (1.25) involves only $\boldsymbol{u}$ and $\boldsymbol{\omega}$, which are, of course, related by

$$\boldsymbol{\omega} = \nabla \wedge \boldsymbol{u}.$$

In particular, if the flow is *two-dimensional,* so that

$$\boldsymbol{u} = [u(x, y, t), v(x, y, t), 0] \tag{1.26}$$

and

$$\boldsymbol{\omega} = (0, 0, \omega),$$

then

$$(\boldsymbol{\omega} \cdot \nabla)\boldsymbol{u} = \omega \frac{\partial \boldsymbol{u}}{\partial z} = 0.$$

It then follows that

$$\frac{\mathrm{D}\omega}{\mathrm{D}t} = 0, \tag{1.27}$$

and we thus conclude, referring back to eqn (1.9), that

In the two-dimensional flow of an ideal fluid subject to a conservative body force $\mathbf{g}$ *the vorticity* ω *of each individual fluid element is conserved.* (1.28)

This result has important applications, which we discuss in Chapter 5. In the particular case of steady flow, eqn (1.27) reduces to

$$(\boldsymbol{u} \cdot \nabla)\omega = 0 \tag{1.29}$$

and consequently

In the steady, two-dimensional flow of an ideal fluid subject to a conservative body force $\mathbf{g}$ *the vorticity* ω *is constant along a streamline.* (1.30)

This, then, is the reason why the steady flow in Fig. 1.8 is irrotational. Note first that there are no regions of closed streamlines in the flow; all the streamlines can be traced back to $x = -\infty$. Now, the vorticity is constant along each one, and hence equal on each one to whatever it is on that particular streamline at $x = -\infty$. As the flow is uniform at $x = -\infty$ the vorticity is zero on all streamlines there. Hence it is zero throughout the flow field in Fig. 1.8.

1.6. Steady flow past a fixed wing

In Fig. 1.9 we show typical measured pressure distributions on the upper and lower surfaces of a fixed wing in steady flow. The pressures on the upper surface are substantially lower than the free-stream value p_∞, while those on the lower surface are a little higher than p_∞. In fact, then, the wing gets most of its lift from a suction effect on its upper surface.

But why is it that the pressures above the wing are less than those below? Well, because the flow is irrotational, the Bernoulli theorem tells us that $p + \frac{1}{2}\rho \boldsymbol{u}^2$ is constant throughout the flow. Explaining the pressure differences, and hence the lift on the

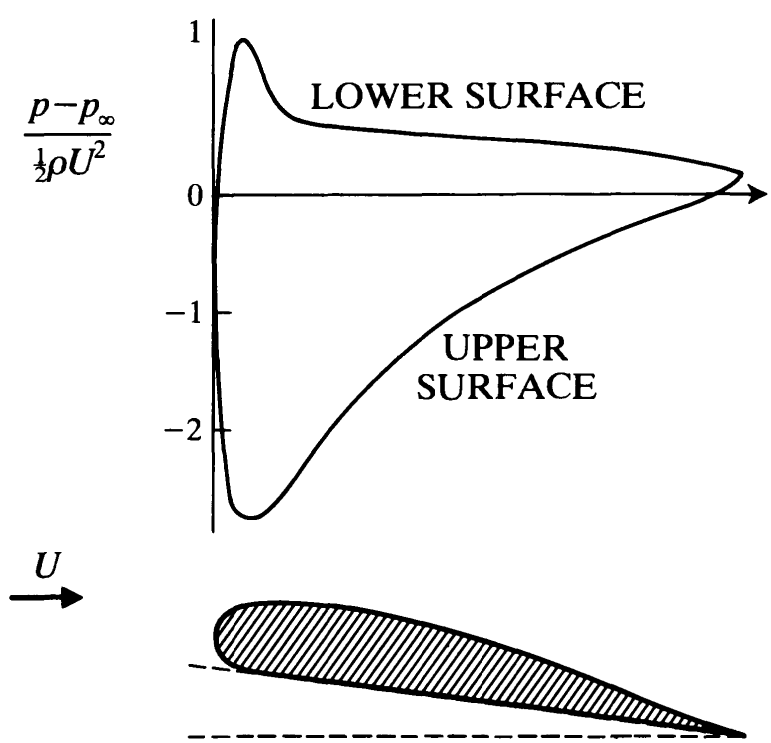

Fig. 1.9. Typical pressure distribution on a wing in steady flow.

wing, thus reduces to explaining why (as in Fig. 1.2) the flow speeds above the wing are greater than those below.

Let us first dispose of one bogus explanation that occasionally appears, namely that the air on the top of the wing flows faster 'because it has farther to go'. There are many woolly aspects to this argument, but it seems to turn principally on the notion that two neighbouring fluid elements, after parting to go their separate ways round the wing, meet up again at the trailing edge, and this is demonstrably false (see Fig. 2.4).

The right way forward to an explanation of the higher flow speeds above the wing is in terms of the concept of circulation.

Circulation

Let C be some closed curve lying in the fluid region. Then the circulation Γ round C is defined as

$$\Gamma = \int_C \boldsymbol{u} \cdot \mathrm{d}\boldsymbol{x}. \tag{1.31}$$

At first sight, perhaps, there cannot be any circulation in an irrotational flow, for Stokes's theorem gives

$$\int_C \boldsymbol{u} \cdot \mathrm{d}\boldsymbol{x} = \int_S (\nabla \wedge \boldsymbol{u}) \cdot \boldsymbol{n}\, \mathrm{d}S, \tag{1.32}$$

and an irrotational flow is, by definition, one for which $\nabla \wedge \boldsymbol{u}$ is zero. But such an argument holds only if the closed curve C in question can be spanned by a surface S which lies wholly in the region of irrotational flow. Thus in the two-dimensional context of Fig. 1.8, for example, for which eqn (1.32) reduces to

$$\Gamma = \int_C u\, \mathrm{d}x + v\, \mathrm{d}y = \int_S \left(\frac{\partial v}{\partial x} - \frac{\partial u}{\partial y}\right) \mathrm{d}x\, \mathrm{d}y, \tag{1.33}$$

it is true that Γ must be zero for any closed curve C not enclosing the wing, but the argument fails for any closed curve that does enclose the wing. The most that can be said about such circuits is that they all have the same value of Γ (Exercise 1.6).

Circulation round a wing is permissible, then, in a steady irrotational flow; but the question still arises as to why there should be any, and, in particular, why it should be negative, corresponding to larger flow speeds above the wing than below.

The Kutta–Joukowski hypothesis

In the case of a wing with a sharp trailing edge, one good reason for non-zero circulation Γ is that there would otherwise be a singularity in the velocity field. The irrotational flow past a wing with $\Gamma = 0$ is sketched in Fig. 1.10(a), but the velocity is infinite at the trailing edge where, loosely speaking, the fluid is having a hard time turning the corner. We show in Chapter 4 that only for one value of the circulation, Γ_K say, is the flow speed finite at the trailing edge, as in Fig. 1.10(b). It is natural to hope that this particular irrotational flow will correspond to the steady flow that is actually observed; this is the *Kutta–Joukowski hypothesis*.

This hypothesis is inevitably somewhat *ad hoc*, resting as it does on the unsatisfactory state of affairs that would otherwise arise because of the sharp trailing edge. (How are we to decide between all the different irrotational flows if the trailing edge is not sharp?) It is, nonetheless, one of the key steps in the development of aerodynamics, and gives results which are in excellent accord with experiment, as we shall shortly see.

The critical value Γ_K depends, naturally, on the flow speed at infinity U and on the size, shape, and orientation of the wing. In Chapter 4 we show that if the wing is thin and symmetrical, of length L, making an angle α with the oncoming stream, then

$$\Gamma_K \doteqdot -\pi U L \sin \alpha. \tag{1.34}$$

Lift

According to ideal flow theory, the *drag* on the wing (the force parallel to the oncoming stream) is zero, but the *lift* (the force

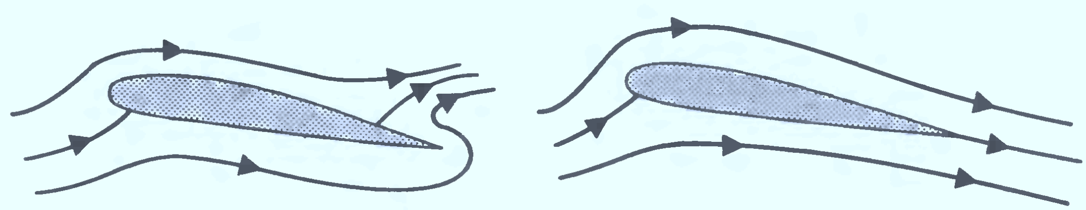

(a) (b)

Fig. 1.10. Irrotational flow past a fixed wing with (a) $\Gamma = 0$ and (b) $\Gamma = \Gamma_K < 0$.

perpendicular to the stream) is

$$\mathscr{L} = -\rho U \Gamma. \tag{1.35}$$

This *Kutta–Joukowski Lift Theorem* is proved in §4.11.

That negative Γ should give positive lift is entirely natural; we have argued as much in the preceding sections. As a precise theorem, however, eqn (1.35) is rather extraordinary, as it holds for irrotational flow (uniform at infinity) past a two-dimensional body of any size or shape; $\mathscr{L}$ depends on the size and shape of the body only inasmuch as Γ does. For the thin symmetrical wing of Fig. 1.10(b), for example, with Γ as in eqn (1.34) by the Kutta–Joukowski condition, the lift is

$$\mathscr{L} \doteqdot \pi \rho U^2 L \sin \alpha. \tag{1.36}$$

Agreement with experiment is good provided that α is only a few degrees (Fig. 1.11). Thereafter the measured lift falls dramatically and diverges substantially from the predictions of inviscid theory, for reasons to be discussed later. The angle α at which this divergence begins may be anywhere between about 6° and 12°, depending on the shape of the wing (see, e.g., Nakayama 1988, pp. 76–80).

Accounting for the flow past a wing at small angles of attack α is nevertheless one of the great, and practically important, successes of ideal-flow theory.

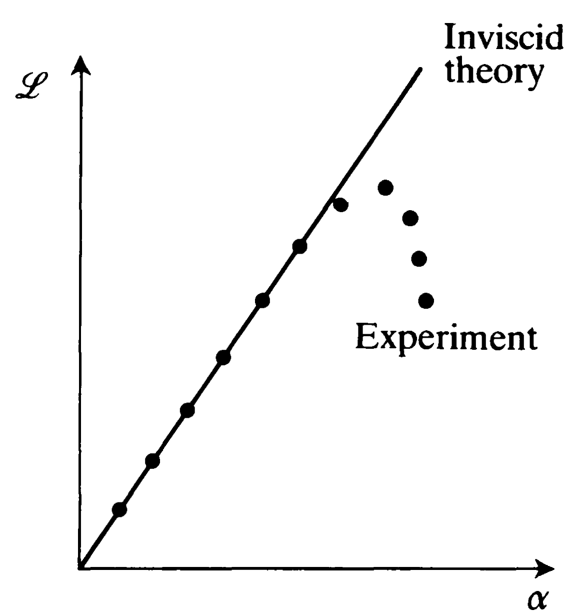

Fig. 1.11. Lift on a symmetric aerofoil.

1.7. Concluding remarks

In this chapter we have introduced some of the basic concepts of fluid dynamics and, at the same time, given some indication of how they figure in one particular branch of the subject, namely aerodynamics. Our treatment of this branch has inevitably been sketchy.

We have, for instance, focused wholly on 2-D aerodynamics, yet any real wing, no matter how long, has ends, and important new phenomena then arise. The circulation round a circuit such as C in Fig. 1.12(a) is essentially that predicted by the 2-D theory (i.e. eqn (1.34)), but plainly the flow cannot be everywhere irrotational, because C can now be spanned by a surface S which lies wholly in the fluid. Indeed, from Stokes's theorem (1.32) we deduce that there must be a positive flux of vorticity out of S, and this is in practice observed as a concentrated *trailing vortex* emanating from the wing-tip as shown. The higher the lift (and

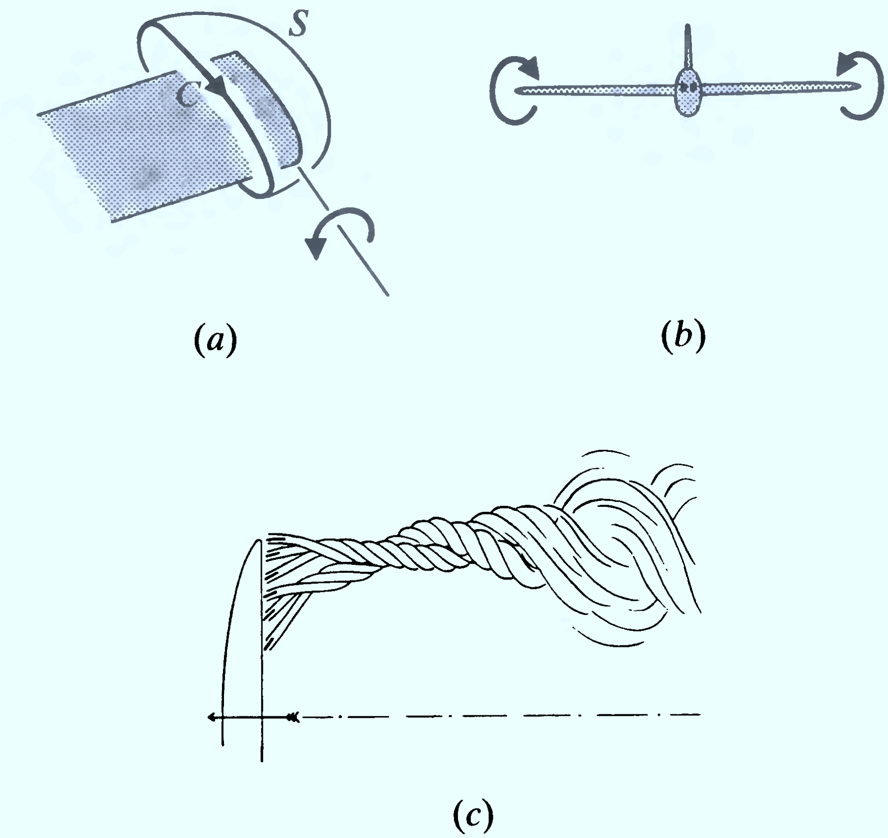

Fig. 1.12. Trailing vortices: (a) definition sketch for application of Stokes's theorem; (b) view from some distance ahead of the aircraft; (c) the original drawing from Lanchester's *Aerodynamics* (1907).

therefore the circulation), the stronger the trailing vortices. Furthermore, the presence of these trailing vortices results in a drag on the wing, even on ideal flow theory, for as they lengthen they contain more and more kinetic energy, and creating all this kinetic energy takes work.

But even within a purely two-dimensional framework we have left some key questions unanswered. We indicated how the Kutta–Joukowski hypothesis provides a rational, although *ad hoc,* basis for deciding the circulation round an aerofoil in steady flight, and we have noted that this gives good agreement with experiment. Yet we have given no account of the dynamical processes by which that circulation is *generated* when the aerofoil starts from a state of rest. It arises, in fact, in response to the 'starting vortex' in §1.1, but why this should be so is far from obvious, and rests on one of the deepest theorems in the subject (§5.1).

Again, the sceptical reader may even be asking: 'But what is all this business about a starting vortex? If the aerofoil and fluid are initially at rest, the vorticity ω is initially zero for each fluid element. By eqn (1.27) it remains zero for each fluid element, even when the aerofoil has been started into motion. Therefore there should not be a starting vortex.'

This is a legitimate conclusion—on the basis of ideal flow theory. While that theory accounts well for the steady flow past an aerofoil, the explanation of how that flow became established involves *viscous* effects in a crucial way.

If this provokes the response: 'But air isn't very viscous, is it?', the answer is, 'No, in some sense air is hardly viscous at all'. Yet, as we shall see, viscous effects are sufficiently subtle that the shedding of the vortex in §1.1, while being an essentially viscous process, would occur no matter how small the viscosity of the fluid happened to be.

Exercises

1.1. Whether a fluid is incompressible or not, each element must conserve its mass as it moves. Consider the rate of mass flow through a fixed closed surface S drawn in the fluid, and use an argument similar to that on p. 7 to show that this *conservation of mass* implies

$$\frac{\partial \rho}{\partial t} + \nabla \cdot (\rho \boldsymbol{u}) = 0, \tag{1.37}$$

where $\rho(\boldsymbol{x}, t)$ denotes the (variable) density of the fluid. Show too that this equation may alternatively be written

$$\frac{\mathrm{D}\rho}{\mathrm{D}t} + \rho\nabla \cdot \boldsymbol{u} = 0. \tag{1.38}$$

It follows that if $\nabla \cdot \boldsymbol{u} = 0$, then $\mathrm{D}\rho/\mathrm{D}t = 0$. What does this mean, exactly, and does it make sense?

1.2. An ideal fluid is rotating under gravity g with constant angular velocity Ω, so that relative to fixed Cartesian axes $\boldsymbol{u} = (-\Omega y, \Omega x, 0)$. We wish to find the surfaces of constant pressure, and hence the surface of a uniformly rotating bucket of water (which will be at atmospheric pressure).

'By Bernoulli,' $p/\rho + \frac{1}{2}\boldsymbol{u}^2 + gz$ is constant, so the constant pressure surfaces are

$$z = \text{constant} - \frac{\Omega^2}{2g}(x^2 + y^2).$$

But this means that the surface of a rotating bucket of water is at its highest in the middle. What is wrong?

Write down the Euler equations in component form, integrate them directly to find the pressure p, and hence obtain the correct shape for the free surface.

1.3. Find the pressure p both inside and outside the core of the Rankine vortex (1.23). Show that the pressure at $r = 0$ is lower than that at $r = \infty$ by an amount $\rho\Omega^2 a^2$ (hence the very low pressure in the centre of a tornado). Deduce that if there is a free surface to the fluid and gravity is acting, then the surface at $r = 0$ is a depth $\Omega^2 a^2/g$ below the surface at $r = \infty$ (hence the dimples in a cup of tea accompanying the vortices that are shed by the edges of the spoon).

1.4. Take the Euler equation for an incompressible fluid of constant density, cast it into an appropriate form, and perform suitable operations on it to obtain the *energy equation*:

$$\frac{\mathrm{d}}{\mathrm{d}t}\int_V \tfrac{1}{2}\rho \boldsymbol{u}^2\,\mathrm{d}V = -\int_S (p' + \tfrac{1}{2}\rho\boldsymbol{u}^2)\boldsymbol{u} \cdot \boldsymbol{n}\,\mathrm{d}S,$$

where V is the region enclosed by a fixed closed surface S drawn in the fluid, and p' denotes $p + \rho\chi$, the non-hydrostatic part of the pressure field.

1.5. For an inviscid fluid we have Euler's equation

$$\frac{\partial \boldsymbol{u}}{\partial t} + \boldsymbol{\omega} \wedge \boldsymbol{u} + \nabla(\tfrac{1}{2}\boldsymbol{u}^2) = -\frac{1}{\rho}\nabla p - \nabla\chi,$$

and, whether or not the fluid is incompressible, we also have conservation of mass (Exercise 1.1):

$$\frac{\mathrm{D}\rho}{\mathrm{D}t} + \rho\nabla\cdot\boldsymbol{u} = 0.$$

Show that

$$\frac{\mathrm{D}}{\mathrm{D}t}\left(\frac{\boldsymbol{\omega}}{\rho}\right) = \left(\frac{\boldsymbol{\omega}}{\rho}\cdot\nabla\right)\boldsymbol{u} - \frac{1}{\rho}\nabla\left(\frac{1}{\rho}\right)\wedge\nabla p. \tag{1.39}$$

Deduce that, if p is a function of ρ alone, the vorticity equation is exactly as in the incompressible, constant density case, except that $\boldsymbol{\omega}$ is replaced by $\boldsymbol{\omega}/\rho$.

1.6. Show that the circulation is the same round all simple closed circuits enclosing the wing in Fig. 1.8. (Hint: sketch two such circuits, and then make a construction so as to create a single closed circuit that does not enclose the wing.)

1.7. Sketch the streamlines for the flow

$$u = \alpha x, \qquad v = -\alpha y, \qquad w = 0,$$

where α is a positive constant.

Let the concentration of some pollutant in the fluid be

$$c(x, y, t) = \beta x^2 y \mathrm{e}^{-\alpha t},$$

for $y > 0$, where β is a constant. Does the pollutant concentration for any particular fluid element change with time?

An alternative way of describing any flow is to specify the position $\boldsymbol{x}$ of each fluid element at time t in terms of the position $\boldsymbol{X}$ of that element at time $t = 0$. For the above flow this 'Lagrangian' description is

$$x = X\mathrm{e}^{\alpha t}, \qquad y = Y\mathrm{e}^{-\alpha t}, \qquad z = Z.$$

Verify by direct calculation that

$$\left(\frac{\partial \boldsymbol{x}}{\partial t}\right)_{\boldsymbol{X}} = \boldsymbol{u}, \qquad \left(\frac{\partial \boldsymbol{u}}{\partial t}\right)_{\boldsymbol{X}} = \frac{\mathrm{D}\boldsymbol{u}}{\mathrm{D}t}$$

in this particular case. Why are these results true in general?

Write c as a function of X, Y, and t.

1.8. Consider the unsteady flow

$$u = u_0, \qquad v = kt, \qquad w = 0,$$

where u_0 and k are positive constants. Show that the streamlines are straight lines, and sketch them at two different times. Also show that any fluid particle follows a parabolic path as time proceeds.

2 Elementary viscous flow

2.1. Introduction

Steady flow past a fixed aerofoil may seem at first to be wholly accounted for by inviscid flow theory. The streamline pattern seems right, and so does the velocity field. In particular, the fluid in contact with the aerofoil appears to slip along the boundary in just the manner predicted by inviscid theory. Yet close inspection reveals that there is in fact no such slip. Instead there is a very thin *boundary layer,* across which the flow velocity undergoes a smooth but rapid adjustment to precisely zero—corresponding to *no slip*—on the aerofoil itself (Fig. 2.1). In this boundary layer inviscid theory fails, and viscous effects are important, even though they are negligible in the main part of the flow.

To see why this should be so we must first make precise what we mean by the term 'viscous'. To this end, consider the case of simple shear flow, so that $\boldsymbol{u} = [u(y), 0, 0]$. The fluid immediately above some level $y = \text{constant}$ exerts a stress, i.e. a force per unit area of contact, on the fluid immediately below, and vice versa. For an inviscid fluid this stress has no tangential component τ, but for a viscous fluid τ is typically non-zero. In this book we shall be concerned with *Newtonian* viscous fluids, and in this case the shear stress τ is proportional to the velocity gradient $\mathrm{d}u/\mathrm{d}y$, i.e.

$$\tau = \mu \frac{\mathrm{d}u}{\mathrm{d}y}, \tag{2.1}$$

where μ is a property of the fluid, called the *coefficient of viscosity*. Many real fluids, such as water or air, behave according to eqn (2.1) over a wide range of conditions (although there are many others, including paints and polymers, which are non-Newtonian, and do not; see Tanner (1988)).

From a fluid dynamical point of view the so-called *kinematic viscosity*

$$\nu = \mu/\rho \tag{2.2}$$

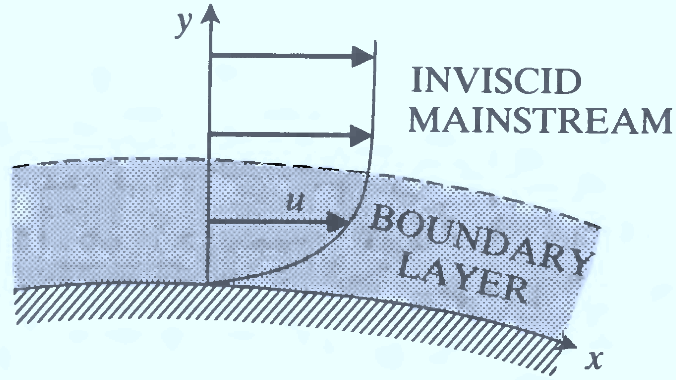

Fig. 2.1. A boundary layer.

is often more significant than μ itself, and some typical values of ν are given in Table 2.1. These values can vary quite substantially with temperature, but throughout much of this book we shall concentrate on a simple model of fluid flow in which μ, ρ, and ν are all constant.

We can see now, in general terms, why viscous effects become important in a boundary layer. The reason is that the velocity gradients in a boundary layer are much larger than they are in the main part of the flow, because a substantial change in velocity is taking place across a very thin layer. In this way the viscous stress (2.1) becomes significant in a boundary layer, even though μ is small enough for viscous effects to be negligible elsewhere in the flow.

But why are boundary layers so important that we begin this chapter with them? The answer is that in certain circumstances

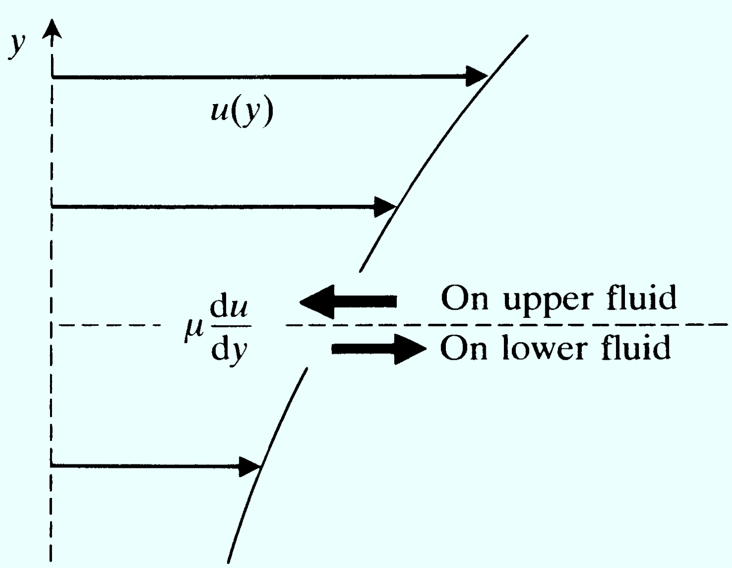

Fig. 2.2. Viscous stresses in a simple shear flow.

Table 2.1. Kinematic viscosity ν (cm^2 s^{-1}) at 15°C.

Water	0.01	($\mu = 0.01$ c.g.s. units)
Air	0.15	($\mu = 0.0002$ c.g.s. units)
Olive oil	1.0	
Glycerine	18	
Golden syrup/treacle	~1200	($\nu \sim 200$ at 27°C)

they may *separate* from the boundary, *thus causing the whole flow of a low-viscosity fluid to be quite different to that predicted by inviscid theory.*

Consider, for example, the flow of a low-viscosity fluid past a circular cylinder. In the first instance it is natural to assume that viscous effects will be negligible in the main part of the flow, which will therefore be irrotational, by the argument of §1.5. If we solve the problem of irrotational flow past a circular cylinder (§4.5) we obtain the streamline pattern of Fig. 2.3(a). This 'solution' is not wholly satisfactory, for it predicts slip on the surface of the cylinder. We might then suppose that a thin viscous boundary layer intervenes to adjust the velocity smoothly to zero on the cylinder itself. But this turns out to be wishful thinking; the observed flow of a low-viscosity fluid past a circular cylinder is, instead, of an altogether different kind, with massive separation of the boundary layer giving rise to a large vorticity-filled *wake* (Fig. 2.3(*b*)).

Why does separation occur? The answer lies in the variation of pressure p along the boundary, as predicted by inviscid theory.

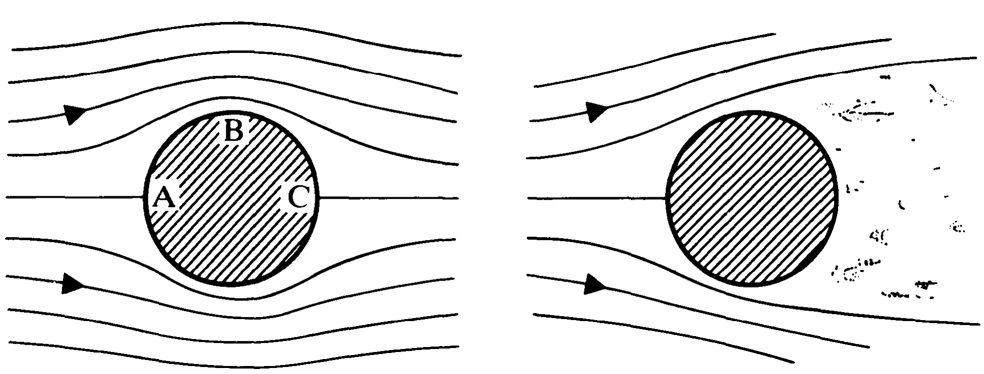

(*a*) (*b*)

Fig. 2.3. Flow past a circular cylinder for (*a*) an inviscid fluid and (*b*) a fluid of small viscosity.

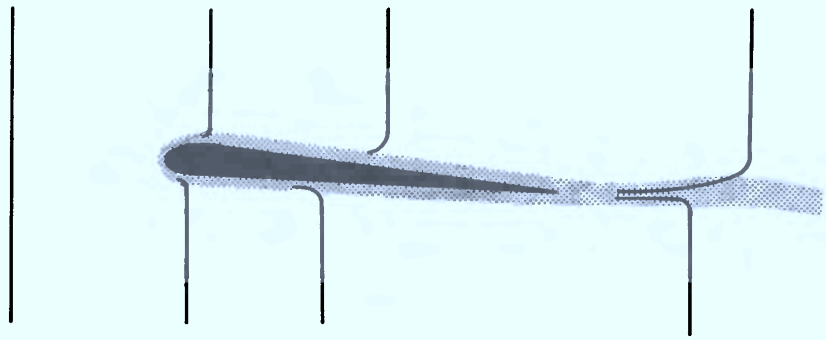

Fig. 2.4. Flow past an aerofoil: the fate of successive lines of fluid particles.

In Fig. 2.3(*a*), inviscid theory predicts that p has a local maximum at the forward stagnation point A, falls to a minimum at B, then increases to a local maximum at C, with $p_A = p_C$. This implies that between B and C there is a substantial increase in pressure along the boundary in the direction of flow. It is this *severe adverse pressure gradient along the boundary* which causes the boundary layer to separate, for reasons which are outlined in §§8.1 and 8.6 (see especially Fig. 8.2.)

An aerofoil, on the other hand, is deliberately designed to avoid such large-scale separation, the key feature being its slowly tapering rear. In Fig. 1.9, for example, the substantial fall in pressure over the first 10% or so of the upper surface is followed by a very *gradual* pressure rise over the remainder. For this reason the boundary layer does not separate until close to the trailing edge, and there is only a very narrow wake (Fig. 2.4). This state of affairs persists as long as the angle of attack α is not too large; if α is greater than a few degrees, the pressure rise over the remainder of the upper surface is no longer gradual,

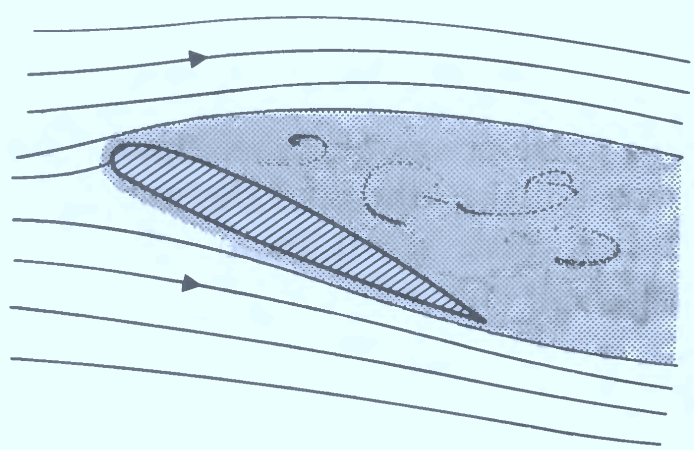

Fig. 2.5. Separated flow past an aerofoil.

large-scale separation takes place, and the aerofoil is said to be *stalled*, as in Fig. 2.5. This is the explanation for the sudden drop in lift in Fig. 1.11.

The most important overall message of this introduction is that *the behaviour of a fluid of small viscosity μ may, on account of boundary layer separation, be completely different to that of a (hypothetical) fluid of no viscosity at all.* From a mathematical point of view, what happens in the limit $\mu \to 0$ may be quite different to what happens when $\mu = 0$.

2.2. The equations of viscous flow

So far we have considered the motion of fluids of small viscosity. Yet there is more to the subject than this, including the opposite extreme of very viscous flow (Chapter 7). It is time, then, to take a more balanced—if brief—look at viscous flow as a whole.

The Navier–Stokes equations

Suppose that we have an incompressible Newtonian fluid of constant density ρ and constant viscosity μ. Its motion is governed by the *Navier–Stokes equations*†

$$\begin{gathered}\frac{\partial \boldsymbol{u}}{\partial t} + (\boldsymbol{u} \cdot \nabla)\boldsymbol{u} = -\frac{1}{\rho}\nabla p + \nu\nabla^2\boldsymbol{u} + \boldsymbol{g}, \\ \nabla \cdot \boldsymbol{u} = 0.\end{gathered} \tag{2.3}$$

These differ from the Euler equations (1.12) by virtue of the viscous term $\nu\nabla^2\boldsymbol{u}$, where ∇^2 denotes the Laplace operator $\partial^2/\partial x^2 + \partial^2/\partial y^2 + \partial^2/\partial z^2$.

The no-slip condition

Observations of real (i.e. viscous) fluid flow reveal that both normal and tangential components of fluid velocity at a rigid boundary must be equal to those of the boundary itself. Thus if the boundary is at rest, $\boldsymbol{u} = 0$ there. The condition on the tangential component of velocity is known as the *no-slip condition,* and it holds for a fluid of any viscosity $\nu \neq 0$, no matter how small ν may be.

† The Navier–Stokes equations are derived from first principles in Chapter 6.

The Reynolds number

Consider a viscous fluid in motion, and let U denote a typical flow speed. Furthermore, let L denote a characteristic length scale of the flow. This is all somewhat subjective, but in dealing with the spin-down of a stirred cup of tea, for instance, 4 cm and 5 cm s^{-1} would be reasonable choices for L and U, while 10 m and 100 m s^{-1} would not. Having thus chosen a value for L and for U we may form the quantity

$$R = \frac{UL}{\nu}, \tag{2.4}$$

which is a pure number known as a *Reynolds number.*

To see why R should be important, note that derivatives of the velocity components, such as $\partial u/\partial x$, will typically be of order U/L—assuming, that is, that the components of $\boldsymbol{u}$ change by amounts of order U over distances of order L. Typically, these derivatives will themselves change by amounts of order U/L over distances of order L, so second derivatives such as $\partial^2 u/\partial x^2$ will be of order U/L^2. In this way we obtain the following order of magnitude estimates for two of the terms in eqn (2.3):

$$\begin{aligned} &\text{inertia term:} && |(\boldsymbol{u}\cdot\nabla)\boldsymbol{u}| = O(U^2/L), \\ &\text{viscous term:} && |\nu\nabla^2\boldsymbol{u}| = O(\nu U/L^2). \end{aligned} \tag{2.5}$$

Provided that these are correct we deduce that

$$\frac{|\text{inertia term}|}{|\text{viscous term}|} = O\left(\frac{U^2/L}{\nu U/L^2}\right) = O(R). \tag{2.6}$$

The Reynolds number is important, then, because it can give a rough indication of the relative magnitudes of two key terms in the equations of motion (2.3). It is not surprising, therefore, that high Reynolds number flows and low Reynolds number flows have quite different general characteristics.

High Reynolds number flow

The case $R \gg 1$ corresponds to what we have hitherto called the motion of a fluid of small viscosity. Equation (2.6) suggests that viscous effects should on the whole be negligible, and flow past a thin aerofoil at small angle of attack provides just one example where this is indeed the case. Even then, however, viscous effects become important in thin boundary layers, where the unusually large velocity gradients make the viscous term much larger than the estimate in eqn (2.5). We show in §§8.1 and 8.2 that the typical thickness δ of such a boundary layer is given by

$$\delta/L = O(R^{-\frac{1}{2}}). \tag{2.7}$$

The larger the Reynolds number, then, the thinner the boundary layer.

A large Reynolds number is *necessary* for inviscid theory to apply over most of the flow field, but it is not sufficient. As we have seen, boundary layer separation can lead to a quite different state of affairs. A further complication at high Reynolds number is that steady flows are often *unstable* to small disturbances, and may, as a result, become *turbulent*. It was in fact in this context that Reynolds first employed the dimensionless parameter that now bears his name (see §9.1).

Low Reynolds number flow

Consider a laboratory experiment in which golden syrup occupies the gap between two circular cylinders, the inner one rotating and the outer one at rest. For reasonable rotation rates of the inner cylinder the Reynolds number might be in the region of 10^{-2} or so; it will certainly be much less than 1. At such Reynolds numbers there is no sign of turbulence, and the flow is extremely well ordered.

The flow is so well ordered, in fact, that if the rotation of the

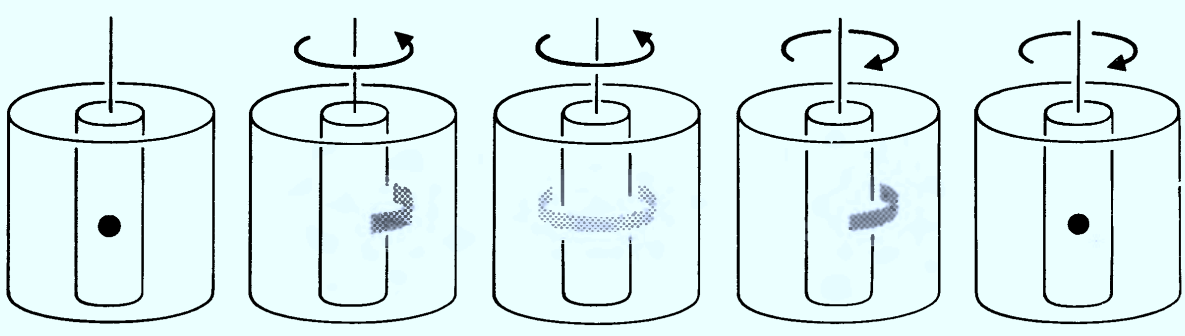

(*a*) (*b*) (*c*) (*d*) (*e*)

Fig. 2.6. The reversibility of a very viscous flow.

inner cylinder is stopped after a few revolutions, and the inner cylinder is then rotated back through the correct number of turns to its original position, a dyed blob of syrup, which has been greatly sheared in the meantime, will return almost exactly to its original configuration as a concentrated blob (Fig. 2.6).

This near *reversibility* is characteristic of low Reynolds number flows, and helps account, in fact, for the unusual swimming techniques that are adopted by certain biological micro-organisms such as the Spermatozoa (§7.5).

2.3. Some simple viscous flows: the diffusion of vorticity

We now turn to some elementary exact solutions of the Navier–Stokes equations. There is, in addition, a major theme running through §§2.3 and 2.4, and that theme is the *viscous diffusion of vorticity,* an important mechanism which was wholly absent in Chapter 1, where ν was zero.

Plane parallel shear flow

Suppose that a viscous fluid is moving so that relative to some set of rectangular Cartesian coordinates

$$\boldsymbol{u} = [u(y, t), 0, 0]. \tag{2.8}$$

Such a flow is termed a plane parallel shear flow. It automatically satisfies $\nabla \cdot \boldsymbol{u} = 0$, as u is independent of x, and in the absence of gravity† the Navier–Stokes equations (2.3) become, in component form:

$$\begin{gathered}\frac{\partial u}{\partial t} = -\frac{1}{\rho}\frac{\partial p}{\partial x} + \nu\frac{\partial^2 u}{\partial y^2},\\ \frac{\partial p}{\partial y} = \frac{\partial p}{\partial z} = 0.\end{gathered} \tag{2.9}$$

The pressure p is thus a function of x and t only. But from eqn (2.9) $\partial p/\partial x$ is equal to the difference between two terms which are independent of x. Thus $\partial p/\partial x$ must be a function of t alone. As we shall see shortly, there are important circumstances in which this fact enables us to deduce that $\partial p/\partial x$ must be zero.

† See footnote on p. 9.

First, however, it is instructive to see how eqn (2.9) may be obtained by a simple and direct application of the expression (2.1).

An ad hoc derivation of the equations of motion for a viscous fluid in plane parallel shear flow

First note that in the absence of viscous forces the corresponding Euler equation

$$\rho \frac{\partial u}{\partial t} = -\frac{\partial p}{\partial x} \tag{2.10}$$

may be deduced by considering an element of fluid of unit length in the z-direction and of small, rectangular cross-section in the x–y plane, with sides of length δx and δy (see Fig. 2.7). The net pressure force on the element in the x-direction is

$$p(x)\,\delta y - p(x+\delta x)\,\delta y \doteqdot -\frac{\partial p}{\partial x}\,\delta x\,\delta y,$$

and this is equal to the product of the element's mass $\rho\,\delta x\,\delta y$ and its acceleration

$$\frac{\mathrm{D}u}{\mathrm{D}t} = \frac{\partial u}{\partial t} + u\frac{\partial u}{\partial x},$$

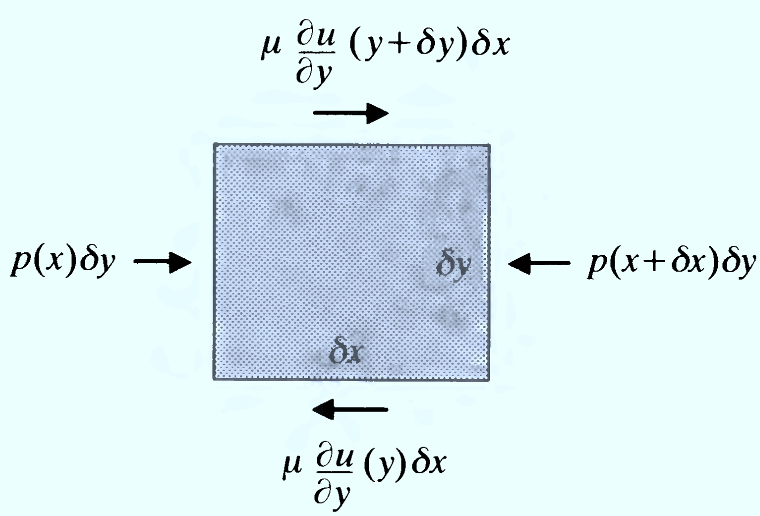

Fig. 2.7. The forces in the x-direction on a small rectangular blob in a plane parallel shear flow.

which reduces simply to $\partial u/\partial t$ because u is independent of x.

In a similar manner we may use eqn (2.1) to deduce that viscous forces on the top and bottom of the element give rise to a net contribution in the x-direction of

$$\mu \left.\frac{\partial u}{\partial y}\right|_{y+\delta y} \delta x - \mu \left.\frac{\partial u}{\partial y}\right|_{y} \delta x \doteqdot \mu \frac{\partial^2 u}{\partial y^2}\,\delta x\,\delta y, \tag{2.11}$$

whence eqn (2.10) becomes modified to

$$\rho \frac{\partial u}{\partial t} = -\frac{\partial p}{\partial x} + \mu \frac{\partial^2 u}{\partial y^2},$$

i.e. to eqn (2.9).

This equation is, of course, valid only for a very restricted class of flows, but the brevity of the above derivation does have its merits. In particular, it brings out rather clearly, via eqns (2.1) and (2.11), why the viscous term in the equation of motion (2.3) involves the *second* derivatives of the velocity field.

The flow due to an impulsively moved plane boundary

Suppose that viscous fluid lies at rest in the region $0 < y < \infty$ and suppose that at $t = 0$ the rigid boundary $y = 0$ is suddenly jerked into motion in the x-direction with constant speed U. By virtue of the no-slip condition the fluid elements in contact with the boundary will immediately move with velocity U. We wish to find how the rest of the fluid responds.

It is natural to look for a flow of the form (2.8), and eqn (2.9) then applies. We assume that the flow is being driven only by the motion of the boundary, i.e. not by any externally applied pressure gradient. This experimental consideration corresponds to asserting that the pressures at $x = \pm\infty$ are equal, and as $\partial p/\partial x$ is independent of x (so that p is a linear function of x) it follows that $\partial p/\partial x$ is zero.

The velocity $u(y, t)$ thus satisfies the classical one-dimensional *diffusion equation*

$$\frac{\partial u}{\partial t} = \nu \frac{\partial^2 u}{\partial y^2}, \tag{2.12}$$

together with the initial condition

$$u(y, 0) = 0, \qquad y > 0,$$

and the boundary conditions

$$u(0, t) = U, \quad t > 0, \qquad u(\infty, t) = 0, \quad t > 0.$$

This whole problem is in fact identical with the problem of the spreading of heat through a thermally conducting solid when its boundary temperature is suddenly raised from zero to some constant.

We may proceed most easily, on this occasion, by seeking a *similarity solution.* We postpone a more rational discussion of this method until §8.3; for the time being we simply observe that the equation is unchanged by the transformation of variables $y \Rightarrow \alpha y$, $t \Rightarrow \alpha^2 t$, α being a constant. This suggests the possibility that there are solutions to eqn (2.12) which are functions of y and t simply through the single combination $y/t^{\frac{1}{2}}$, for this 'similarity' variable would itself be unchanged by such a transformation. Inspection of eqn (2.12) suggests that it may be more convenient still to take $y/(\nu t)^{\frac{1}{2}}$ as the similarity variable. Thus if we try

$$u = f(\eta), \qquad \text{where } \eta = y/(\nu t)^{\frac{1}{2}}, \tag{2.13}$$

so that

$$\frac{\partial u}{\partial t} = f'(\eta)\frac{\partial \eta}{\partial t} = -f'(\eta)\frac{y}{2\nu^{\frac{1}{2}}t^{\frac{3}{2}}},$$

$$\frac{\partial u}{\partial y} = f'(\eta)\frac{\partial \eta}{\partial y} = f'(\eta)\frac{1}{\nu^{\frac{1}{2}}t^{\frac{1}{2}}}, \qquad \text{etc.,}$$

we obtain, from eqn (2.12),

$$f'' + \tfrac{1}{2}\eta f' = 0.$$

Integrating,

$$f' = B\mathrm{e}^{-\eta^2/4},$$

whence

$$f = A + B\int_0^\eta \mathrm{e}^{-s^2/4}\,\mathrm{d}s,$$

where A and B are constants of integration, to be determined from the initial and boundary conditions. By virtue of eqn (2.13) these reduce to

$$f(\infty) = 0, \qquad f(0) = U,$$

so that

$$u = U\left[1 - \frac{1}{\pi^{\frac{1}{2}}}\int_0^{\eta} e^{-s^2/4}\,ds\right] \tag{2.14}$$

is the solution of the problem, where $\eta = y/(\nu t)^{\frac{1}{2}}$.

The simple form of the initial and boundary conditions was essential to the success of the method. The underlying reason lies in the nature of the similarity solution (2.14) itself. As its name implies, the velocity profiles $u(y)$ are, at different times, all geometrically similar. At time t_1 the velocity u is a function of $y/(\nu t_1)^{\frac{1}{2}}$; at a later time t_2 the velocity u is the *same* function of $y/(\nu t_2)^{\frac{1}{2}}$. All that happens as time goes on is that the velocity profile becomes stretched out, as indicated in Fig. 2.8. We would not expect this to be the case if, for instance, an upper boundary were present, and the solution is, indeed, not then of similarity form (see eqn (2.21)).

At time t the effects of the motion of the plane boundary are largely confined to a distance of order $(\nu t)^{\frac{1}{2}}$ from the boundary; u is less than 1% of U at $y = 4(\nu t)^{\frac{1}{2}}$. In this way viscous effects gradually communicate the motion of the boundary to the whole fluid.

A more fundamental way of viewing this process, open to considerable generalization, is in terms of the diffusion of vorticity. The vorticity is

$$\omega = -\frac{\partial u}{\partial y} = \frac{U}{(\pi \nu t)^{\frac{1}{2}}} e^{-y^2/4\nu t}, \tag{2.15}$$

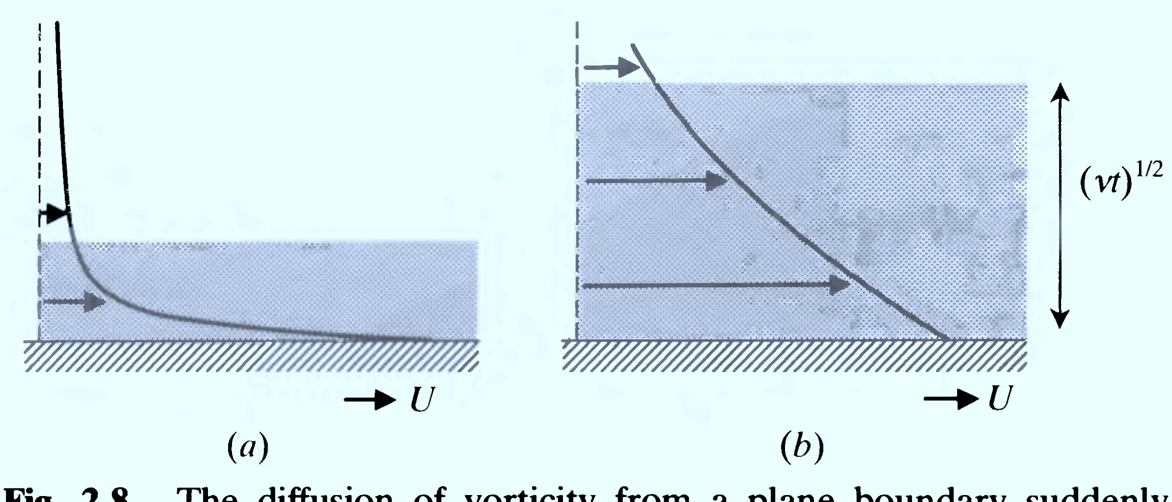

Fig. 2.8. The diffusion of vorticity from a plane boundary suddenly moved with velocity U. The solid line indicates the velocity profile at some early time (a) and some later time (b); the shading indicates the region of significant vorticity.

and this is exponentially small beyond a distance of order $(\nu t)^{\frac{1}{2}}$ from the boundary. The spreading of vorticity by viscous action thus smooths out what was, initially, a *vortex sheet,* i.e. an infinite concentration of vorticity at the boundary $(y=0,\ t\to 0)$ with none elsewhere $(y>0,\ t\to 0)$.

Finally we may state these broad conclusions in a slightly different way. Vorticity diffuses a distance of order $(\nu t)^{\frac{1}{2}}$ in time t. Equivalently, *the time taken for vorticity to diffuse a distance of order L is of the order*

$$\text{viscous diffusion time} = O(L^2/\nu). \tag{2.16}$$

Steady flow under gravity down an inclined plane

This next solution of the Navier–Stokes equations serves to make one or two elementary points about technique.

It may be argued that the key step in solving any flow problem, having decided on a sensible coordinate system, is to decide the number of independent variables (e.g. x, y, z, t) on which $\boldsymbol{u}$ depends, and the rule is 'the fewer, the better'.

In the present problem $\boldsymbol{u}$ is zero on $y=0$ (see Fig. 2.9), by virtue of the no-slip condition, so $\boldsymbol{u}$ must depend on y. In the absence of any a priori reason why $\boldsymbol{u}$ needs to depend on anything else we examine the possibility that there is a two-dimensional steady flow solution in which $\boldsymbol{u} = [u(y), v(y), 0]$.

Now, it is only common sense in any problem to *turn to the incompressibility condition at an early stage*, for of the two

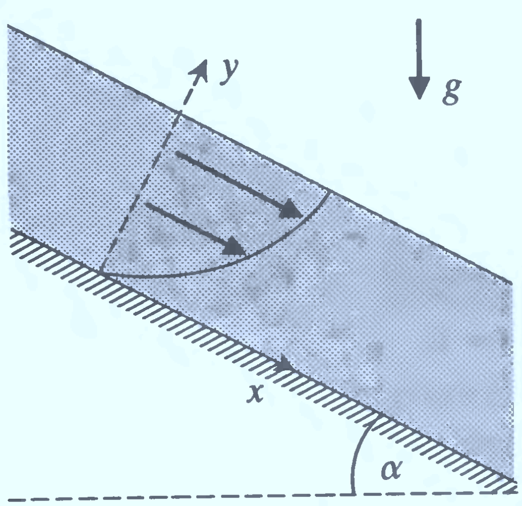

Fig. 2.9. Steady flow of a viscous fluid down an inclined plane.

equations (2.3) it is by far the simpler. In the present instance it tells us immediately that

$$dv/dy = 0,$$

i.e. that v is a constant. But $v = 0$ on $y = 0$, so v is zero everywhere.

Substituting $\boldsymbol{u} = [u(y), 0, 0]$ into the momentum equation (2.3), with the gravitational body force included, we obtain

$$\begin{aligned} 0 &= -\frac{1}{\rho}\frac{\partial p}{\partial x} + \nu\frac{d^2u}{dy^2} + g \sin\alpha, \\ 0 &= -\frac{1}{\rho}\frac{\partial p}{\partial y} \qquad\qquad - g\cos\alpha. \end{aligned} \tag{2.17}$$

Integrating the second of these we find

$$p = -\rho g y \cos\alpha + f(x),$$

where $f(x)$ is an arbitrary function of x.

Now, the free surface must be $y = h$, where h is a constant, because all the streamlines are parallel to the plane. At this free surface the tangential stress must be zero and the pressure p must be equal to atmospheric pressure p_0 (see Exercise 6.3), so

$$p = p_0 \quad \text{and} \quad \mu\frac{du}{dy} = 0 \qquad \text{at } y = h, \tag{2.18}$$

by virtue of eqn (2.1). Consequently,

$$p - p_0 = \rho g(h - y)\cos\alpha,$$

whence $\partial p/\partial x$ is zero. Equation (2.17) then reduces to

$$\nu\frac{d^2u}{dy^2} = -g\sin\alpha,$$

and we may easily integrate this twice, applying the boundary conditions

$$u = 0 \quad \text{at} \quad y = 0, \qquad \mu\frac{du}{dy} = 0 \quad \text{at} \quad y = h,$$

to obtain

$$u = \frac{g}{2\nu}y(2h - y)\sin\alpha. \tag{2.19}$$

The velocity profile is therefore parabolic, as shown in Fig. 2.9. The volume flux down the plane, per unit length in the z-direction, is

$$Q = \int_0^h u \, \mathrm{d}y = \frac{gh^3}{3\nu} \sin \alpha.$$

Another example of vorticity diffusion

Consider the problem in Fig. 2.10, in which a lower rigid boundary $y = 0$ is suddenly moved with speed U, while an upper rigid boundary to the fluid, $y = h$, is held at rest. As in an earlier subsection, we argue that $\boldsymbol{u} = [u(y, t), 0, 0]$ will satisfy eqn (2.12):

$$\frac{\partial u}{\partial t} = \nu \frac{\partial^2 u}{\partial y^2}, \tag{2.20}$$

subject to the initial condition

$$u(y, 0) = 0, \qquad 0 < y < h;$$

but this time the boundary conditions will be

$$u(0, t) = U, \quad t > 0, \qquad u(h, t) = 0, \quad t > 0.$$

The equation is homogeneous, but the boundary conditions are not. Before using the method of separation of variables and

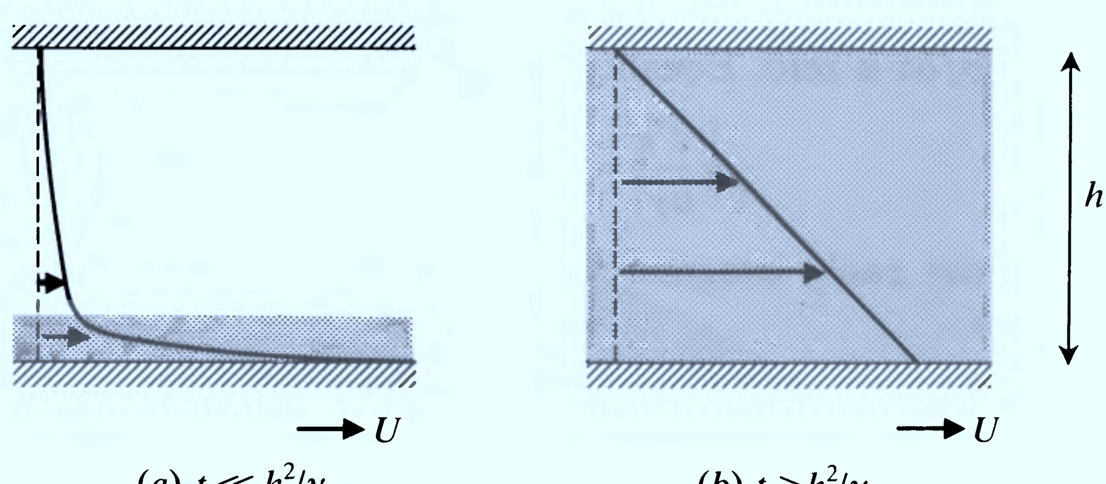

Fig. 2.10. Flow between two rigid boundaries, one suddenly moved with speed U and one held fixed. Shading indicates regions of significant vorticity.

Fourier series we therefore reformulate the problem by first seeking a *steady* solution that satisfies the boundary conditions; this is clearly $U(1-y/h)$. We therefore write

$$u = U(1-y/h) + u_1,$$

where

$$\frac{\partial u_1}{\partial t} = \nu \frac{\partial^2 u_1}{\partial y^2},$$

$$u_1(y, 0) = -U(1-y/h), \qquad 0<y<h,$$

$$u_1(0, t) = 0, \qquad t>0, \qquad u_1(h, t) = 0, \quad t>0.$$

The boundary conditions are now homogeneous. By the method of separation of variables we find that the functions

$$\exp(-n^2\pi^2\nu t/h^2)\sin(n\pi y/h), \qquad n = 1, 2, \ldots.$$

all satisfy the equation for u_1 and the boundary conditions for u_1 at $y = 0, h$. None of these individually satisfies the initial condition for u_1, but by writing

$$u_1 = \sum_{n=1}^{\infty} A_n \exp(-n^2\pi^2\nu t/h^2)\sin(n\pi y/h),$$

we may use Fourier theory to determine the A_n such that

$$\sum_{n=1}^{\infty} A_n \sin(n\pi y/h) = -U(1-y/h) \qquad \text{in } 0<y<h,$$

thus satisfying the initial condition. In this way we find

$$A_n = -\frac{2}{h}\int_0^h U(1-y/h)\sin(n\pi y/h)\,dy = -2U/n\pi,$$

and the solution is therefore

$$u(y, t) = U(1-y/h) - \frac{2U}{\pi}\sum_{n=1}^{\infty}\frac{1}{n}\exp(-n^2\pi^2\nu t/h^2)\sin(n\pi y/h). \tag{2.21}$$

The main feature of this solution is that for times $t \gtrsim h^2/\nu$ (cf. eqn (2.16)) the flow has almost reached its steady state, as in Fig. 2.10(b), and the vorticity is almost distributed uniformly throughout the fluid.

2.4. Flow with circular streamlines

The Navier–Stokes equations are

$$\frac{\partial \boldsymbol{u}}{\partial t} + (\boldsymbol{u} \cdot \nabla)\boldsymbol{u} = -\frac{1}{\rho}\nabla p + \nu \nabla^2 \boldsymbol{u},$$

$$\nabla \cdot \boldsymbol{u} = 0,$$

and when written out in cylindrical polar coordinates they become

$$\begin{aligned}
\frac{\partial u_r}{\partial t} + (\boldsymbol{u} \cdot \nabla)u_r - \frac{u_\theta^2}{r} &= -\frac{1}{\rho}\frac{\partial p}{\partial r} + \nu\left(\nabla^2 u_r - \frac{u_r}{r^2} - \frac{2}{r^2}\frac{\partial u_\theta}{\partial \theta}\right)\\
\frac{\partial u_\theta}{\partial t} + (\boldsymbol{u} \cdot \nabla)u_\theta + \frac{u_r u_\theta}{r} &= -\frac{1}{\rho r}\frac{\partial p}{\partial \theta} + \nu\left(\nabla^2 u_\theta + \frac{2}{r^2}\frac{\partial u_r}{\partial \theta} - \frac{u_\theta}{r^2}\right)\\
\frac{\partial u_z}{\partial t} + (\boldsymbol{u} \cdot \nabla)u_z &= -\frac{1}{\rho}\frac{\partial p}{\partial z} + \nu \nabla^2 u_z,
\end{aligned} \tag{2.22}$$

$$\frac{1}{r}\frac{\partial}{\partial r}(r u_r) + \frac{1}{r}\frac{\partial u_\theta}{\partial \theta} + \frac{\partial u_z}{\partial z} = 0,$$

where

$$(\boldsymbol{u} \cdot \nabla) = u_r \frac{\partial}{\partial r} + \frac{u_\theta}{r}\frac{\partial}{\partial \theta} + u_z \frac{\partial}{\partial z},$$

$$\nabla^2 = \frac{1}{r}\frac{\partial}{\partial r}\left(r\frac{\partial}{\partial r}\right) + \frac{1}{r^2}\frac{\partial^2}{\partial \theta^2} + \frac{\partial^2}{\partial z^2},$$

(see eqn (A.35)).

Note the 'extra' terms that arise; the r-component of $(\boldsymbol{u} \cdot \nabla)\boldsymbol{u}$ is not $(\boldsymbol{u} \cdot \nabla)u_r$, for instance, but $(\boldsymbol{u} \cdot \nabla)u_r - u_\theta^2/r$ instead. This kind of thing occurs because $\boldsymbol{u} = u_r\boldsymbol{e}_r + u_\theta\boldsymbol{e}_\theta + u_z\boldsymbol{e}_z$, and *some of the unit vectors involved change with* θ:

$$\frac{\partial \boldsymbol{e}_r}{\partial \theta} = \boldsymbol{e}_\theta, \qquad \frac{\partial \boldsymbol{e}_\theta}{\partial \theta} = -\boldsymbol{e}_r, \qquad \frac{\partial \boldsymbol{e}_z}{\partial \theta} = 0, \tag{2.23}$$

(see eqn (A.29)). When $(\boldsymbol{u} \cdot \nabla)\boldsymbol{u}$ and $\nu \nabla^2 \boldsymbol{u}$ are expanded carefully using these expressions they may be seen to yield eqn (2.22).

Taking explicit account of the change in direction of unit vectors may alternatively be avoided by use of the identities

$$(\boldsymbol{u} \cdot \nabla)\boldsymbol{u} = (\nabla \wedge \boldsymbol{u}) \wedge \boldsymbol{u} + \nabla(\tfrac{1}{2}\boldsymbol{u}^2), \tag{2.24}$$

$$\nabla^2 \boldsymbol{u} = \nabla(\nabla \cdot \boldsymbol{u}) - \nabla \wedge (\nabla \wedge \boldsymbol{u}). \tag{2.25}$$

For this purpose we recall

$$\nabla \wedge \boldsymbol{u} = \frac{1}{r}\begin{vmatrix} \boldsymbol{e}_r & r\boldsymbol{e}_\theta & \boldsymbol{e}_z \\ \dfrac{\partial}{\partial r} & \dfrac{\partial}{\partial \theta} & \dfrac{\partial}{\partial z} \\ u_r & ru_\theta & u_z \end{vmatrix} \tag{2.26}$$

(see Exercise 2.13).

The differential equation for circular flow

Consider solutions to the Navier–Stokes equations of the form

$$\boldsymbol{u} = u_\theta(r, t)\boldsymbol{e}_\theta, \tag{2.27}$$

so that the streamlines are circular. The incompressibility condition $\nabla \cdot \boldsymbol{u} = 0$ is automatically satisfied for any flow of the form (2.27).

Rather than use the remaining equations in the ready-made form (2.22) it is instructive to derive them, for the flow (2.27), using the expressions (2.23). Thus

$$(\boldsymbol{u} \cdot \nabla)\boldsymbol{u} = \frac{u_\theta}{r}\frac{\partial}{\partial \theta}[u_\theta(r, t)\boldsymbol{e}_\theta] = \frac{u_\theta^2}{r}\frac{\partial \boldsymbol{e}_\theta}{\partial \theta} = -\frac{u_\theta^2}{r}\boldsymbol{e}_r, \tag{2.28}$$

while

$$\nu\,\nabla^2\boldsymbol{u} = \nu\left(\frac{\partial^2}{\partial r^2} + \frac{1}{r}\frac{\partial}{\partial r} + \frac{1}{r^2}\frac{\partial^2}{\partial \theta^2} + \frac{\partial^2}{\partial z^2}\right)[u_\theta(r, t)\boldsymbol{e}_\theta],$$

and

$$\frac{1}{r^2}\frac{\partial^2}{\partial \theta^2}[u_\theta \boldsymbol{e}_\theta] = \frac{1}{r^2}\frac{\partial}{\partial \theta}\left(u_\theta\frac{\partial \boldsymbol{e}_\theta}{\partial \theta}\right) = \frac{-1}{r^2}\frac{\partial}{\partial \theta}(u_\theta \boldsymbol{e}_r) = -\frac{u_\theta}{r^2}\boldsymbol{e}_\theta,$$

so

$$\nu\,\nabla^2\boldsymbol{u} = \nu\left(\frac{\partial^2 u_\theta}{\partial r^2} + \frac{1}{r}\frac{\partial u_\theta}{\partial r} - \frac{u_\theta}{r^2}\right)\boldsymbol{e}_\theta. \tag{2.29}$$

When $\boldsymbol{u} = u_\theta(r, t)\boldsymbol{e}_\theta$ the Navier–Stokes equations therefore reduce to

$$-\frac{u_\theta^2}{r} = -\frac{1}{\rho}\frac{\partial p}{\partial r},$$

$$\frac{\partial u_\theta}{\partial t} = -\frac{1}{\rho r}\frac{\partial p}{\partial \theta} + \nu\left(\frac{\partial^2 u_\theta}{\partial r^2} + \frac{1}{r}\frac{\partial u_\theta}{\partial r} - \frac{u_\theta}{r^2}\right),$$

$$0 = -\frac{1}{\rho}\frac{\partial p}{\partial z},$$

as we might have deduced more quickly from eqn (2.22).

Now, u_θ is a function of r and t only, so from the second equation the same must be true of $\partial p/\partial\theta$, so $\partial p/\partial\theta = P(r, t)$, say. Integrating:

$$p = P(r, t)\theta + f(r, t),$$

as $\partial p/\partial z = 0$. We conclude that $P(r, t) = 0$, for otherwise p would be a multivalued function of position (different at $\theta = 0$ and at $\theta = 2\pi$, say). Thus

$$\frac{\partial u_\theta}{\partial t} = \nu\left(\frac{\partial^2 u_\theta}{\partial r^2} + \frac{1}{r}\frac{\partial u_\theta}{\partial r} - \frac{u_\theta}{r^2}\right) \tag{2.30}$$

is the evolution equation for a viscous flow with $\boldsymbol{u} = u_\theta(r, t)\boldsymbol{e}_\theta$.

Steady flow between rotating cylinders

For steady flow we have

$$r^2\frac{\mathrm{d}^2 u_\theta}{\mathrm{d}r^2} + r\frac{\mathrm{d}u_\theta}{\mathrm{d}r} - u_\theta = 0,$$

with general solution

$$u_\theta = Ar + \frac{B}{r}. \tag{2.31}$$

If the fluid occupies the gap $r_1 \leqslant r \leqslant r_2$ between two circular cylinders which rotate with angular velocities Ω_1 and Ω_2, then we may apply the no-slip condition at each cylinder to obtain

$$A = \frac{\Omega_2 r_2^2 - \Omega_1 r_1^2}{r_2^2 - r_1^2}, \qquad B = \frac{(\Omega_1 - \Omega_2)r_1^2 r_2^2}{r_2^2 - r_1^2}. \tag{2.32}$$

The most interesting thing about this flow is the manner in which it becomes unstable if Ω_1 is too large, so that superbly regular and axisymmetric *Taylor vortices* appear (see §9.4, especially Fig. 9.8).

Spin-down in an infinitely long circular cylinder

Suppose viscous fluid occupies the region $r \leqslant a$ within a circular cylinder of radius a, and suppose that both cylinder and fluid are initially rotating with uniform angular velocity Ω, so that

$$u_\theta = \Omega r, \qquad r \leqslant a, \qquad t = 0.$$

Suppose that the cylinder is then suddenly brought to rest. We need to solve

$$\frac{\partial u_\theta}{\partial t} = \nu\left(\frac{\partial^2 u_\theta}{\partial r^2} + \frac{1}{r}\frac{\partial u_\theta}{\partial r} - \frac{u_\theta}{r^2}\right)$$

with the above initial condition and the boundary condition

$$u_\theta = 0 \qquad \text{at } r = a, \quad t > 0.$$

The problem may be tackled in a Fourier-series type manner, as for eqn (2.21), but the separable solutions now involve Bessel functions, and

$$u_\theta(r, t) = -2\Omega a \sum_{n=1}^{\infty} \frac{\mathrm{J}_1(\lambda_n r/a)}{\lambda_n \mathrm{J}_0(\lambda_n)} \exp\left(-\lambda_n^2 \frac{\nu t}{a^2}\right). \qquad (2.33)$$

Here λ_n denote the positive values of λ at which $\mathrm{J}_1(\lambda) = 0$, and J_k denotes the Bessel function of order k. All the terms of the series decay rapidly with t; the one that survives longest is the first one, and $\lambda_1 \doteqdot 3.83$. The 'spin-down' process is therefore well under way in a time of order $a^2/\nu\lambda_1^2$, i.e. in the classic viscous diffusion time (2.16).

If we apply this to a stirred cup of tea, with $a = 4\,\mathrm{cm}$ and $\nu = 10^{-2}\,\mathrm{cm^2\,s^{-1}}$ for water, we obtain a 'spin-down' time of about 2 minutes. This is much too long; casual observation suggests that u_θ drops to about $1/\mathrm{e}$ of its original value in about 15 s. The discrepancy arises because straightforward diffusion of (negative) vorticity from the side walls is not the key process by which a stirred cup of tea comes to rest; the bottom of the cup—wholly absent in the present model—plays a crucial role (see Fig. 5.6.)

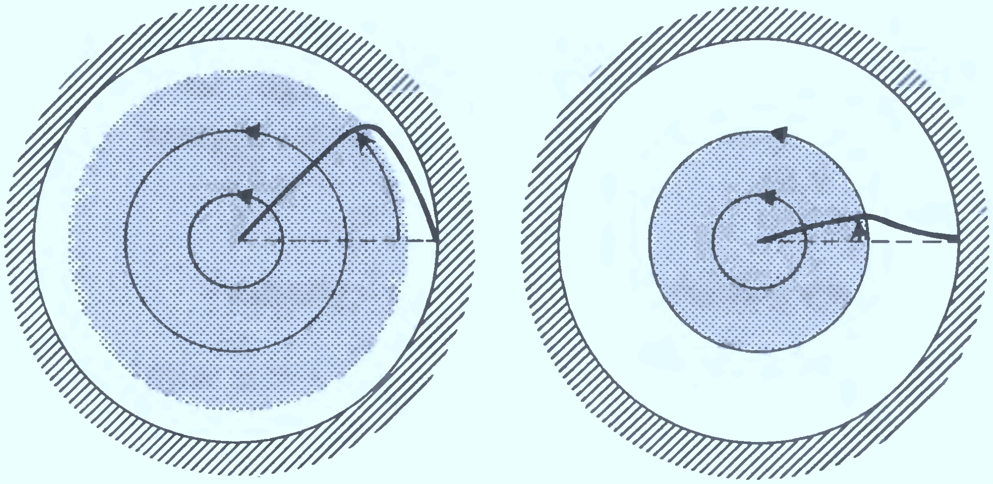

(*a*) (*b*)

Fig. 2.11. 'Spin-down' in an infinitely long circular cylinder. Initially there is vorticity 2Ω everywhere, but negative vorticity diffuses inward from the stationary boundary $r = a$, so that the (shaded) region of significant vorticity shrinks with time.

Viscous decay of a line vortex

The line vortex

$$\boldsymbol{u} = \frac{\Gamma_0}{2\pi r}\boldsymbol{e}_\theta, \tag{2.34}$$

where Γ_0 is a constant, has zero vorticity in $r > 0$ but infinite vorticity at $r = 0$. In a viscous fluid, then, this flow does not persist; the vorticity diffuses outward as time goes on.

To examine this process it is convenient to take the circulation

$$\Gamma(r, t) = 2\pi r u_\theta(r, t) \tag{2.35}$$

as the dependent variable of the problem. In place of eqn (2.30) we then obtain

$$\frac{\partial \Gamma}{\partial t} = \nu\left(\frac{\partial^2 \Gamma}{\partial r^2} - \frac{1}{r}\frac{\partial \Gamma}{\partial r}\right). \tag{2.36}$$

The initial condition is

$$\Gamma(r, 0) = \Gamma_0.$$

We require u_θ finite at $r = 0$ at any later time, so

$$\Gamma(0, t) = 0, \qquad t > 0.$$

This problem is very similar to that in which a plane rigid boundary is jerked into motion (see eqn (2.14)); we leave it as an exercise to seek, as in that case, a similarity solution in which

$$\Gamma = f(\eta), \qquad \text{where } \eta = r/(\nu t)^{\frac{1}{2}}.$$

In this way we may discover that

$$\Gamma = \Gamma_0(1 - \mathrm{e}^{-r^2/4\nu t}),$$

so

$$u_\theta = \frac{\Gamma_0}{2\pi r}(1 - \mathrm{e}^{-r^2/4\nu t}). \tag{2.37}$$

At distances greater than about $(4\nu t)^{\frac{1}{2}}$ from the axis the circulation is almost unaltered, because very little vorticity has yet diffused that far out. At small distances from the axis, however, where $r \ll (4\nu t)^{\frac{1}{2}}$, the flow is no longer remotely irrotational; indeed

$$u_\theta \doteqdot \frac{\Gamma_0}{8\pi\nu t} r \qquad \text{for} \qquad r \ll (4\nu t)^{\frac{1}{2}}, \tag{2.38}$$

which corresponds to almost uniform rotation with angular velocity $\Gamma_0/8\pi\nu t$. The intensity of the vortex thus decreases with time as the 'core' spreads radially outward (Fig. 2.12).

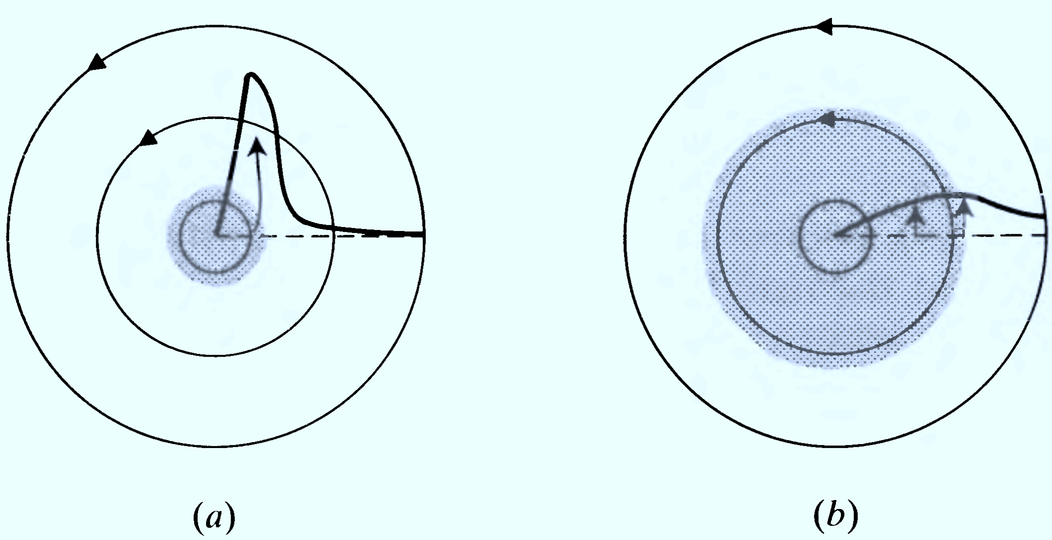

(*a*) (*b*)

Fig. 2.12. The viscous diffusion of a vortex.

2.5. The convection and diffusion of vorticity

If we take the curl of the momentum equation (2.3) we obtain

$$\frac{\partial \boldsymbol{\omega}}{\partial t} + (\boldsymbol{u} \cdot \nabla)\boldsymbol{\omega} = (\boldsymbol{\omega} \cdot \nabla)\boldsymbol{u} + \nu \nabla^2 \boldsymbol{\omega}, \tag{2.39}$$

(cf. eqn (1.25)), and in the case of a 2-D flow this reduces to

$$\frac{\partial \omega}{\partial t} + (\boldsymbol{u} \cdot \nabla)\omega = \nu\left(\frac{\partial^2 \omega}{\partial x^2} + \frac{\partial^2 \omega}{\partial y^2}\right). \tag{2.40}$$

In Chapter 1 we set the viscosity ν to zero from the outset; ω was then conserved by individual fluid elements in 2-D flow. Changes in ω at a particular point in space took place only by the *convection* of vorticity from elsewhere in the fluid, and this process is represented by the second term in eqn (2.40). In §§2.3 and 2.4, on the other hand, we looked at some simple viscous flow problems in which the term $(\boldsymbol{u} \cdot \nabla)\omega$ happened to be identically zero; in other words, we isolated *diffusion* of vorticity as a mechanism, this being represented by the third term in eqn (2.40).

In general, there is both diffusion and convection of vorticity in a viscous fluid flow, and we end this chapter with two examples.

2-D flow near a stagnation point

The main features of this exact solution of the Navier–Stokes equations (Exercise 2.14) are as follows. First, there is an inviscid 'mainstream' flow

$$u = \alpha x, \qquad v = -\alpha y, \tag{2.41}$$

where α is a positive constant. This fails to satisfy the no-slip condition at the rigid boundary $y = 0$, but the mainstream flow speed $\alpha\,|x|$ increases with distance $|x|$ along the boundary. By Bernoulli's theorem, the mainstream pressure p *decreases* with distance along the boundary in the flow direction (Fig. 2.13), so we may hope for a thin, unseparated boundary layer which adjusts the velocity to satisfy the no-slip condition (see §2.1). This is indeed the case, as Exercise 2.14 shows, and the boundary layer, in which all the vorticity is concentrated, has thickness

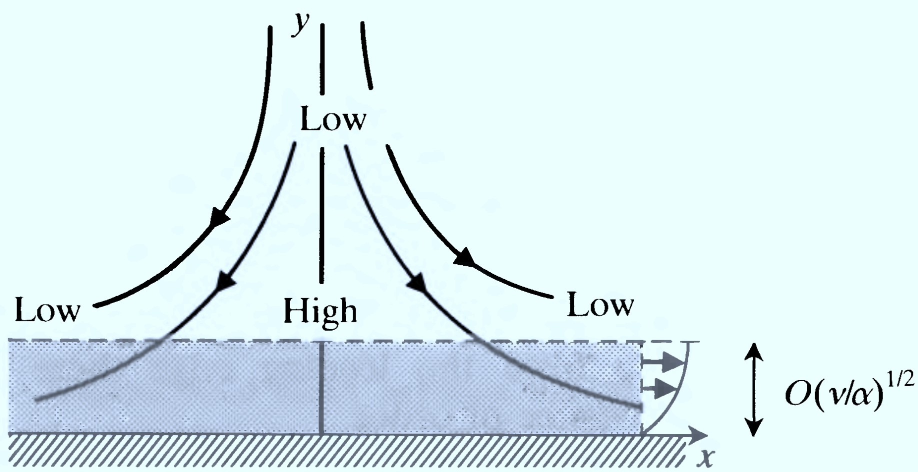

Fig. 2.13. Flow towards a 2-D stagnation point.

$\delta = O(\nu/\alpha)^{\frac{1}{2}}$. In this boundary layer there is a steady state balance between the viscous diffusion of vorticity from the wall and the convection of vorticity towards the wall by the flow. Thus if ν decreases the diffusive effect is weakened, while if α increases the convective effect is enhanced; in either case the boundary layer becomes thinner.

High Reynolds number flow past a flat plate

In uniform flow past a flat plate with a leading edge, as in Fig. 2.14, there is no flow component convecting vorticity towards the plate to counter the diffusion of vorticity from it, so the boundary layer becomes progressively thicker with downstream distance x. (In less formal terms, the layers of fluid closest to the centreline are the first to be slowed down as they pass the leading edge, and they in turn gradually slow down the layers of fluid which are further away.)

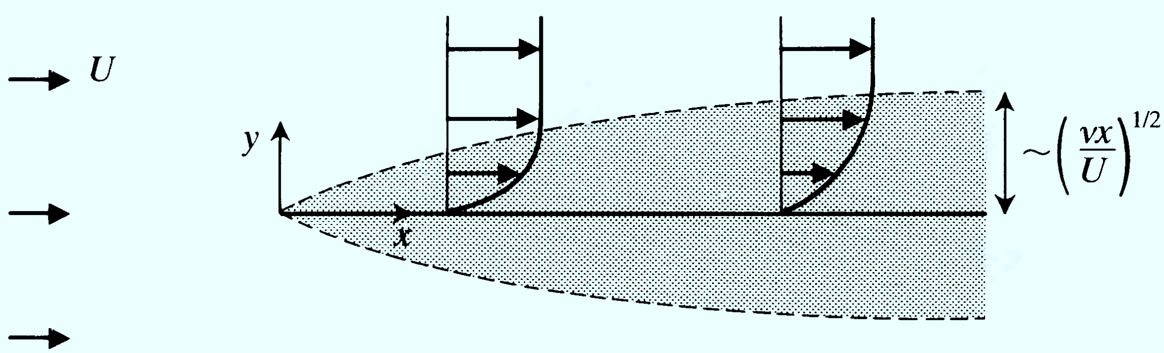

Fig. 2.14. The boundary layer on a flat plate.

We may estimate the boundary layer thickness δ by a simple argument based on the related problem in which the flat plate is instead suddenly pulled to the left, with speed U, through fluid which was previously at rest. From Fig. 2.8 we infer that at time t after the plate is moved vorticity will have diffused out a distance of order $(\nu t)^{\frac{1}{2}}$. But by this time the leading edge of the plate will have moved a distance $x = Ut$ to the left. It follows that at distance x downstream from the leading edge there will be significant vorticity a distance of order

$$\delta \sim (\nu x/U)^{\frac{1}{2}} \tag{2.42}$$

from the plate, but not beyond.

This crude estimate for the growth of the boundary layer with downstream distance x in Fig. 2.14 is indeed confirmed by the appropriate solution of the boundary layer equations (see §8.3). For a plate of finite length L the thickness (2.42) is in keeping with the claim (2.7) and is small compared with L at all points of the plate if $R = UL/\nu \gg 1$.

Exercises

2.1. Give an order of magnitude estimate of the Reynolds number for:

(i) flow past the wing of a jumbo jet at $150\,\mathrm{m\,s^{-1}}$ (roughly half the speed of sound);

(ii) the experiment in §1.1 with, say, $L = 2\,\mathrm{cm}$ and $U = 5\,\mathrm{cm\,s^{-1}}$;

(iii) a thick layer of golden syrup draining off a spoon;

(iv) a spermatozoan with tail length of $10^{-3}\,\mathrm{cm}$ swimming at $10^{-2}\,\mathrm{cm\,s^{-1}}$ in water.

Give an order of magnitude estimate of the thickness of the boundary layer in case (i).

2.2. The problem of 2-D steady viscous flow past a circular cylinder of radius a involves finding a velocity field $\boldsymbol{u} = [u(x, y), v(x, y), 0]$ which satisfies

$$(\boldsymbol{u} \cdot \nabla)\boldsymbol{u} = -\frac{1}{\rho}\nabla p + \nu\,\nabla^2\boldsymbol{u}, \qquad \nabla \cdot \boldsymbol{u} = 0,$$

together with the boundary conditions

$$\boldsymbol{u} = 0 \quad \text{on } x^2 + y^2 = a^2; \qquad \boldsymbol{u} \to (U, 0, 0) \quad \text{as } x^2 + y^2 \to \infty.$$

Rewrite this problem in *dimensionless form* by using the dimensionless variables

$$\mathbf{x}' = \mathbf{x}/a, \qquad \mathbf{u}' = \mathbf{u}/U, \qquad p' = p/\rho U^2$$

in places of $\mathbf{x}$, $\mathbf{u}$, and p. Without attempting to solve the problem, show that the streamline pattern can depend on ν, a, and U only in the combination $R = Ua/\nu$, so that flows at equal Reynolds numbers are geometrically similar.

2.3. (i) Viscous fluid flows between two stationary rigid boundaries $y = \pm h$ under a constant pressure gradient $P = -\mathrm{d}p/\mathrm{d}x$. Show that

$$u = \frac{P}{2\mu}(h^2 - y^2), \qquad v = w = 0.$$

(ii) Viscous fluid flows down a pipe of circular cross-section $r = a$ under a constant pressure gradient $P = -\mathrm{d}p/\mathrm{d}z$. Show that

$$u_z = \frac{P}{4\mu}(a^2 - r^2), \qquad u_r = u_\theta = 0.$$

[These are called *Poiseuille flows* (Fig. 2.15), after the physician who first studied (ii) in connection with blood flow. Their instability at high Reynolds number constitutes one of the most important problems of fluid dynamics (see §9.1).]

2.4. Two incompressible viscous fluids of the same density ρ flow, one on top of the other, down an inclined plane making an angle α with the horizontal. Their viscosities are μ_1 and μ_2, the lower fluid is of depth h_1 and the upper fluid is of depth h_2. Show that

$$u_1(y) = [(h_1 + h_2)y - \tfrac{1}{2}y^2]\frac{g \sin \alpha}{\nu_1},$$

so that the velocity of the lower fluid $u_1(y)$ is dependent on the depth h_2, but not the viscosity, of the upper fluid. Why is this?

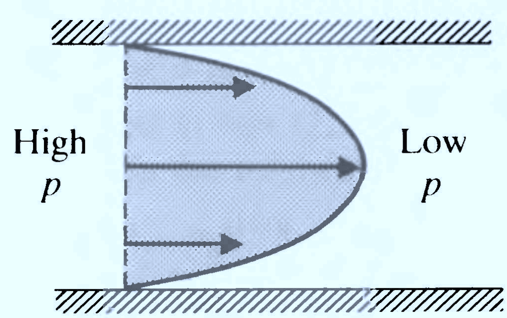

Fig. 2.15. Poiseuille flow.

2.5. Viscous fluid is at rest in a two-dimensional channel between two stationary rigid walls $y = \pm h$. For $t \geqslant 0$ a constant pressure gradient $P = -\mathrm{d}p/\mathrm{d}x$ is imposed. Show that $u(y, t)$ satisfies

$$\frac{\partial u}{\partial t} = \nu \frac{\partial^2 u}{\partial y^2} + \frac{P}{\rho},$$

and give suitable initial and boundary conditions. Find $u(y, t)$ in the form of a Fourier series, and show that the flow approximates to steady channel flow when $t \gg h^2/\nu$.

2.6. Viscous fluid flows between two rigid boundaries $y = 0$, $y = h$, the lower boundary moving in the x-direction with constant speed U, the upper boundary being at rest. The boundaries are porous, and the vertical velocity v is $-v_0$ at each one, v_0 being a given constant (so that there is an imposed flow across the system). Show that the resulting flow is

$$u = U\left(\frac{\mathrm{e}^{-v_0 y/\nu} - \mathrm{e}^{-v_0 h/\nu}}{1 - \mathrm{e}^{-v_0 h/\nu}}\right), \qquad v = -v_0.$$

Show that the horizontal velocity profile $u(y)$ is as in Fig. 2.16, so that when $v_0 h/\nu$ is large the downflow v_0 confines the vorticity to a very thin layer adjacent to $y = 0$.

[This is probably the mathematically simplest example of a steady boundary layer, but it is untypical in that the boundary layer thickness is proportional to ν, rather than to $\nu^{\frac{1}{2}}$ (see eqn (2.7)).]

2.7. Incompressible fluid occupies the space $0 < y < \infty$ above a plane rigid boundary $y = 0$ which oscillates to and fro in the x-direction with velocity $U \cos \omega t$. Show that the velocity field $\boldsymbol{u} = [u(y, t), 0, 0]$ satisfies

$$\frac{\partial u}{\partial t} = \nu \frac{\partial^2 u}{\partial y^2}$$

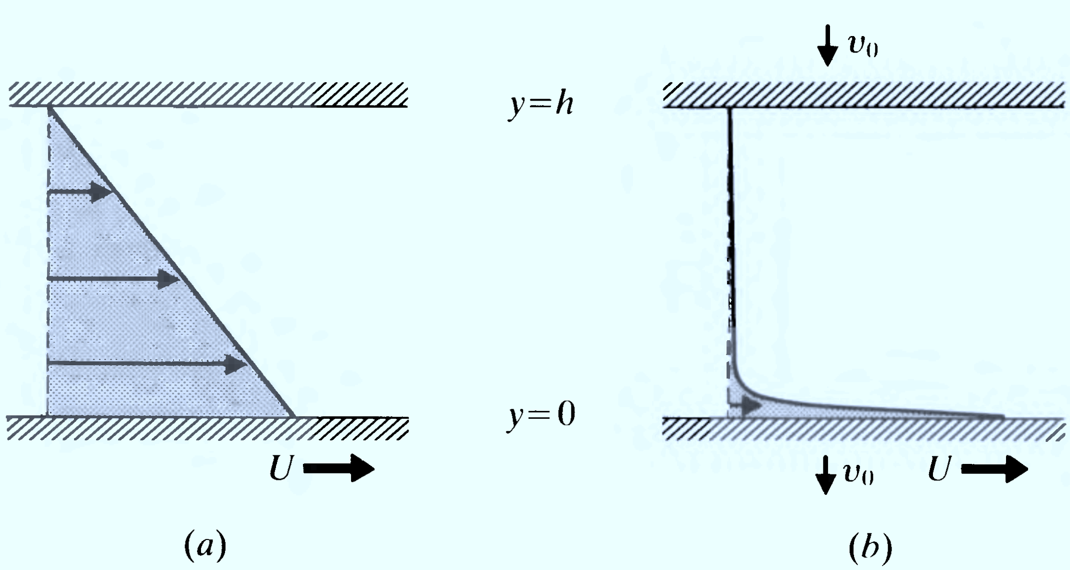

Fig. 2.16. Wall-driven channel flow with (a) $v_0 = 0$ and (b) $v_0 h/\nu \gg 1$.

(there being no applied pressure gradient), and by seeking a solution of the form

$$u = \mathscr{R}[f(y)e^{i\omega t}],$$

where $\mathscr{R}$ denotes 'real part of', show that

$$u(y, t) = Ue^{-ky}\cos(ky - \omega t),$$

where $k = (\omega/2\nu)^{\frac{1}{2}}$.

Sketch the velocity profile at some time t, and note that there is hardly any motion beyond a distance of order $(\nu/\omega)^{\frac{1}{2}}$ from the boundary.

2.8. A circular cylinder of radius a rotates with constant angular velocity Ω in a viscous fluid. Show that the line vortex flow

$$\mathbf{u} = \frac{\Omega a^2}{r}\mathbf{e}_\theta, \qquad r \geqslant a,$$

is an exact solution of the equations and boundary conditions. Describe roughly how the vorticity changes with time when the cylinder is suddenly started into rotation with angular velocity Ω from a state of rest. Likewise, discuss the case in which an outer cylinder $r = b$ is simultaneously given an angular velocity $\Omega a^2/b^2$.

2.9. A viscous flow is generated in $r \geqslant a$ by a circular cylinder $r = a$ which rotates with constant angular velocity Ω. There is also a radial inflow which results from a uniform suction on the (porous) cylinder, so that $u_r = -U$ on $r = a$. Show that

$$u_r = -Ua/r \qquad \text{for } r \geqslant a,$$

and that

$$r^2\frac{d^2u_\theta}{dr^2} + (R+1)r\frac{du_\theta}{dr} + (R-1)u_\theta = 0,$$

where $R = Ua/\nu$.

Show that if $R < 2$ there is just one solution of this equation which satisfies the no-slip condition on $r = a$ and has finite circulation $\Gamma = 2\pi r u_\theta$ at infinity, but that if $R > 2$ there are many such solutions.

2.10. Show that, as claimed in eqn (2.37), a line vortex of strength Γ_0 decays by viscous diffusion in the following manner:

$$u_\theta = \frac{\Gamma_0}{2\pi r}(1 - e^{-r^2/4\nu t}).$$

Calculate and sketch the vorticity as a function of r at two different times.

2.11. Viscous fluid occupies the region $0<z<h$ between two rigid boundaries $z=0$ and $z=h$. The lower boundary is at rest, the upper boundary rotates with constant angular velocity Ω about the z-axis. Show that a steady solution of the full Navier–Stokes equations of the form

$$\boldsymbol{u} = u_\theta(r, z)\boldsymbol{e}_\theta$$

is not possible, so that any rotary motion $u_\theta(r, z)$ in this system must be accompanied by a *secondary flow* $(u_r, u_z \neq 0)$.

2.12. Viscous fluid is inside an infinitely long circular cylinder $r=a$ which is rotating with angular velocity Ω, so that $u_\theta = \Omega r$ for $r \leqslant a$. The cylinder is suddenly brought to rest at $t=0$. Rewrite the evolution equation (2.30) in the form

$$\frac{\partial u_\theta}{\partial t} = \frac{\nu}{r}\frac{\partial}{\partial r}\left(r\frac{\partial u_\theta}{\partial r}\right) - \frac{\nu u_\theta}{r^2},$$

and thereby show that

$$\frac{\mathrm{d}E}{\mathrm{d}t} + \frac{2\nu}{a^2}E \leqslant 0,$$

where

$$E = \tfrac{1}{2}\int_0^a r u_\theta^2 \,\mathrm{d}r,$$

which is proportional to the kinetic energy of the flow. Hence show that $E \to 0$ as $t \to \infty$.

[This may seem a little pointless, given that the exact solution (2.33) is available, but the above approach is in fact of very general value, and provides the basis for the proof, in §9.7, of an important uniqueness theorem.]

2.13. Re-derive the results (2.28) and (2.29) by the alternative route involving eqns (2.24), (2.25), and (2.26).

2.14. Consider in $y \geqslant 0$ the 2-D flow

$$u = \alpha x f'(\eta), \qquad v = -(\nu\alpha)^{\frac{1}{2}} f(\eta),$$

where

$$\eta = (\alpha/\nu)^{\frac{1}{2}} y.$$

Show that it is an exact solution of the Navier–Stokes equations which (i) satisfies the boundary conditions at the stationary rigid boundary $y=0$ and (ii) takes the asymptotic form $u \sim \alpha x$, $v \sim -\alpha y$ far from the

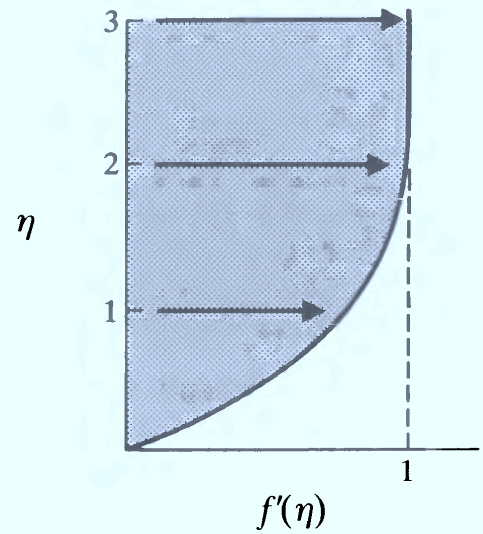

Fig. 2.17. The velocity profile in the boundary layer near a 2-D stagnation point.

boundary (see Fig. 2.13) if

$$f''' + ff'' + 1 - f'^2 = 0,$$

with

$$f(0) = f'(0) = 0, \qquad f'(\infty) = 1.$$

[The differential equation for $f(\eta)$ is solved numerically, and $f'(\eta)$ is shown in Fig. 2.17. Notably, $f'(3) = 0.998$, so beyond a distance of $3(\nu/\alpha)^{\frac{1}{2}}$ from the boundary the flow is effectively inviscid and irrotational, with $u \doteq \alpha x$ and $v \doteq -\alpha y$.]

2.15. If a flat plate is fixed between $(0, 0)$ and $(0, L)$ in Fig. 2.13, with $L \gg (\nu/\alpha)^{\frac{1}{2}}$, one might at first think that the flow would not be much affected, for the plate lies along one of the streamlines of the original flow. Why is it, then, that the observed flow is quite different, as in Fig. 2.18?

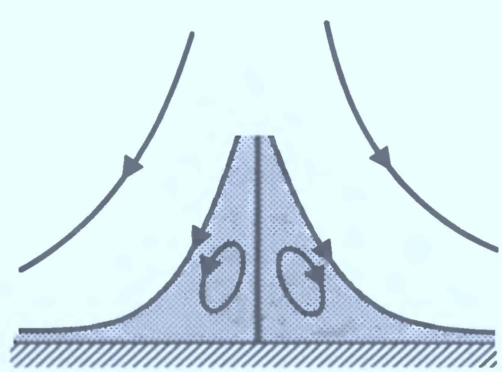

Fig. 2.18. High Reynolds number stagnation-point flow with a protruding flat plate.

4 Classical aerofoil theory

4.1. Introduction

Let us begin by noting some of the key events in the early days of aerodynamics.

1894 F. W. Lanchester presents a paper, 'The soaring of birds and the possibilities of mechanical flight', to a meeting of the Birmingham Natural History and Philosophical Society. It contains the elements of the circulation theory of lift, but not in conventional terms.

1897 Lanchester submits a written version of his paper for publication by the Physical Society. It is rejected.

1901 The Wright brothers encounter failure with their first attempts at glider design. One of them is heard to mutter that 'nobody will fly for a thousand years'.

1902 Kutta publishes a short paper, 'Lifting forces in flowing fluids'. It contains the solution for 2-D irrotational flow past a circular arc, with circulation round the surface and a finite velocity at the trailing edge (Exercise 4.8). The connection between circulation and lift is recognized, though not in the form of the general theorem (1.35).

1903 17 December: The Wright brothers achieve their first powered flight. It lasts for 12 seconds, although they improve on this later the same day.

1904 Prandtl presents his paper on boundary layers to the Third International Congress of Mathematicians at Heidelberg (see §8.1).

1906 Joukowski publishes the lift theorem (1.35):

> If an irrotational two-dimensional fluid current, having at infinity the velocity V_∞, surrounds any closed contour on which the circulation of velocity is Γ, the force of the aerodynamic pressure acts on this contour in a direction perpendicular to the velocity and has the value
>
> $$L' = \rho_\infty V_\infty \Gamma.$$

The direction of this force is found by causing to rotate through a right angle the vector V_∞ around its origin, in an inverse direction to that of the circulation.

1907 Lanchester publishes his *Aerodynamics*, although some of the most important results in the book date from as early as 1892. He was certainly years ahead of everyone else in recognizing the inevitability, and the importance, of trailing vortices from the tip of a wing of finite length (§1.7).

A list like this is a concise way of presenting some of the facts, but it can be misleading, for the events within it were, at the time, almost wholly unconnected. Thus Lanchester, Kutta, and Joukowski came to their various conclusions about aerodynamics quite independently, and Wilbur Wright, had he known, would probably not have had much time for any of them. He and his brother relied greatly on their own experimental work on wind-tunnel flows past aerofoils of various shapes, but as late as 1909 he wrote to Lanchester:

...I note such differences of information, theory, and even ideals, as to make it quite out of the question to reach common ground..., so I think it will save me much time if I follow my usual plan and let the truth make itself apparent in actual practice.

Our first aim in this chapter is to establish that for uniform irrotational flow past an aerofoil with a sharp trailing edge there is just one value of the circulation Γ for which the velocity is finite everywhere (Kutta–Joukowski condition). In particular, we seek to show that in the case of a thin symmetrical aerofoil of length L making an angle of attack α with the oncoming stream the value Γ is given by

$$\Gamma = -\pi UL \sin \alpha. \tag{4.1}$$

We set about doing this by first solving the comparatively easy problem of irrotational flow past a circular cylinder, and then using the method of conformal mapping to infer the irrotational flow past 2-D objects of more wing-like cross-section.

We must add one important warning before we start. The present chapter is full of irrotational flows which involve slip at rigid boundaries. While any particular flow may well serve a quite different purpose, *it will represent correctly the motion of a viscous fluid at high Reynolds number only if the slip velocity can* *be adjusted to zero successfully, by a viscous boundary layer, without separation.* Rough guidelines on whether or not separation will occur have already been presented in §2.1.

4.2. Velocity potential and stream function

The velocity potential

The velocity potential ϕ is something that exists *only if* $\nabla \wedge \boldsymbol{u} = 0$; it is defined at any point P by

$$\phi = \int_{\mathrm{O}}^{\mathrm{P}} \boldsymbol{u} \cdot \mathrm{d}\boldsymbol{x} \tag{4.2}$$

where O is some arbitrary fixed point. In a simply connected fluid region ϕ is independent of the path between O and P, and thus a single-valued function of position (Exercise 4.1.) Partial differentiation of eqn (4.2) gives

$$\boldsymbol{u} = \nabla\phi, \tag{4.3}$$

and the vector identity (A.2) at once confirms that this flow is irrotational, as desired.

This representation of an irrotational flow, eqn (4.3), is valid also in multiply connected fluid regions, but the integral in eqn (4.2) may then depend on the path from O to P, in which case ϕ will be a multivalued function of position. In this case, it is worth noting at once that the circulation round any closed curve C in the flow is given by

$$\Gamma = \oint_C \boldsymbol{u} \cdot \mathrm{d}\boldsymbol{x} = \oint_C \nabla\phi \cdot \mathrm{d}\boldsymbol{x} = [\phi]_C, \tag{4.4}$$

where the last expression denotes the change (if any) in ϕ after one circuit round C (see eqn (A.12)).

Let us take some examples. The uniform flow $\boldsymbol{u} = (U, 0, 0)$ has velocity potential $\phi = Ux$ (plus an insignificant arbitrary constant, which has no effect on the flow (4.3)). The stagnation point flow of Exercise 1.7:

$$u = \alpha x, \qquad v = -\alpha y, \qquad w = 0$$

is irrotational, and writing

$$\partial\phi/\partial x = \alpha x, \qquad \partial\phi/\partial y = -\alpha y, \qquad \partial\phi/\partial z = 0$$

we may integrate to obtain

$$\phi = \tfrac{1}{2}\alpha(x^2 - y^2).$$

In both these cases ϕ is a single-valued function of position; there is therefore no circulation round any closed circuit lying in the flow domain.

Now take the line vortex flow (1.21):

$$\boldsymbol{u} = \frac{k}{r}\boldsymbol{e}_\theta,$$

which is an irrotational flow *except at the origin,* where it is not defined. To meet this difficulty, consider the flow domain to be $r \geqslant a$, which is not simply connected, for there are now some closed curves (i.e. those which enclose $r = a$) which cannot be shrunk to a point without leaving the flow domain. To find the velocity potential we integrate

$$\frac{\partial \phi}{\partial r} = 0, \qquad \frac{1}{r}\frac{\partial \phi}{\partial \theta} = \frac{k}{r}, \qquad \frac{\partial \phi}{\partial z} = 0,$$

and thus obtain

$$\phi = k\theta,$$

which is a multivalued function of position. As we go round any circuit not enclosing $r = a$ it is clear that θ, and hence ϕ, will return, at the end of that circuit, to its original value. There is therefore no circulation round such a circuit. But as we go round any closed curve which winds once round the cylinder $r = a$, θ increases by 2π, and the circulation round such a circuit will therefore be $\Gamma = 2\pi k$. Thus all circuits which wind once round the cylinder have the same circulation (cf. Exercise 1.6).

The stream function

This is a useful device for representing flows which are *incompressible and two-dimensional.* The essential idea is to write

$$u = \frac{\partial \psi}{\partial y}, \qquad v = -\frac{\partial \psi}{\partial x}, \tag{4.5}$$

thus automatically satisfying the 2-D incompressibility condition

$$\frac{\partial u}{\partial x} + \frac{\partial v}{\partial y} = 0. \tag{4.6}$$

That such a function $\psi(x, y, t)$ may be found can be shown by a similar argument to that used above (Exercise 4.1).

An important property of ψ follows immediately from eqn (4.5), for

$$(\boldsymbol{u} \cdot \nabla)\psi = u\frac{\partial \psi}{\partial x} + v\frac{\partial \psi}{\partial y} = \frac{\partial \psi}{\partial y}\frac{\partial \psi}{\partial x} - \frac{\partial \psi}{\partial x}\frac{\partial \psi}{\partial y} = 0, \quad (4.7)$$

so ψ *is constant along a streamline*. This gives an effective way of finding the streamlines for a 2-D incompressible flow; if we can just find $\psi(x, y, t)$ the equations for the streamlines can be written down immediately.

A useful way of viewing the representation (4.5) is as

$$\boldsymbol{u} = \nabla \wedge (\psi \boldsymbol{k}), \quad (4.8)$$

where $\boldsymbol{k}$ is the unit vector in the z-direction. It provides, in particular, a way of obtaining the plane polar counterparts to eqn (4.5). Regarding ψ instead as a function of r, θ, and t, we obtain at once

$$u_r = \frac{1}{r}\frac{\partial \psi}{\partial \theta}, \qquad u_\theta = -\frac{\partial \psi}{\partial r}, \quad (4.9)$$

and such a flow automatically satisfies the 2-D incompressibility condition in plane polar coordinates:

$$\frac{1}{r}\frac{\partial}{\partial r}(ru_r) + \frac{1}{r}\frac{\partial u_\theta}{\partial \theta} = 0 \quad (4.10)$$

(see eqn (A.35)).

4.3. The complex potential

Suppose now that we have a flow which is (i) two-dimensional, (ii) incompressible, and (iii) irrotational. Then the velocity field can be represented by both eqns (4.3) and (4.5), so that

$$u = \frac{\partial \phi}{\partial x} = \frac{\partial \psi}{\partial y}, \qquad v = \frac{\partial \phi}{\partial y} = -\frac{\partial \psi}{\partial x}. \quad (4.11)$$

The second of the equations in each pair constitute the well known Cauchy–Riemann equations of complex variable theory, and provided that the partial derivatives in eqn (4.11) are continuous it follows that

$$w = \phi + i\psi \tag{4.12}$$

is an analytic function of the complex variable $z = x + iy$ (Priestley 1985, pp. 16, 184). We call $w(z)$ the *complex potential.*

One of the most important properties of a 2-D incompressible, irrotational flow is that its velocity potential and stream function both satisfy Laplace's equation, so

$$\frac{\partial^2\phi}{\partial x^2} + \frac{\partial^2\phi}{\partial y^2} = 0 \tag{4.13}$$

and

$$\frac{\partial^2\psi}{\partial x^2} + \frac{\partial^2\psi}{\partial y^2} = 0, \tag{4.14}$$

as may be seen directly from eqn (4.11).

The velocity components u and v are directly related to dw/dz, which is most conveniently calculated as follows:

$$\frac{dw}{dz} = \frac{\partial\phi}{\partial x} + i\frac{\partial\psi}{\partial x} = u - iv. \tag{4.15}$$

(Note the negative sign.) The flow speed at any point is therefore

$$q = (u^2 + v^2)^{\frac{1}{2}} = \left|\frac{dw}{dz}\right|. \tag{4.16}$$

We now consider a number of examples.

Uniform flow at an angle α to the x-axis

Here

$$u = U\cos\alpha, \qquad v = U\sin\alpha,$$

so $dw/dz = Ue^{-i\alpha}$, and therefore

$$w = Uze^{-i\alpha}. \tag{4.17}$$

Line vortex

We may write this flow as

$$\boldsymbol{u} = \frac{\Gamma}{2\pi r}\boldsymbol{e}_\theta, \tag{4.18}$$

where Γ is the circulation round any simple circuit enclosing the vortex, and we already know from the previous section that

$$\phi = \Gamma\theta/2\pi. \tag{4.19}$$

Using eqn (4.9) we may also write

$$\frac{1}{r}\frac{\partial\psi}{\partial\theta} = 0, \qquad -\frac{\partial\psi}{\partial r} = \frac{\Gamma}{2\pi r},$$

whence

$$\psi = -\frac{\Gamma}{2\pi}\log r.$$

Thus

$$\phi + \mathrm{i}\psi = \frac{\Gamma}{2\pi}(\theta - \mathrm{i}\log r) = -\frac{\mathrm{i}\Gamma}{2\pi}(\log r + \mathrm{i}\theta),$$

and the complex potential for a line vortex at the origin is therefore

$$w = -\frac{\mathrm{i}\Gamma}{2\pi}\log z. \tag{4.20}$$

By the same token, the complex potential for a line vortex at $z = z_0$ is

$$w = -\frac{\mathrm{i}\Gamma}{2\pi}\log(z - z_0). \tag{4.21}$$

2-D irrotational flow near a stagnation point

If the complex potential $w(z)$ is analytic in some region it will possess a Taylor series expansion in the neighbourhood of any point z_0 in that region (Priestley 1985, p. 69), i.e.

$$w(z) = w(z_0) + (z - z_0)w'(z_0) + \tfrac{1}{2}(z - z_0)^2 w''(z_0) + \dots.$$

Now, the first term is an inconsequential constant which makes no difference to $\mathrm{d}w/\mathrm{d}z$, and if $z = z_0$ is a *stagnation point* for the flow, then $w'(z_0) = 0$, by virtue of eqn (4.15). Unless $w''(z_0)$ also happens to be zero, it follows that the flow in the immediate neighbourhood of the stagnation point will be determined by the

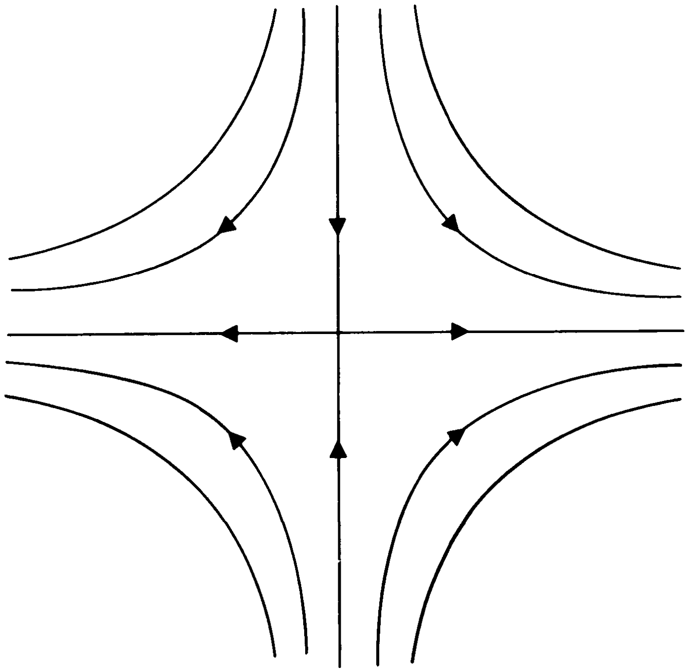

Fig. 4.1. 2-D irrotational flow near a stagnation point.

quadratic term in the above expression. Now, $w''(z_0)$ will typically be complex, $\alpha e^{i\beta}$, say, but by first shifting our coordinates:

$$z - z_0 = z_1,$$

so that the stagnation point is at $z_1 = 0$, and then rotating them so that

$$z_1 e^{i\beta/2} = z_2,$$

we may write

$$w = \text{constant} + \tfrac{1}{2}\alpha z_2^2 + \ldots.$$

Dropping the inconsequential constant, we see that relative to suitably located and orientated coordinates the complex potential in the neighbourhood of a stagnation point is

$$w = \tfrac{1}{2}\alpha z^2, \tag{4.22}$$

where α is real, the corresponding flow being

$$u = \alpha x, \qquad v = -\alpha y \tag{4.23}$$

(cf. Exercise 1.7). The stream function is

$$\psi = \alpha xy, \tag{4.24}$$

so the streamlines are rectangular hyperbolae, as in Fig. 4.1.

4.4. The method of images

Suppose there is a line vortex of strength Γ at a distance d from a rigid plane wall $x = 0$, as in Fig. 4.2(*a*). A clever trick for obtaining the flow is to imagine that the region $x \leqslant 0$ is also filled with fluid and that there is an equal and opposite vortex, i.e. of strength $-\Gamma$, at the mirror-image point, as in Fig. 4.2(*b*). The reason for doing this is that the x-components of velocity of the two vortices obviously cancel on $x = 0$, so there is no normal velocity component there. Thus the complex potential

$$w = -\frac{\mathrm{i}\Gamma}{2\pi}\log(z-d) + \frac{\mathrm{i}\Gamma}{2\pi}\log(z+d) \tag{4.25}$$

serves not only for the flow problem in Fig. 4.2(*b*) but, in $x \geqslant 0$, for the flow in the presence of a wall in Fig. 4.2(*a*). This is a simple example of the *method of images*, which is all about getting flows that satisfy boundary conditions.

Let us examine the flow in Fig. 4.2 a little more carefully. The stream function ψ is obtained by writing

$$\phi + \mathrm{i}\psi = -\frac{\mathrm{i}\Gamma}{2\pi}\log\left(\frac{z-d}{z+d}\right), \tag{4.26}$$

and the streamlines are therefore

$$\left|\frac{z-d}{z+d}\right| = \text{constant}. \tag{4.27}$$

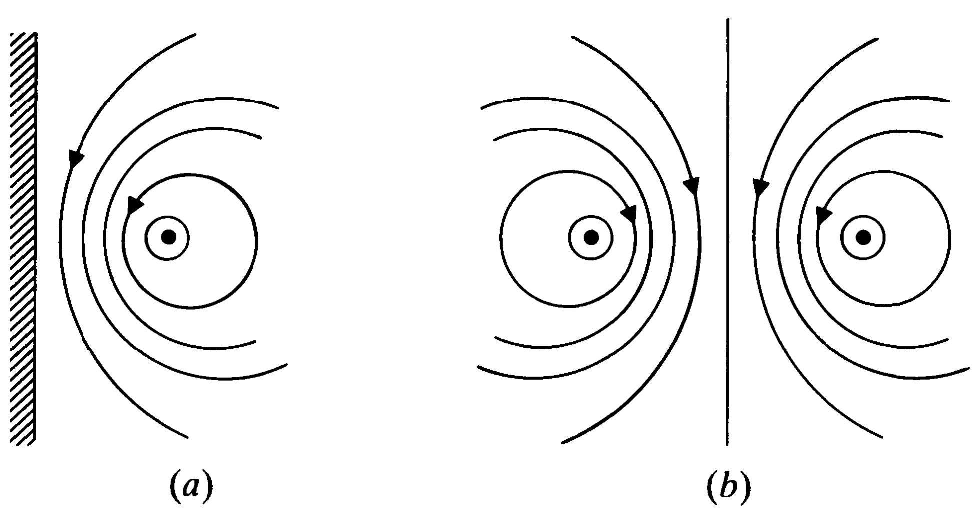

Fig. 4.2. Flows due to line vortices.

These are circles, the so-called coaxal circles of elementary geometry. Each circle cuts the circle $|z| = d$ orthogonally, and if the centre of any circle is distant c_1 and c_2 from the two vortices, then $c_1 c_2 = a^2$, where a is its radius.

It is a simple matter, then, to write down the flow inside a circular cylinder $|z| = a$ due to a line vortex at $z = c < a$: it will be as if the cylinder were not present and there were, instead, an equal and opposite line vortex at $z = a^2/c$. The complex potential for the flow in Fig. 4.3 is therefore

$$w = -\frac{\mathrm{i}\Gamma}{2\pi}\log(z - c) + \frac{\mathrm{i}\Gamma}{2\pi}\log\left(z - \frac{a^2}{c}\right). \tag{4.28}$$

While it is not a matter of major concern at present, eqns (4.25) and (4.28) are, in fact, only *instantaneous* complex potentials corresponding to the momentary positions of the vortices; the vortices, and the whole streamline patterns associated with them, in fact move in a manner to be described in §5.6.

Milne-Thomson's circle theorem

Suppose we have a flow with complex potential $w = f(z)$, where all the singularities of $f(z)$ lie in $|z| > a$. Then

$$w = f(z) + \overline{f(a^2/\bar{z})}, \tag{4.29}$$

where an overbar denotes complex conjugate, is the complex potential of a flow with (i) the same singularities as $f(z)$ in $|z| > a$ and (ii) $|z| = a$ as a streamline.

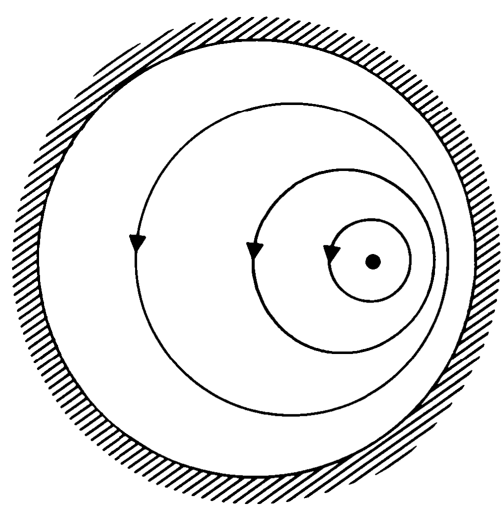

Fig. 4.3. Flow due to a line vortex inside a circular cylinder.

The last property makes the circle theorem a sort of automated method of images for circular boundaries. To prove it, note first that as all the singularities of $f(z)$ are in $|z| > a$, all those of $f(a^2/\bar{z})$ are in $|a^2/\bar{z}| > a$, i.e. in $|z| < a$. Second, on the circle itself we have $z\bar{z} = a^2$, so

$$w = f(z) + \overline{f(z)} \qquad \text{on } |z| = a. \tag{4.30}$$

Thus w is real on $|z| = a$, so $\psi = 0$ there, so $|z| = a$ is a streamline.

An elementary application of the circle theorem follows in the next section.

4.5. Irrotational flow past a circular cylinder

Consider irrotational flow, uniform with speed U at infinity, past a fixed circular cylinder $|z| = a$. If the stream is parallel to the x-axis the complex potential for the undisturbed flow is $f(z) = Uz$, which has a singularity only at infinity. Applying the circle theorem we find

$$f(a^2/\bar{z}) = Ua^2/\bar{z}, \qquad \overline{f(a^2/\bar{z})} = Ua^2/z,$$

so

$$w(z) = U\left(z + \frac{a^2}{z}\right) \tag{4.31}$$

is the complex potential of an irrotational flow, uniform at infinity, having $|z| = a$ as a streamline.

It is not the only irrotational flow satisfying these conditions; we may plainly superimpose a line vortex flow of arbitrary strength Γ to give

$$w(z) = U\left(z + \frac{a^2}{z}\right) - \frac{\mathrm{i}\Gamma}{2\pi}\log z \tag{4.32}$$

as the complex potential of a more general irrotational flow having no normal velocity at $|z| = a$, yet being uniform, with speed U, at infinity.

Nevertheless, consider first the case (4.31) in which there is no circulation round the cylinder. Putting $z = re^{\mathrm{i}\theta}$ we find that

$$\phi = U\left(r + \frac{a^2}{r}\right)\cos\theta \tag{4.33}$$

and

$$\psi = U\left(r - \frac{a^2}{r}\right)\sin\theta, \tag{4.34}$$

whence†

$$u_r = U\left(1 - \frac{a^2}{r^2}\right)\cos\theta, \qquad u_\theta = -U\left(1 + \frac{a^2}{r^2}\right)\sin\theta. \tag{4.35}$$

The flow is symmetric fore and aft of the cylinder, and some of the streamlines are sketched in Fig. 4.4(a).

There is evidently *slip* on the cylinder—according to this irrotational flow theory, at any rate—for

$$u_\theta = -2U\sin\theta \qquad \text{at } r = a. \tag{4.36}$$

In discussing this it is convenient to use instead $u_s = -u_\theta$, which is positive, and $s = (\pi - \theta)a$, which is the distance along the top of the cylinder from the forward stagnation point. Thus

$$u_s = 2U\sin\frac{s}{a}, \tag{4.37}$$

and

$$\frac{\mathrm{d}u_s}{\mathrm{d}s} = \frac{2U}{a}\cos\frac{s}{a}.$$

The slip velocity therefore rises from zero at the front stagnation point to a maximum of $2U$ at $\theta = \pi/2$; it then decreases again to zero at the rear stagnation point.

When there is circulation Γ round the cylinder, as in eqn (4.32), the velocity components are

$$u_r = U\left(1 - \frac{a^2}{r^2}\right)\cos\theta, \qquad u_\theta = -U\left(1 + \frac{a^2}{r^2}\right)\sin\theta + \frac{\Gamma}{2\pi r}. \tag{4.38}$$

Anticipating the applications to aerofoil theory that lie ahead, we have taken Γ to be negative in Fig. 4.4, so that the superimposed circulatory flow is clockwise. The character of the streamline

† We do not, of course, need the full apparatus of complex variable theory and circle theorem to establish this particular result; there is a much simpler way (Exercise 4.4).

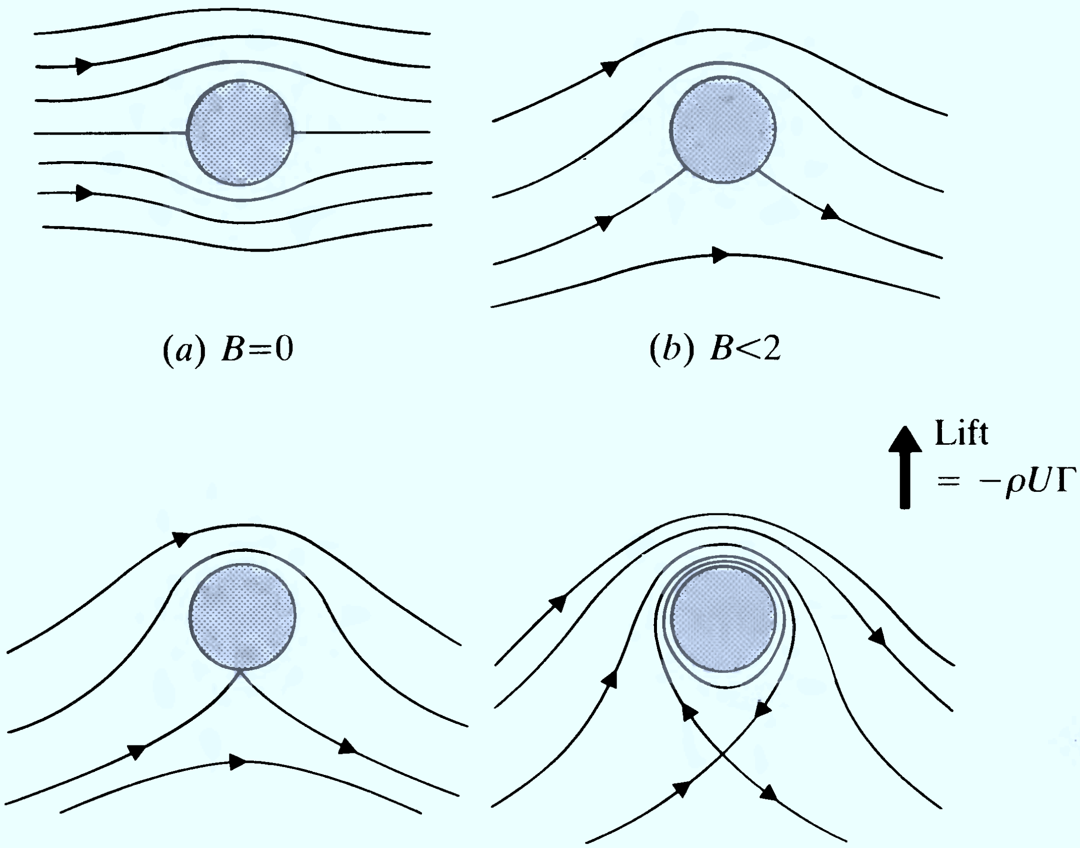

Fig. 4.4. Irrotational flows past a circular cylinder.

pattern depends crucially on the parameter

$$B = -\Gamma/2\pi U a, \tag{4.39}$$

which is then positive.

One notable feature of the flow that changes with B is the location of the stagnation points. When $B < 2$ there are two of them, both located on the cylinder $r = a$, at $\sin\theta = -\frac{1}{2}B$. They therefore move round as B is increased and coalesce when $B = 2$ at $\theta = 3\pi/2$. When $B > 2$ there is only one stagnation point, and it lies off the cylinder at

$$\frac{r}{a} = \frac{B}{2} + \left(\frac{B^2}{4} - 1\right)^{\frac{1}{2}}, \qquad \theta = \frac{3\pi}{2}. \tag{4.40}$$

This stagnation point thus moves further and further away from the cylinder as B increases, and the region of closed streamlines adjacent to the cylinder becomes steadily larger.

The net force on the cylinder may be calculated from the pressure distribution on $r = a$. As the cylinder is a streamline, and the motion is steady, Bernoulli's theorem gives

$$p + \tfrac{1}{2}\rho \mathbf{u}^2 = \text{constant} \qquad \text{on } r = a,$$

whence

$$\frac{p}{\rho} = \text{constant} - 2U^2 \sin^2\theta + \frac{U\Gamma}{\pi a} \sin\theta \qquad \text{on } r = a.$$

This pressure distribution is symmetric fore and aft of the cylinder (i.e. unchanged by the transformation $\theta \Rightarrow \pi - \theta$), so any net force must be perpendicular to the oncoming stream. The force on a small element $a\,\mathrm{d}\theta$ of the cylinder is $pa\,\mathrm{d}\theta$ (per unit length in the z-direction). The y-component of this force is $-pa\sin\theta\,\mathrm{d}\theta$, and there is therefore a net force on the cylinder of

$$\rho \int_0^{2\pi} \left(2U^2 \sin^2\theta - \frac{U\Gamma}{\pi a}\sin\theta\right) a \sin\theta\,\mathrm{d}\theta = -\rho U \Gamma \qquad (4.41)$$

in the y-direction, in keeping with the far more general Kutta–Joukowski Lift Theorem of §4.11.

There is positive 'lift', then, if $\Gamma < 0$, and it is easy to see why this should be so, as we have already observed in §1.6. On top of the cylinder in Fig. 4.4 the circulatory flow reinforces the oncoming stream (if $\Gamma < 0$), leading to high speeds and low pressures. Beneath the cylinder the circulatory flow opposes the oncoming stream, leading to low speeds—as evinced by the stagnation points—and high pressures.

Before proceeding further we should emphasize again that we are currently using the irrotational flows in Fig. 4.4 purely as a mathematical device for the calculation of irrotational flows past a thin aerofoil. We are deferring, in particular, all question of whether the flows of Fig. 4.4 are *themselves* observable for a real (i.e. viscous) fluid, whether at high Reynolds number or otherwise (see §§5.7 and 8.6, cf. §7.7).

For what follows it is convenient, in fact, to take the oncoming stream at an angle α to the x-axis. The complex potential of the undisturbed flow is $Uz\mathrm{e}^{-\mathrm{i}\alpha}$, by virtue of eqn (4.17). Applying the circle theorem and superposing a line vortex flow of strength Γ then gives

$$w(z) = U\left(z\mathrm{e}^{-\mathrm{i}\alpha} + \frac{a^2}{z}\mathrm{e}^{\mathrm{i}\alpha}\right) - \frac{\mathrm{i}\Gamma}{2\pi}\log z \qquad (4.42)$$

as our starting point, and this corresponds to the flows of Fig. 4.4 turned anticlockwise through an angle α.

4.6. Conformal mapping

Let $w(z)$ be the complex potential of some 2-D irrotational flow in the z-plane, with $w = \phi + i\psi$. Suppose now that we choose

$$Z = f(z) \tag{4.43}$$

as some analytic function of z, with an inverse

$$z = F(Z) \tag{4.44}$$

which is an analytic function of Z. Then

$$W(Z) = w\{F(Z)\} \tag{4.45}$$

is an analytic function of Z. Now write

$$Z = X + iY \tag{4.46}$$

and split $W(Z)$ into its real and imaginary parts:

$$W(Z) = \Phi(X, Y) + i\Psi(X, Y). \tag{4.47}$$

As W is an analytic function of Z, Φ and Ψ satisfy the Cauchy–Riemann equations, and it follows that the two functions

$$u_*(X, Y) = \partial\Phi/\partial X = \partial\Psi/\partial Y, \qquad v_*(X, Y) = \partial\Phi/\partial Y = -\partial\Psi/\partial X, \tag{4.48}$$

represent the velocity components of an irrotational, incompressible flow in the Z-plane.

Further, because $W(Z)$ and $w(z)$ take the same value at corresponding points of the two planes (i.e. points related by eqns (4.43) or (4.44)) it follows that Ψ and ψ are the same at corresponding points. Thus streamlines are mapped into streamlines. In particular, a fixed rigid boundary in the z-plane, which is necessarily a streamline, gets mapped into a streamline in the Z-plane, which could accordingly be viewed as a rigid boundary for the flow in the Z-plane. The key question, then, is: Given flow past a circular cylinder in the z-plane (see eqn (4.42)), can we choose the mapping (4.43) so as to obtain in the Z-plane uniform flow past a more wing-like shape?

What happens to the circulation round a closed circuit is important in this connection. Evidently Φ and ϕ are the same at corresponding points of the two planes, and it follows that if we go once round some closed circuit of the z-plane and obtain some consequent change in ϕ, we will obtain the same change in Φ on going once round the corresponding circuit in the Z-plane. Appealing to eqn (4.4), then, we see that the circulations round two such corresponding circuits must be the same.

What happens to the flow at infinity is also of importance. Plainly

$$\frac{\mathrm{d}W}{\mathrm{d}Z}=\frac{\mathrm{d}w/\mathrm{d}z}{\mathrm{d}Z/\mathrm{d}z}, \tag{4.49}$$

so

$$u_*-\mathrm{i}v_*=(u-\mathrm{i}v)/f'(z). \tag{4.50}$$

If we want to map uniform flow past some object into the same uniform flow past another object we must therefore choose $f(z)$ such that $f'(z)\to 1$ as $|z|\to\infty$.

One last general observation concerns a strictly local property of conformal mapping which gives the method its name. Take some point z_0 in the z-plane, with a corresponding point Z_0 in the Z-plane, and let $f^{(n)}(z_0)$ be the first non-vanishing derivative of the function $f(z)$ at z_0. Typically, n will be 1, but there will be occasions in what follows when $f'(z_0)=0$ but $f''(z_0)\neq 0$, in which case $n=2$. Let δz denote a small element in the z-plane, originating at $z=z_0$, and let δZ denote the corresponding element in the Z-plane, originating at $Z=Z_0$. By expanding $f(z)$ in a Taylor series we find that

$$\delta Z=\frac{(\delta z)^n}{n!}f^{(n)}(z_0)+O(\delta z)^{n+1}.$$

To first order in small quantities, then,

$$\arg(\delta Z)=n\arg(\delta z)+\arg\{f^{(n)}(z_0)\},$$

and it follows that if δz_1 and δz_2 denote two small elements in the z-plane, both originating at z_0, then

$$\arg(\delta Z_2)-\arg(\delta Z_1)=n[\arg(\delta z_2)-\arg(\delta z_1)]. \tag{4.51}$$

Thus when two short intersecting elements in the z-plane are mapped into two short intersecting elements in the Z-plane, the angle between them is multiplied by n. Usually, $n=1$, and such angles are preserved. The shape of a small figure in the z-plane (e.g. a small parallelogram) is then preserved by the mapping—hence the name 'conformal'.

A very effective transformation for our purposes is the Joukowski transformation,

$$Z = z + \frac{c^2}{z}, \tag{4.52}$$

and we shall exploit the fact that $f'(\pm c) = 0$ but $f''(\pm c) \neq 0$, so that angles between two short line elements which intersect at either $z = c$ or $z = -c$ are doubled by the transformation. The inverse of eqn (4.52) is

$$z = \tfrac{1}{2}Z + (\tfrac{1}{4}Z^2 - c^2)^{\frac{1}{2}}, \tag{4.53}$$

although we have to take steps to pin down the meaning of this, for there are branch points at $Z = \pm 2c$. In all that follows we shall (i) cut the Z-plane along the real axis between $Z = -2c$ and $Z = 2c$, which stops eqn (4.53) from being multivalued, and (ii) interpret $(\frac{1}{4}Z^2 - c^2)^{\frac{1}{2}}$ as meaning that branch of the function which behaves like $\frac{1}{2}Z$ (as opposed to $-\frac{1}{2}Z$) as $|Z| \to \infty$, which ensures that $z \sim Z$ when $|Z|$ is large.

4.7. Irrotational flow past an elliptical cylinder

Consider the effect of the Joukowski transformation (4.52) on the circle $z = a\mathrm{e}^{\mathrm{i}\theta}$, where $0 \leqslant c \leqslant a$. Plainly

$$X + \mathrm{i}Y = \left(a + \frac{c^2}{a}\right)\cos\theta + \mathrm{i}\left(a - \frac{c^2}{a}\right)\sin\theta,$$

so the circle is mapped into the ellipse

$$\frac{X^2}{(a + c^2/a)^2} + \frac{Y^2}{(a - c^2/a)^2} = 1 \tag{4.54}$$

in the Z-plane (see Fig. 4.5).

Substituting eqn (4.53) into eqn (4.42) we thus obtain

$$W(Z) = U\mathrm{e}^{-\mathrm{i}\alpha}[\tfrac{1}{2}Z + (\tfrac{1}{4}Z^2 - c^2)^{\frac{1}{2}}] + U\mathrm{e}^{\mathrm{i}\alpha}\frac{a^2}{c^2}[\tfrac{1}{2}Z - (\tfrac{1}{4}Z^2 - c^2)^{\frac{1}{2}}]$$

$$-\frac{\mathrm{i}\Gamma}{2\pi}\log[\tfrac{1}{2}Z + (\tfrac{1}{4}Z^2 - c^2)^{\frac{1}{2}}] \tag{4.55}$$

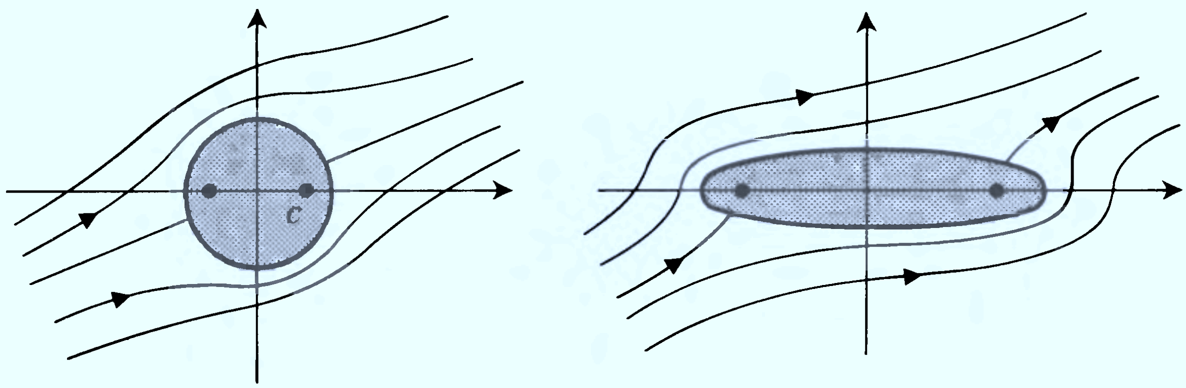

(a) z−plane (b) Z−plane

Fig. 4.5. Flow past an elliptical cylinder by conformal mapping; no circulation.

as the complex potential for uniform flow at an angle α past the ellipse (4.54), with circulation Γ. It is an elementary, but messy, exercise to write $Z = X + \mathrm{i}Y$ and then extract the imaginary part of $W(Z)$, namely $\Psi(X, Y)$. The streamlines are sketched in Fig. 4.5(b) for the case $\Gamma = 0$.

4.8. Irrotational flow past a finite flat plate

If we choose $c = a$, so that

$$Z = z + \frac{a^2}{z}, \tag{4.56}$$

the ellipse (4.54) collapses to a flat plate of length $4a$. Consider the velocity components u_* and v_* in the Z-plane:

$$u_* - \mathrm{i}v_* = \frac{\mathrm{d}W}{\mathrm{d}Z} = \frac{\mathrm{d}w/\mathrm{d}z}{\mathrm{d}Z/\mathrm{d}z} = \left(U\mathrm{e}^{-\mathrm{i}\alpha} - U\mathrm{e}^{\mathrm{i}\alpha}\frac{a^2}{z^2} - \frac{\mathrm{i}\Gamma}{2\pi z}\right)\bigg/\left(1 - \frac{a^2}{z^2}\right). \tag{4.57}$$

Using eqn (4.53) we can write them in terms of Z, but the comparative simplicity of eqn (4.57) can be more helpful for many purposes.

In particular, the flow speed is in general infinite at the ends of the plate ($Z = \pm 2a$), as these points correspond to the points $z = \pm a$. The status of these sharp edges as singular points in the flow is confirmed by a glance at the streamline pattern for the case $\Gamma = 0$ in Fig. 4.6(a).

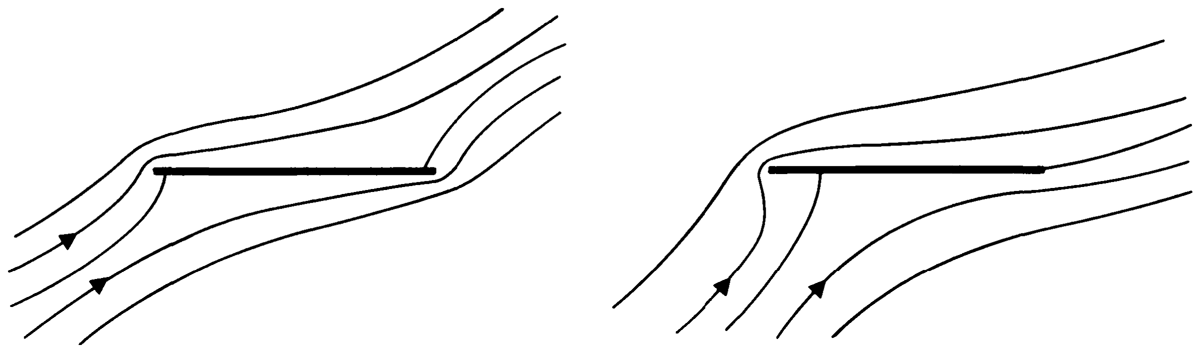

(*a*) $\Gamma=0$ (*b*) $\Gamma=-4\pi Ua\sin\alpha$

Fig. 4.6. Irrotational flow past a finite flat plate.

Notably, however, the singularity at the trailing edge $Z=2a$ (i.e. $z=a$) may be removed *if the circulation* Γ *is chosen so that the numerator in eqn* (4.57) *vanishes at the trailing edge.* Thus if

$$Ue^{-i\alpha}-Ue^{i\alpha}-\frac{i\Gamma}{2\pi a}=0,$$

i.e. if

$$\Gamma=-4\pi Ua\sin\alpha, \tag{4.58}$$

then by writing $z=a+\varepsilon$ in both the numerator and denominator of eqn (4.57) and taking the limit as $\varepsilon\to 0$ we find

$$u_*\to U\cos\alpha,\quad v_*\to 0\qquad \text{as } Z\to 2a,$$

so that the flow leaves the trailing edge smoothly and parallel to the plate, as in Fig. 4.6(*b*). The sense of the circulation is clockwise (for $\alpha>0$), and this is why we chose to represent the effects of a clockwise circulation in Fig. 4.4.

Of course, the presence of this circulation still leaves a singularity in the velocity field at the leading edge in Fig. 4.6(*b*).

4.9. Flow past a symmetric aerofoil

In view of Figs 4.5 and 4.6 it will come as no surprise that if we use the mapping (4.56) on a circle in the z-plane which passes through $z=a$ but which encloses $z=-a$, we obtain an aerofoil with a rounded nose but a sharp trailing edge, as in Fig. 4.7(*b*). If the centre of the circle is on the real axis in the z-plane, at $z=-\lambda$, say, the aerofoil is symmetric and given in terms of the

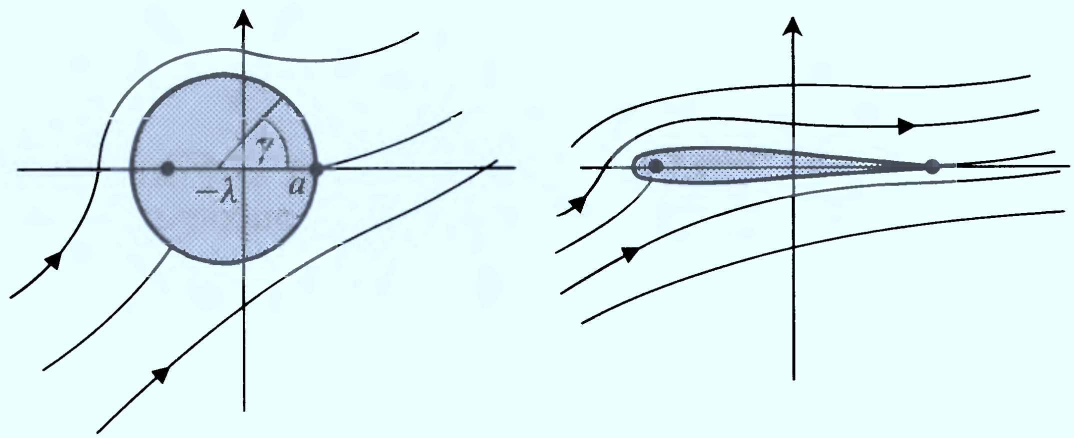

(*a*) z-plane (*b*) Z-plane

Fig. 4.7. Flow past a symmetric Joukowski aerofoil by conformal mapping.

parameter γ by

$$Z = -\lambda + (a+\lambda)e^{i\gamma} + \frac{a^2}{-\lambda + (a+\lambda)e^{i\gamma}}. \tag{4.59}$$

Its shape and thickness depend on λ.

The complex potential $W(Z)$ corresponding to uniform flow past this aerofoil at angle of attack α is obtained by first modifying eqn (4.42) to take account of the new radius and location of the cylinder in the z-plane:

$$w(z) = U\left[(z+\lambda)e^{-i\alpha} + \frac{(a+\lambda)^2}{(z+\lambda)}e^{i\alpha}\right] - \frac{i\Gamma}{2\pi}\log(z+\lambda),$$

and then substituting $z = \frac{1}{2}Z + (\frac{1}{4}Z^2 - a^2)^{\frac{1}{2}}$.

The counterpart to eqn (4.57) is

$$\frac{dW}{dZ} = \left\{U\left[e^{-i\alpha} - \left(\frac{a+\lambda}{z+\lambda}\right)^2 e^{i\alpha}\right] - \frac{i\Gamma}{2\pi(z+\lambda)}\right\}\Big/\left(1 - \frac{a^2}{z^2}\right), \tag{4.60}$$

but now it is only the vanishing of the denominator at $z = a$ ($Z = 2a$) that causes concern, for $z = -a$ corresponds to a point in the Z-plane which is inside the aerofoil. The value of Γ which makes the numerator in eqn (4.60) zero at the trailing edge ($z = a$) is

$$\Gamma = -4\pi U(a+\lambda)\sin\alpha. \tag{4.61}$$

The flow is then smooth and free of singularities everywhere, as shown in Fig. 4.7(b), and this is an example of the *Kutta–Joukowski condition* at work.

When $\lambda \ll a$ the aerofoil described by eqn (4.59) is thin and symmetric, with length approximately $4a$ and maximum thickness $3\sqrt{3}\lambda$. By neglecting λ in comparison with a in eqn (4.61) we obtain the classic expression (4.1).

4.10. The forces involved: Blasius's theorem

Let there be a steady flow with complex potential $w(z)$ about some fixed body which has as its boundary the closed contour C, as in Fig. 4.8. If F_x and F_y are the components of the net force (per unit length) on the body, then

$$F_x - \mathrm{i}F_y = \tfrac{1}{2}\mathrm{i}\rho \oint_C \left(\frac{\mathrm{d}w}{\mathrm{d}z}\right)^2 \mathrm{d}z. \tag{4.62}$$

This is *Blasius's theorem.*

To prove it, let s denote arc length along C, and let θ denote the angle made with the x-axis by the tangent to C. Then the force (per unit length) on a small element δs of the boundary is $(-\sin\theta, \cos\theta)p\,\delta s$, so

$$\delta F_x - \mathrm{i}\,\delta F_y = -p(\sin\theta + \mathrm{i}\cos\theta)\,\delta s = -p\mathrm{i}e^{-\mathrm{i}\theta}\,\delta s.$$

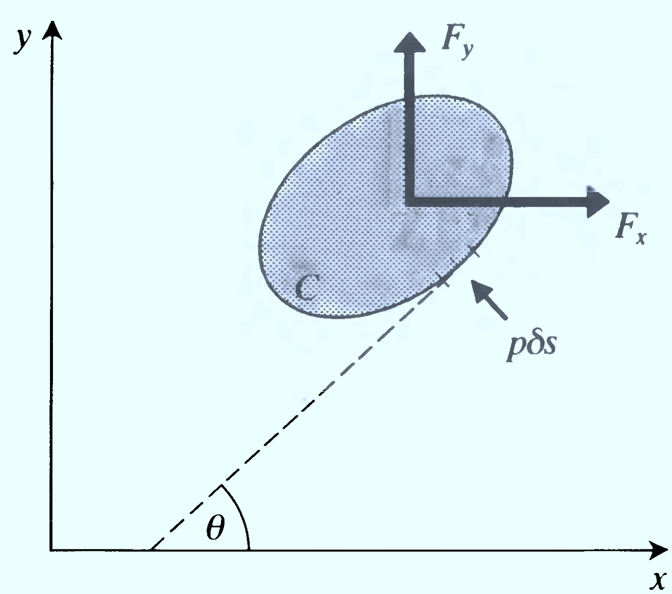

Fig. 4.8. Definition sketch for proof of Blasius's theorem.

Now, C is a streamline for the flow, so

$$u = q\cos\theta, \quad v = q\sin\theta \qquad \text{on } C,$$

where $q = (u^2+v^2)^{\frac{1}{2}}$, so

$$\frac{\mathrm{d}w}{\mathrm{d}z} = u - \mathrm{i}v = q\mathrm{e}^{-\mathrm{i}\theta} \text{ on } C.$$

Using Bernoulli's equation we may write

$$\delta F_x - \mathrm{i}\,\delta F_y = (\tfrac{1}{2}\rho q^2 - k)\mathrm{i}\mathrm{e}^{-\mathrm{i}\theta}\,\delta s,$$

where k is a constant, and substituting for q we find

$$\delta F_x - \mathrm{i}\,\delta F_y = \tfrac{1}{2}\mathrm{i}\rho\left(\frac{\mathrm{d}w}{\mathrm{d}z}\right)^2 \mathrm{e}^{\mathrm{i}\theta}\,\delta s - k\mathrm{i}(\delta x - \mathrm{i}\,\delta y).$$

Now, $\mathrm{e}^{\mathrm{i}\theta}\,\delta s = \delta z$. On integrating round the closed contour C the final term disappears and we obtain eqn (4.62).

In a similar way we may establish a formula for $\mathcal{N}$, the moment about the origin of the forces on the body:

$$\mathcal{N} = \text{Real part of}\left[-\tfrac{1}{2}\rho\oint_C z\left(\frac{\mathrm{d}w}{\mathrm{d}z}\right)^2 \mathrm{d}z\right] \tag{4.63}$$

(see Exercise 4.5).

We now consider two examples.

Uniform flow past a circular cylinder

We have, of course, already calculated the net force in this case by direct integration of the pressure distribution in §4.5. Nevertheless, the complex potential is, in the case $\alpha = 0$:

$$w = U\left(z + \frac{a^2}{z}\right) - \frac{\mathrm{i}\Gamma}{2\pi}\log z,$$

so applying Blasius's theorem:

$$F_x - \mathrm{i}F_y = \tfrac{1}{2}\mathrm{i}\rho\oint_C\left[U\left(1 - \frac{a^2}{z^2}\right) - \frac{\mathrm{i}\Gamma}{2\pi z}\right]^2 \mathrm{d}z.$$

When the integrand is expanded only the z^{-1} term gives a contribution to the integral. The coefficient of that term is

$-\mathrm{i}U\Gamma/\pi$, so a simple application of the residue calculus gives

$$F_x - \mathrm{i}F_y = \tfrac{1}{2}\mathrm{i}\rho \cdot 2\pi\mathrm{i} \cdot \left(-\frac{\mathrm{i}U\Gamma}{\pi}\right) = \mathrm{i}\rho U\Gamma.$$

Thus

$$F_x = 0, \qquad F_y = -\rho U\Gamma, \tag{4.64}$$

as found previously.

Uniform flow past an elliptical cylinder

Consider for simplicity the case when there is no circulation, as in Fig. 4.5(*b*). By the Kutta–Joukowski Lift Theorem (§4.11) there will be no net force on the ellipse, but there will in general be a torque about the origin given by eqn (4.63), i.e.

$$\text{Real part of}\left[-\tfrac{1}{2}\rho\oint_{\text{ellipse}} Z\left(\frac{\mathrm{d}W}{\mathrm{d}Z}\right)^2 \mathrm{d}Z\right].$$

Now, the expression (4.55) for W in terms of $Z = z + c^2/z$ is quite complicated, even in the case $\Gamma = 0$. It is more sensible, then, to write

$$\frac{\mathrm{d}W}{\mathrm{d}Z} = \frac{\mathrm{d}w}{\mathrm{d}z}\frac{\mathrm{d}z}{\mathrm{d}Z}$$

and change the variable of integration from Z to z, so calculating

$$\text{Real part of}\left[-\tfrac{1}{2}\rho\oint_{|z|=a} Z\left(\frac{\mathrm{d}w}{\mathrm{d}z}\right)^2 \frac{\mathrm{d}z}{\mathrm{d}Z}\,\mathrm{d}z\right].$$

Now, when $\Gamma = 0$,

$$w = U\left(z\mathrm{e}^{-\mathrm{i}\alpha} + \frac{a^2}{z}\mathrm{e}^{\mathrm{i}\alpha}\right),$$

so the torque on the ellipse is the real part of

$$-\tfrac{1}{2}\rho U^2 \oint_{|z|=a}\left(z + \frac{c^2}{z}\right)\left(\mathrm{e}^{-\mathrm{i}\alpha} - \frac{a^2}{z^2}\mathrm{e}^{\mathrm{i}\alpha}\right)^2\left(1 - \frac{c^2}{z^2}\right)^{-1} \mathrm{d}z.$$

The integrand has poles at $-c$, 0, and c, all within the contour (as $0 < c < a$). Expanding the whole integrand in a Laurent series valid for $|z| > c$, and therefore valid on the integration contour, we obtain

$$\left(z+\frac{c^2}{z}\right)\left(e^{-2i\alpha}-\frac{2a^2}{z^2}+\frac{a^4}{z^4}e^{2i\alpha}\right)\left(1+\frac{c^2}{z^2}+\frac{c^4}{z^4}+\ldots\right).$$

The coefficient of z^{-1} is

$$c^2e^{-2i\alpha}-2a^2+c^2e^{-2i\alpha},$$

and the torque on the ellipse is therefore the real part of

$$-\tfrac{1}{2}\rho U^2\cdot 2\pi i\cdot(2c^2e^{-2i\alpha}-2a^2),$$

i.e.

$$\mathcal{N}=-2\pi\rho U^2c^2\sin 2\alpha. \tag{4.65}$$

For the flow in Fig. 4.5(*b*) the torque is negative, i.e. clockwise. More generally, it is such as to tend to align the ellipse so that it is broadside-on to the stream.

4.11. The Kutta–Joukowski Lift Theorem

Consider steady flow past a two-dimensional body, the cross-section of which is some simple closed curve C, as in Fig. 4.9. Let the flow be uniform at infinity, with speed U in the x-direction, and let the circulation round the body be Γ. Then

$$F_x=0,\qquad F_y=-\rho U\Gamma. \tag{4.66}$$

To prove this theorem, first choose the origin O so that it lies inside the body. Then, assuming the flow to be free of singularities, $\mathrm{d}w/\mathrm{d}z$ will be an analytic function of z in the flow domain and can be expanded in a Laurent series valid for $R<|z|<\infty$, where R is the radius of the smallest circle centred on O which encloses the body. Furthermore, the form of this series must be

$$\frac{\mathrm{d}w}{\mathrm{d}z}=U+\frac{a_1}{z}+\frac{a_2}{z^2}+\ldots \tag{4.67}$$

because the flow is uniform, speed U, at infinity.

Now, we stated Blasius's theorem in the form of an integral (4.62) taken round the contour C of the body, but if the flow is free of singularities we may, by a cross-cut argument and use of Cauchy's theorem, take the integral equally well round any simple closed contour C' which surrounds the body. In

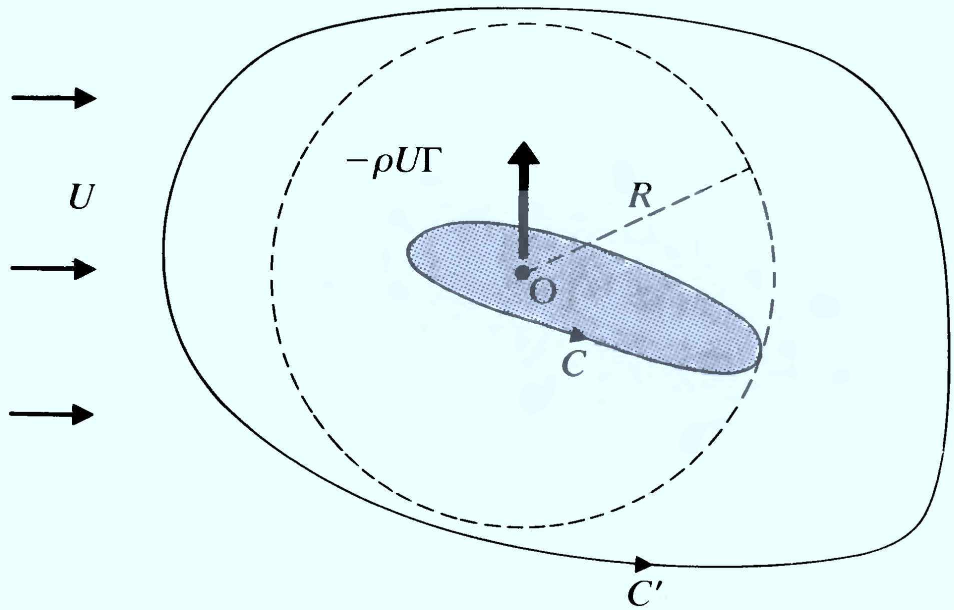

Fig. 4.9. Definition sketch for proof of the Kutta–Joukowski Lift Theorem.

particular, if we take it round a contour C', such as that in Fig. 4.9, which lies wholly in the region $|z| > R$, we may use eqn (4.67) to write

$$F_x - \mathrm{i}F_y = \tfrac{1}{2}\mathrm{i}\rho \oint_{C'} \left(U + \frac{a_1}{z} + \frac{a_2}{z^2} + \ldots\right)^2 \mathrm{d}z.$$

On expanding the integrand only the z^{-1} term contributes to the integral, and with residue $2Ua_1$ at $z = 0$ this gives

$$F_x - \mathrm{i}F_y = \tfrac{1}{2}\mathrm{i}\rho \cdot 2\pi\mathrm{i} \cdot 2Ua_1 = -2\pi\rho U a_1. \tag{4.68}$$

To find a_1, use eqn (4.67) to write

$$2\pi\mathrm{i}a_1 = \oint_{C'} \frac{\mathrm{d}w}{\mathrm{d}z}\,\mathrm{d}z,$$

where C' lies wholly in $|z| > R$. We may then appeal again to Cauchy's theorem and a cross-cut argument to justify taking the integral round C instead of C', as $\mathrm{d}w/\mathrm{d}z$ is analytic in the whole of the flow region. Thus

$$2\pi\mathrm{i}a_1 = \oint_{C} \frac{\mathrm{d}w}{\mathrm{d}z}\,\mathrm{d}z = [w]_C = [\phi + \mathrm{i}\psi]_C.$$

But C is a streamline, so the change in ψ after one journey round C is zero. The change in ϕ, on the other hand, is simply Γ, the circulation round the body (see eqn (4.4)). Thus

$$2\pi i a_1 = \Gamma, \tag{4.69}$$

and substituting this in eqn (4.68) establishes the theorem, eqn (4.66).

4.12. Lift: the deflection of the airstream

Notwithstanding the importance of circulation, the Kutta–Joukowski condition, and the theorem of §4.11, an aerofoil obtains lift essentially by imparting downward momentum to the oncoming airstream. In the case of a single aerofoil in an infinite expanse of fluid this elementary truth is disguised, perhaps, by the way that the deflection of the airstream tends to zero at infinity. But in uniform flow past an infinite array of aerofoils, as in Fig. 4.10, there is a finite deflection of the airstream at infinity, so that the downward momentum flux is more readily apparent. Moreover, the deflection is related in a most instructive way to both the circulation and the lift. For this reason, it is worth exploring, and to do this we first need a reformulation of the equation of motion.

The steady momentum equation in integral form

For steady flow, and in the absence of body forces, Euler's equation (1.12) reduces to

$$\rho(\boldsymbol{u} \cdot \nabla)\boldsymbol{u} = -\nabla p,$$

and using a suffix notation and the summation convention this may be written

$$\rho u_j \frac{\partial u_i}{\partial x_j} = -\frac{\partial p}{\partial x_i}.$$

Let us integrate this over some fixed region V which is enclosed by a fixed surface S, so that fluid is flowing in through some parts of S and out at others. Then the left-hand side becomes

$$\begin{aligned}\int_V \rho u_j \frac{\partial u_i}{\partial x_j}\,\mathrm{d}V &= \int_V \rho \frac{\partial}{\partial x_j}(u_j u_i)\,\mathrm{d}V = \int_S \rho u_j u_i n_j\,\mathrm{d}S \\ &= \int_S \rho(\boldsymbol{u} \cdot \boldsymbol{n})u_i\,\mathrm{d}S,\end{aligned}$$

the first equation holding because $\partial u_j/\partial x_j = \nabla \cdot \boldsymbol{u} = 0$, and the second holding by virtue of eqn (A.18). Thus

$$\int_S \rho(\boldsymbol{u} \cdot \boldsymbol{n})u_i \, \mathrm{d}S = -\int_V \frac{\partial p}{\partial x_i} \mathrm{d}V = -\int_S pn_i \, \mathrm{d}S,$$

where we have used eqn (A.15). In vector terms, then,

$$-\int_S p\boldsymbol{n} \, \mathrm{d}S = \int_S \rho\boldsymbol{u}(\boldsymbol{u} \cdot \boldsymbol{n}) \, \mathrm{d}S. \tag{4.70}$$

Now, $\rho\boldsymbol{u}$ is the momentum per unit volume of a fluid element, and $(\boldsymbol{u} \cdot \boldsymbol{n})\,\delta S$ is the volume rate at which fluid is leaving a small portion δS of the surface S, so the right-hand side represents the rate at which momentum is getting carried out of S. The equation states, then, that the total force on S is equal to the rate at which momentum is carried out of S.

Flow past a stack of aerofoils

Let the (identical) aerofoils be a distance d apart, as in Fig. 4.10. Consider the flow in and out of the control surface ABCDA, where AB and DC are portions of identical streamlines a distance d apart, AD being far upstream, where the velocity is $(U, 0)$, and BC being far downstream, where we assume the velocity to be

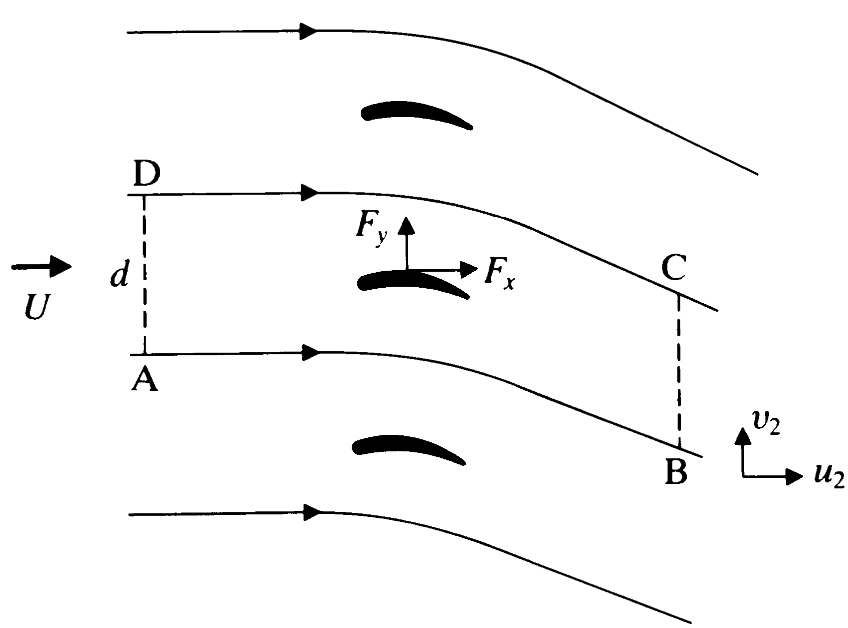

Fig. 4.10. Flow past a stack of aerofoils.

uniform again, but equal to (u_2, v_2). Now, because the fluid is incompressible the volume flux across AD must be equal to that across BC, so $Ud = u_2 d$, and therefore

$$u_2 = U. \tag{4.71}$$

We now apply the result (4.70) to the fixed region S which lies within ABCDA but excludes the aerofoil. If the lift on the aerofoil is F_y there is a vertical component of force $-F_y$ on S. (There is no other y-component to the first term in eqn (4.70), for those at BC and DA are zero and those at AB and CD cancel, because at any given x the pressures on AB and CD will be the same, as the flow repeats periodically in the y-direction.) There is no flux of momentum across either AB or CD, for they are streamlines, and there is no flux of vertical momentum across AD. Vertical momentum is, however, flowing out of BC at a rate $\rho v_2 U d$ (per unit length in the z-direction). Equating this to the force exerted on S by the aerofoil, we have

$$F_y = -\rho U v_2 d. \tag{4.72}$$

In this way we see clearly how the lift is related to the deflection of the airstream; a downward deflection $(v_2 < 0)$ corresponds to positive lift. Moreover, it is clear, too, how the circulation is related to this deflection, and hence to the lift itself, for the circulation round ABCDA is

$$\Gamma = v_2 d, \tag{4.73}$$

as the contribution from DA is zero and those from AB and CD cancel. Thus

$$F_y = -\rho U \Gamma, \tag{4.74}$$

so that the Kutta–Joukowski result for a single aerofoil in fact holds in this rather different situation also.

4.13. D'Alembert's paradox

Consider the steady flow of an ideal fluid around a 3-D body which is placed in a long straight channel of uniform cross-section (Fig. 4.11). Let us apply eqn (4.70) to the fixed region bounded by the obstacle, two fixed cross-sections S_1 and S_2, and the channel walls. The net force in the downstream direction on the

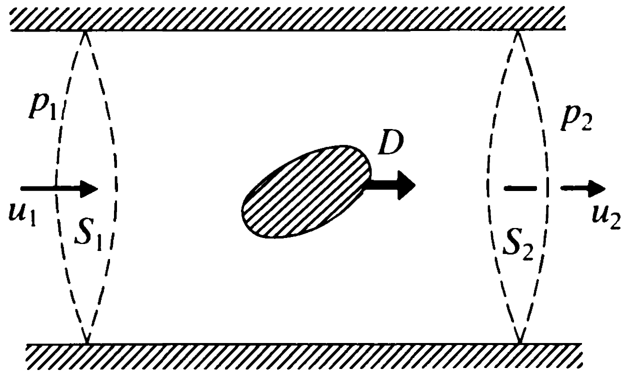

Fig. 4.11. Definition sketch for D'Alembert's paradox.

boundary of this region is

$$\int_{S_1} p_1 \, \mathrm{d}S - \int_{S_2} p_2 \, \mathrm{d}S - D,$$

where D is the drag exerted by the fluid on the obstacle. According to eqn (4.70), this net force is equal to the downstream component of the flux of momentum out of the region, which is

$$\rho \int_{S_2} u_2^2 \, \mathrm{d}S - \rho \int_{S_1} u_1^2 \, \mathrm{d}S,$$

where u_1 and u_2 are the velocity components parallel to the channel walls at S_1 and S_2. Thus

$$D = \int_{S_1} (p_1 + \rho u_1^2) \, \mathrm{d}S - \int_{S_2} (p_2 + \rho u_2^2) \, \mathrm{d}S. \qquad (4.75)$$

Now let us assume that the flow is uniform with speed U_0 far upstream, so that the pressure is a constant, p_0, there. Let us assume that conditions far downstream are similarly uniform; then considerations of mass flow show that the speed must again be U_0 far downstream, as the cross-sectional area of the channel has not changed. Applying the Bernoulli streamline theorem (1.16) to a streamline that runs along the channel walls from $x = -\infty$ to $x = +\infty$ we find that the uniform pressure far downstream must again be p_0.

If, then, we let the cross-sections S_1 and S_2 in Fig. 4.11 recede to infinity in the upstream and downstream directions, we see that the two competing integrals in eqn (4.75) tend to the same limit, and we therefore deduce that

$$D = 0. \tag{4.76}$$

This is one of several ways of presenting *D'Alembert's paradox*, namely that steady, uniform flow of an ideal fluid past a fixed body gives no drag on the body.

Another instructive way of viewing this result is as follows. Consider a finite rigid body which has as its boundary a simple closed surface S, and suppose that it is immersed in an infinite expanse of ideal fluid, the entire system being initially at rest. Suppose that the body now moves with speed $U(t)$ in the negative x-direction. The resulting flow is necessarily irrotational (§5.2), and it is, at any instant, unique (Exercise 5.24), determined entirely by the instantaneous normal component of velocity at the surface of the body. Indeed, at any instant the kinetic energy $T(t)$ of the fluid is proportional to the square of $U(t)$, the constant of proportionality being simply a function of the shape and size of the body (see, e.g., Exercise 5.27). Now, if D is the drag exerted on the body (i.e. the force opposite to the direction of $U(t)$), then the rate at which the fluid does work on the body is $-DU$. Equivalently, the body does work on the fluid at a rate DU, and the only way this energy can appear, in the present circumstances,† is as the kinetic energy of the fluid. So

$$DU = \mathrm{d}T/\mathrm{d}t. \tag{4.77}$$

There is therefore a drag on the body during the starting process, because the body needs to do work to set up all the kinetic energy of the fluid. But suppose that after a certain time the translational velocity U is held constant. D is then zero, according to eqn (4.77), because the kinetic energy of the fluid remains constant (although it is redistributed, of course, in a rather trivial way, as the whole streamline pattern shifts to follow the body).

The above energy argument can be adapted quite easily for 2-D flow past a 2-D object, provided that there is no circulation; if there is circulation round the object the kinetic energy T is typically infinite, and the argument based on eqn (4.77) breaks

† Equation (4.77) does not hold for a viscous fluid, because this energy can then be dissipated (§6.5). Nor does it hold when water waves or sound waves are present, because they can radiate energy to infinity (see, e.g., §3.7).

down. The result nevertheless obtains; according to the Kutta–Joukowski Lift Theorem (4.66) the drag is zero, whether or not there is any circulation.

The result flies in the face of common experience; bodies moving through a fluid are usually subject to a substantial resistance, or drag. In Fig. 4.12 we see the drag on a circular cylinder plotted as a function of the Reynolds number, and it remains substantial even when R is changed from 10^2 to 10^7, which is equivalent to decreasing the viscosity by five orders of magnitude. But then, as the sketches indicate, the flow as a whole shows no sign of settling down to the form in Fig. 4.4(*a*) as $\nu \rightarrow 0$. This is because the mainstream flow speed would, in that event, decrease very substantially along the boundary at the rear of the cylinder, and there would therefore be a strong adverse pressure gradient. An attached boundary layer cannot cope with that (see §2.1), and separation of the boundary layer leads instead to a substantial *wake* behind the cylinder. This wake changes in character with increasing R, as in Fig. 4.12, but shows no sign of disappearing as $R \rightarrow \infty$.

D'Alembert described his result of zero drag as 'a singular paradox'. His original argument (*c.* 1745) was in fact quite different to any of those above, and applied only to flow past

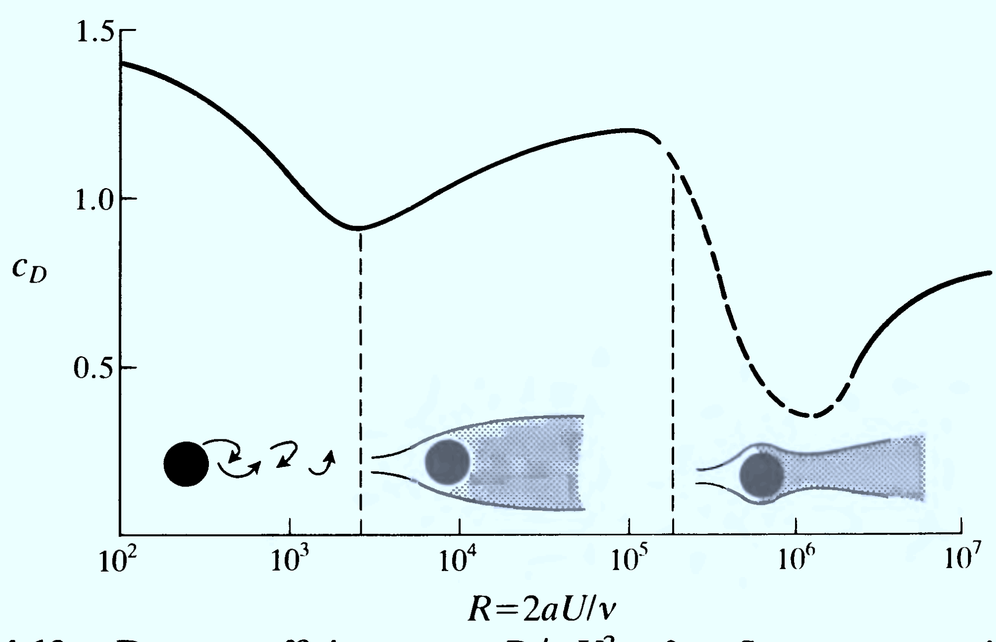

Fig. 4.12. Drag coefficient $c_D = D/\rho U^2 a$ for flow past a circular cylinder of radius a.

bodies, such as a sphere, that have fore–aft symmetry (see Exercise 5.26). Such an appeal to symmetry is unnecessary, and Euler came across the full 'paradox' quite independently. His argument involved consideration of the balance of momentum, but it differed significantly from the first argument presented above, not least because the concept of internal pressure p was not secure at the time (see §6.1).

Lighthill (1986) argues that 'D'Alembert's paradox' might better be designated 'D'Alembert's theorem', for if only a body is designed so as to avoid the kind of boundary layer separation evident in Fig. 4.12, then very low drag forces may indeed be achieved. The key feature in this respect is a long, slowly tapering rear to the body—as with an aerofoil—for this typically implies a very *weak* adverse pressure gradient at the rear of the body, enabling the boundary layer to remain attached. For flow past such a 'streamlined' body c_D is typically $O(R^{-\frac{1}{2}})$ as $R \to \infty$ (see eqn (8.24)).

Exercises

4.1. (i) Show that in a simply connected region of irrotational fluid motion the integral (4.2) is independent of the path between O and P.

(ii) Show that in a simply connected region of two-dimensional, incompressible fluid motion the integral

$$\psi = \int_O^P u\,dy - v\,dx$$

is independent of the path between O and P, and hence serves as a definition of the stream function.

4.2. The velocity field

$$u_r = \frac{Q}{2\pi r}, \qquad u_\theta = 0,$$

where Q is a constant, is called a *line source* flow if $Q > 0$ and a *line sink* if $Q < 0$. Show that it is irrotational and that it satisfies $\nabla \cdot \boldsymbol{u} = 0$, save at $r = 0$, where it is not defined. Find the velocity potential and the stream function, and show that the complex potential is

$$w = \frac{Q}{2\pi} \log z.$$

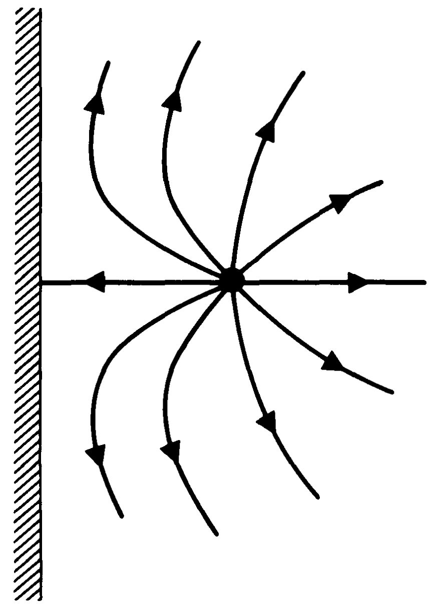

Fig. 4.13. Irrotational flow due to a line source near a wall.

Observe that the stream function is a multivalued function of position. Why does this not contradict part (ii) of Exercise 4.1?

Fluid occupies the region $x \geqslant 0$, and there is a plane rigid boundary at $x = 0$. Find the complex potential for the flow due to a line source at $z = d > 0$, and show that the pressure at $x = 0$ decreases to a minimum at $|y| = d$ and thereafter increases with $|y|$.

[Any attempt to reproduce the flow of Fig. 4.13 at high Reynolds number would be fraught with difficulties. A viscous boundary layer would be present, to satisfy the no-slip condition, but for $|y| > d$ the substantial adverse pressure gradient along the boundary would make separation inevitable (see §2.1). More fundamentally still, there are considerable practical difficulties in producing a line source, as opposed to a line sink, at high Reynolds number. These are more easily seen by considering the corresponding 3-D problem; a point sink can be simulated quite well by sucking at a small tube inserted in the fluid, but blowing down such a tube produces not a point source but a highly directional and usually turbulent jet (see, e.g. Lighthill 1986, pp. 100–103). The streamline pattern in Fig. 4.13 may nevertheless be observed in a *Hele–Shaw cell* (§7.7), although viscous effects are then paramount throughout the whole flow, so the pressure distribution is not given by Bernoulli's equation.]

4.3. An irrotational 2-D flow has stream function $\psi = A(x - c)y$, where A and c are constants. A circular cylinder of radius a is introduced, its centre being at the origin. Find the complex potential, and hence the stream function, of the resulting flow. Use Blasius's theorem (4.62) to calculate the force exerted on the cylinder.

4.4. Show that the problem of irrotational flow past a circular cylinder may be formulated in terms of the velocity potential $\phi(r, \theta)$ as follows:

$$\frac{\partial^2 \phi}{\partial r^2} + \frac{1}{r}\frac{\partial \phi}{\partial r} + \frac{1}{r^2}\frac{\partial^2 \phi}{\partial \theta^2} = 0,$$

with

$$\phi \sim Ur\cos\theta \quad \text{as } r \to \infty, \qquad \partial\phi/\partial r = 0 \quad \text{on } r = a,$$

and obtain the solution (4.33) by using the method of separation of variables.

When there is circulation round the cylinder, derive eqn (4.40), and confirm that the stagnation points vary in position with the parameter B in the manner of Fig. 4.4.

4.5. Establish the expression (4.63) for the moment, $\mathcal{N}$, of forces on a body in irrotational flow, using an argument similar to that for Blasius's theorem.

4.6. By writing $z = a + \varepsilon$ in eqn (4.57) and taking the limit $\varepsilon \to 0$ check that the choice of circulation (4.58) does indeed lead to a finite velocity at the trailing edge.

4.7. According to eqns (4.1) and (4.66), the force on a thin symmetric aerofoil with a sharp trailing edge is

$$\mathscr{L} = \pi\rho U^2 L \sin\alpha$$

in a direction *perpendicular to the uniform stream.* This amounts to a component $\mathscr{L}\cos\alpha$ perpendicular to the aerofoil and a component $\mathscr{L}\sin\alpha$ parallel to the aerofoil, directed towards the leading edge. This latter component is, at first sight, rather curious; it might be thought that the net effect of a pressure distribution on a thin symmetric aerofoil should be almost normal to the aerofoil. That it is not is due to *leading edge suction*, i.e. a severe drop in pressure in the immediate vicinity of the rounded leading edge, this pressure drop being sufficient to make itself felt despite the small thickness of the wing on which it acts.

To see evidence of this, consider the extreme case of flow past a flat plate with circulation, as in Fig. 4.6(*b*) or Fig. 4.15. First, use eqns (4.56) and (4.57), on $z = ae^{i\theta}$, with Γ chosen according to eqn (4.58), to show that the flow speed on the plate is

$$U\left|\cos\alpha \pm \left(\frac{1-s}{1+s}\right)^{\frac{1}{2}}\sin\alpha\right|,$$

where the upper/lower sign corresponds to the upper/lower side of the plate, and s denotes $X/2a$, which therefore runs between -1 at the leading edge and $+1$ at the trailing edge.

Show that the corresponding pressure distributions are

$$p(s) = p(1) - \tfrac{1}{2}\rho U^2\left[\left(\frac{1-s}{1+s}\right)\sin^2\alpha \pm 2\left(\frac{1-s}{1+s}\right)^{\frac{1}{2}}\sin\alpha\cos\alpha\right],$$

(see Fig. 4.14). Note that there is a (negative) pressure singularity at the leading edge, whereas if the leading edge were rounded this pressure drop would be finite.

As far as the force component normal to the plate is concerned, note that the pressure difference across the plate is

$$p_D = 2\rho U^2\left(\frac{1-s}{1+s}\right)^{\frac{1}{2}}\sin\alpha\cos\alpha.$$

This too has a singularity at the leading edge, but it is integrable. Show that

$$\int_{-2a}^{2a} p_D \, \mathrm{d}X = \mathscr{L}\cos\alpha,$$

in keeping with the Kutta–Joukowski Lift Theorem.

Finally, show that eqn (4.65) holds even if there is circulation Γ round the ellipse, and then take the case $c = a$ to show that the torque on a flat plate about the origin is $-\mathscr{L}a\cos\alpha$, i.e. as if the whole lift force $\mathscr{L}$ were

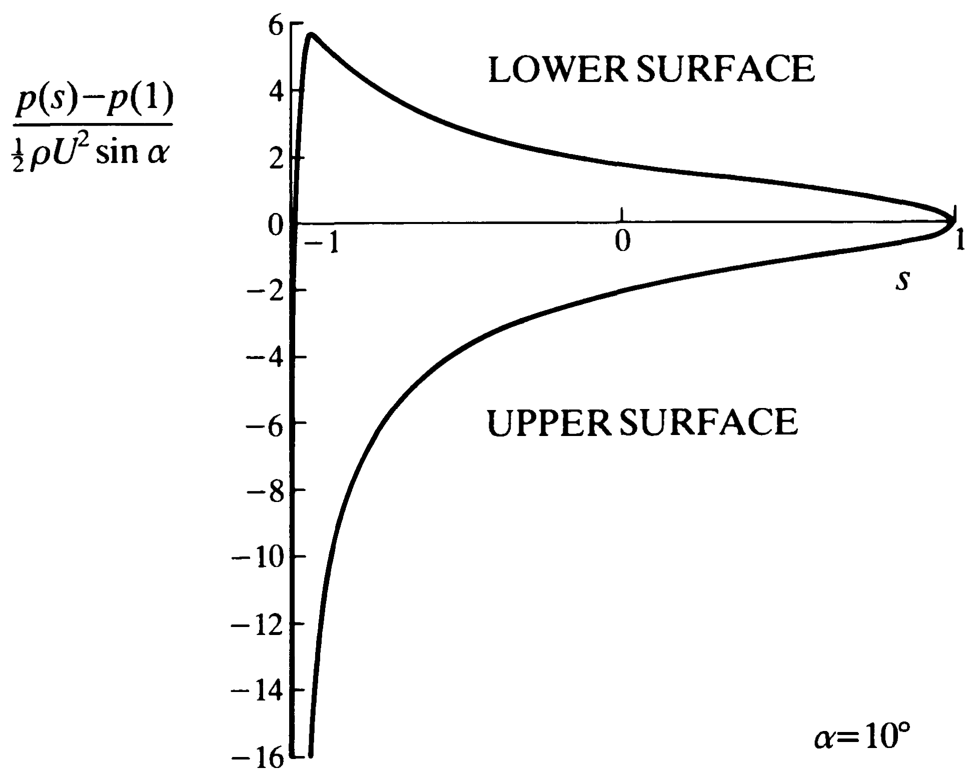

Fig. 4.14. Theoretical pressure distribution on a flat plate at a 10° angle of attack.

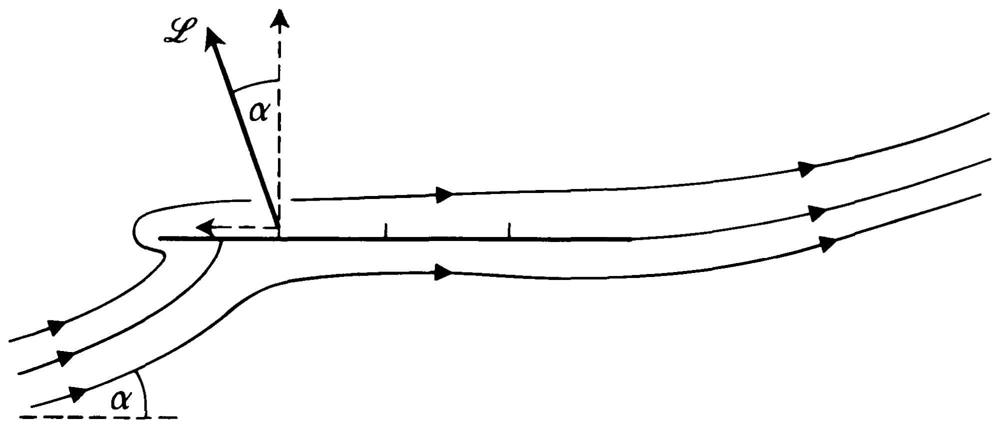

Fig. 4.15. The torque on a flat plate in uniform flow is as if the lift $\mathscr{L}$ were concentrated at a point one-quarter of the way along the plate from the leading edge.

applied at a point one-quarter of the way along the plate, as indicated in Fig. 4.15.

[The fact that this point is independent of α is of practical value, and makes for smooth control of an aircraft.]

4.8. Show that the Joukowski transformation $Z = z + a^2/z$ can be written in the form

$$\frac{Z - 2a}{Z + 2a} = \left(\frac{z - a}{z + a}\right)^2,$$

so that, in particular,

$$\arg(Z - 2a) - \arg(Z + 2a) = 2[\arg(z - a) - \arg(z + a)].$$

Consider the circle in the z-plane which passes through $z = -a$ and $z = a$ and has centre $\mathrm{i}a \cot \beta$. Show that the above transformation takes it into a circular arc between $Z = -2a$ and $Z = 2a$, with subtended angle 2β (Fig. 4.16). Obtain an expression for the complex potential in the Z-plane, when the flow is uniform, speed U, and parallel to the real axis. Show that the velocity will be finite at both the leading and trailing edges if

$$\Gamma = -4\pi U a \cot \beta.$$

[This exceptional circumstance arises only when the undisturbed flow is parallel to the chord line of the arc.]

4.9. Provided that $f'(z_0) \neq 0$, points in the neighbourhood of $z = z_0$ are mapped by $Z = f(z)$, according to Taylor's theorem, in such a way that

$$Z - Z_0 = f'(z_0)(z - z_0) + O(z - z_0)^2,$$

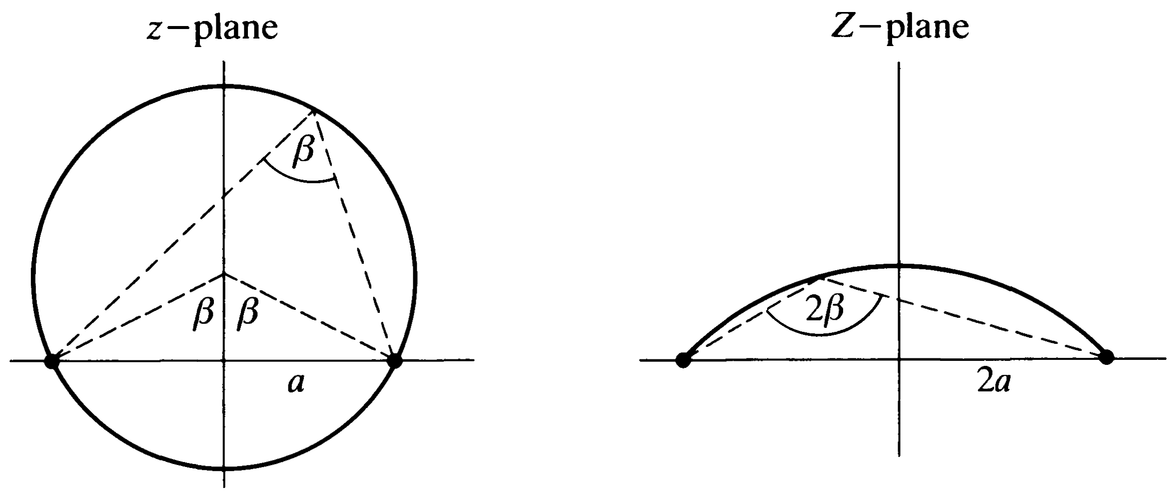

Fig. 4.16. Generation of a circular arc by a Joukowski transformation.

where $Z_0 = f(z_0)$. Use this to show that a line source of strength Q at $z = z_0$ is mapped into a line source of strength Q at $Z = Z_0$, provided that $f'(z_0) \neq 0$.

Fluid occupies the region between two plane rigid boundaries at $y = \pm b$, and there is a line source of strength Q at $z = 0$. Find the complex potential $w(z)$ for the flow

(i) by the method of images,

(ii) by using the mapping $Z = e^{\alpha z}$ with a suitably chosen $\alpha > 0$.

4.10. Use the momentum equation in its integral form (4.70) to show that there is a non-zero drag

$$F_x = \rho\Gamma^2/2d$$

on each of the aerofoils in Fig. 4.10.

Is this at odds with the Kutta–Joukowski Lift Theorem (4.66)?

5 Vortex motion

5.1. Kelvin's circulation theorem

THEOREM. *Let an inviscid, incompressible fluid of constant density be in motion in the presence of a conservative body force* $\boldsymbol{g} = -\nabla\chi$ *per unit mass. Let* $C(t)$ *denote a closed circuit that consists of the same fluid particles as time proceeds (Fig.* 5.1). *Then the circulation*

$$\Gamma = \int_{C(t)} \boldsymbol{u} \cdot \mathrm{d}\boldsymbol{x} \tag{5.1}$$

round $C(t)$ *is independent of time.*

Proof. We appeal to the following lemma:

$$\frac{\mathrm{d}}{\mathrm{d}t}\int_{C(t)} \boldsymbol{u} \cdot \mathrm{d}\boldsymbol{x} = \int_{C(t)} \frac{\mathrm{D}\boldsymbol{u}}{\mathrm{D}t} \cdot \mathrm{d}\boldsymbol{x} \tag{5.2}$$

(Exercise 5.2). Then, by Euler's equation (1.12),

$$\frac{\mathrm{d}\Gamma}{\mathrm{d}t} = -\int_{C(t)} \nabla\left(\frac{p}{\rho} + \chi\right) \cdot \mathrm{d}\boldsymbol{x} = -\left[\frac{p}{\rho} + \chi\right]_C,$$

where the last term denotes the change in $p/\rho + \chi$ on going once round C (see eqn (A.12)). But this change is zero, as p, ρ, and χ are all single-valued functions of position. This proves the theorem.

Notes on the theorem

(a) C denotes a 'dyed' circuit, composed of the same fluid particles as time proceeds; the result is not true in general if C is a closed curve fixed in space.

(b) The conditions of incompressibility and constant density are not essential: Kelvin established his result subject to weaker restrictions (Exercise 5.4).

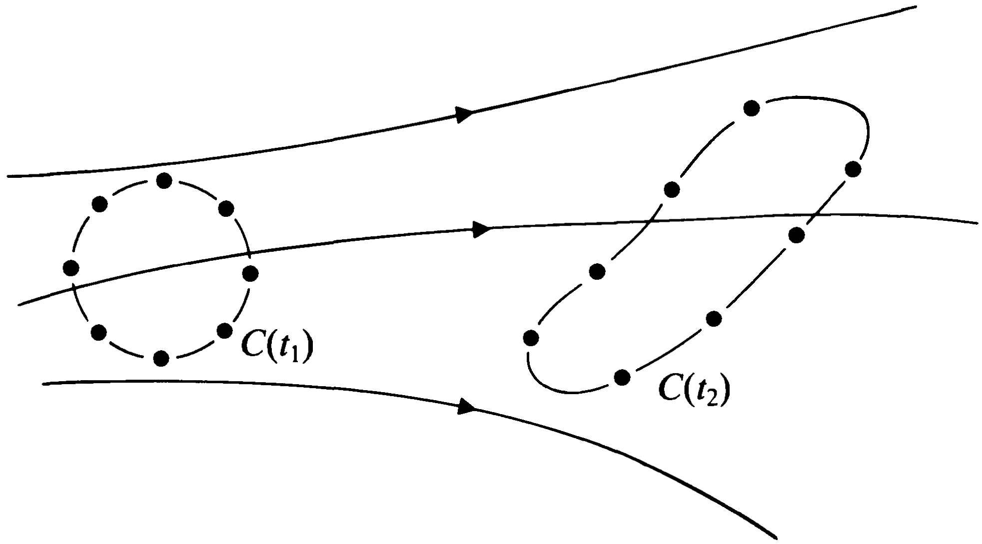

Fig. 5.1. Definition sketch for Kelvin's theorem, showing eight fluid particles along a 'dyed' circuit C at time t_1, and their positions at time t_2.

(c) The theorem does not require the fluid region to be simply connected, i.e. it does not require the dyed circuit C to be spannable by a surface S lying wholly in the fluid.

(d) The inviscid equations of motion enter the proof only in helping to evaluate a line integral round C, so if viscous forces happened to be important elsewhere in the flow, i.e. off the curve C, this would not affect the conclusion that Γ remains constant round C.

The generation of lift on an aerofoil

We mentioned in §1.1 how the shedding of a starting vortex is essential to the generation of lift on an aerofoil, and we now investigate why this should be so.

Consider the situation at a time t after the start. Vorticity and viscous forces will be confined to (i) a thin boundary layer on the aerofoil, (ii) a thin wake, and (iii) the rolled-up 'core' of the starting vortex, as indicated by the shading in Fig. 5.2. Consider now a dyed circuit abcda which is large enough to have been clear of all these regions since the start of the motion. As the original state was one of rest the circulation round that circuit was originally zero. By Kelvin's circulation theorem, then, the circulation round that circuit will still be zero at time t (see especially note (d) above). Thus if we sketch in a line aec—an

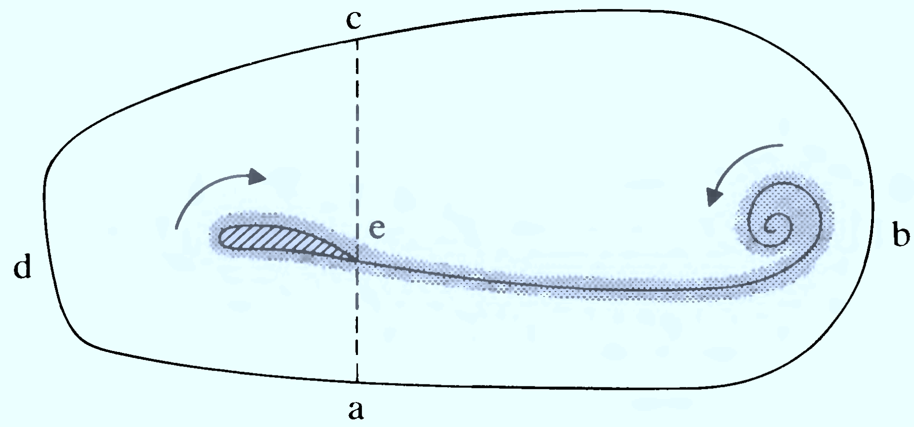

Fig. 5.2. The generation of circulation by means of vortex shedding.

instantaneous line in space at time t such that the curve aecda encloses the aerofoil but not the wake or the starting vortex—then the circulation round aecda must be equal and opposite to that round abcea.

What happens, then, as the aerofoil starts to move, is that positive vorticity is shed in the form of a starting vortex. By Stokes's theorem,

$$\int_S \boldsymbol{\omega} \cdot \boldsymbol{n} \, \mathrm{d}S = \int_C \boldsymbol{u} \cdot \mathrm{d}\boldsymbol{x},$$

this gives a positive circulation round abcea. This in turn implies, by the preceding argument, a negative circulation round aecda, and this circulation is very evident in some classic photographs taken by Prandtl and Tietjens (see, e.g., Batchelor 1967, Plate 13). The vortex shedding continues until the circulation round the aerofoil is sufficient to make the main, irrotational flow smooth at the trailing edge, as in Fig. 1.10(b), at which stage no further net vorticity is shed into the wake from the boundary layers on the upper and lower surfaces of the aerofoil. Thereafter the aerofoil retains its final 'Kutta–Joukowski' value of the circulation.

A novel mechanism of lift generation for hovering insects

An exotic variation on the above theme was discovered by Weis-Fogh (1973, 1975) in the hovering motions of the tiny chalcid wasp *Encarsia formosa* (wing chord ~0.2 mm). This insect claps its wings together, then flings them open about a

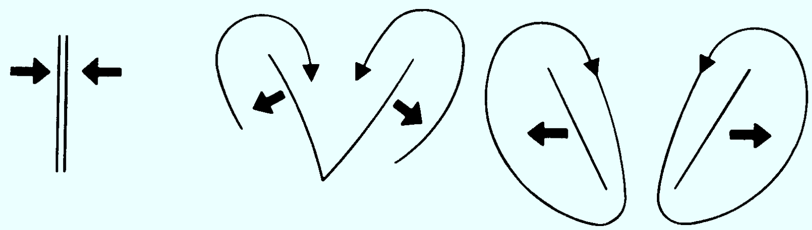

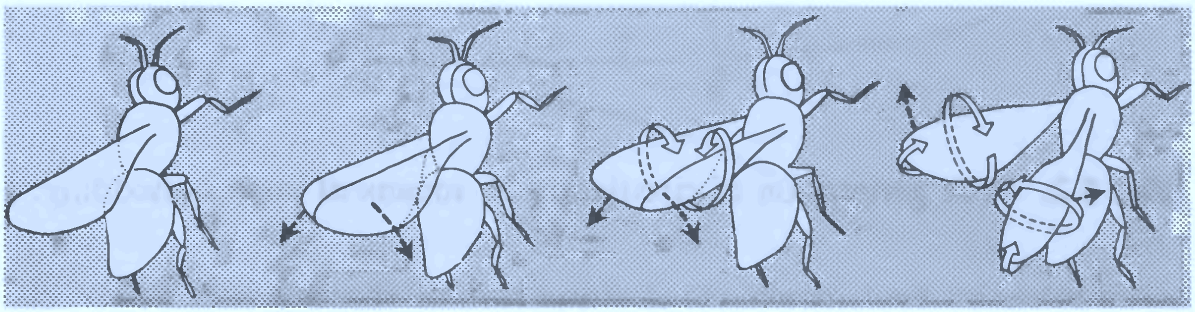

Fig. 5.3. The Weis-Fogh mechanism of lift generation. The first three sketches give a 2-D model of (*a*) the 'clap', (*b*) the 'fling', and (*c*) the parting of the wings. The remaining sketches (after Dalton 1977) show the mechanism in practice, and the final sketch indicates also the flow associated with the vortex (not shown) that extends, in a circular arc, between the wing tips (cf. Fig. 1.12).

horizontal line of contact, so that air has to rush in to fill the gap (Fig. 5.3(*b*)). Then it moves its wings apart, by which time each one has acquired during the 'fling' movement a circulation of the correct sign to give lift in the subsequent motion.

In practice, viscous effects are important, especially in causing large leading-edge separation vortices (see the excellent photographs in Spedding and Maxworthy 1986). Nevertheless, one remarkable feature of this novel lift generation mechanism is that it could work, in principle, in a strictly inviscid fluid (Lighthill 1973). In this sense it differs markedly from the conventional method for lift generation which we have just discussed, for that relies in an essential way on viscous effects for boundary layer formation, separation at the trailing edge, and consequent vortex shedding. In the Weis-Fogh mechanism the circulation round one wing essentially acts as the starting vortex for the other.

At first sight, perhaps, Kelvin's circulation theorem does not permit the situation in Fig. 5.3(*c*) for a strictly inviscid fluid: if one views the circuits there as dyed circuits then the circulations round them must have remained constant. Yet one cannot claim that those circulations are zero, even if the fluid were wholly at rest at stage (a), for neither dyed circuit at stage (c) was a *closed* circuit at stage (b), an unusual circumstance that arises only because the topology of the fluid domain has changed in the meantime.

The word 'meantime' gives, in fact, rather too leisurely an impression; *Encarsia formosa* goes through the sequence in Fig. 5.3 roughly 400 times a second.

5.2. The persistence of irrotational flow

Let an inviscid, incompressible fluid of constant density move in the presence of a conservative body force. Then if a portion of the fluid is initially in irrotational motion, that portion will always be in irrotational motion.

To prove this *Cauchy–Lagrange theorem* suppose that the vorticity $\boldsymbol{\omega} = \nabla \wedge \boldsymbol{u}$ were *not* identically zero throughout that portion of fluid at a later time. By virtue of Stokes's theorem:

$$\int_C \boldsymbol{u} \cdot \mathrm{d}\boldsymbol{x} = \int_S \boldsymbol{\omega} \cdot \boldsymbol{n} \, \mathrm{d}S,$$

and it would then be possible to select some small closed dyed circuit around which the circulation would be non-zero. But this would violate Kelvin's circulation theorem, because the circulation round such a circuit must initially have been zero, on account of Stokes's theorem and the fact that $\boldsymbol{\omega}$ was initially zero. Our initial assumption must therefore be false. This completes the proof.

For 2-D flows the result is obvious from the vorticity equation (1.27); if ω is zero for a portion of the fluid at $t = 0$ then, according to eqn (1.27), ω remains zero for each fluid element constituting that portion for all time t. But in three dimensions the result is not obvious from eqn (1.25), and it is here that the theorem comes into its own. (Although it is of course quite evident that if $\boldsymbol{\omega}$ is everywhere zero at $t = 0$ then $\boldsymbol{\omega} = 0$ everywhere for all t is *one* solution of eqn (1.25).)

Irrotational flows are important, then, even in three dimensions. The velocity field can then be written as

$$\boldsymbol{u} = \nabla \phi, \tag{5.3}$$

and ϕ will be a single-valued function of position when the flow region is simply connected (see §4.2). [In other circumstances—as, for example, with the irrotational part of the flow due to a vortex ring (Fig. 5.7(*b*))—ϕ may be multivalued.] As the fluid is incompressible, $\nabla \cdot \boldsymbol{u} = 0$, so ϕ satisfies *Laplace's equation*

$$\nabla^2 \phi = 0. \tag{5.4}$$

The general theory of irrotational flow is a classical and important part of fluid dynamics, and we explore something of it in Exercises 5.23–5.29. We should emphasize, however, that much of the present chapter is concerned with fluid motions in which the vorticity is *not* zero, in which case there is no such thing as a velocity potential ϕ and $\boldsymbol{u}$ *cannot* be written in the form (5.3).

5.3. The Helmholtz vortex theorems

A *vortex line* is, at any particular time t, a curve which has the same direction as the vorticity vector

$$\boldsymbol{\omega} = \nabla \wedge \boldsymbol{u} \tag{5.5}$$

at each point. Mathematically, then, a vortex line $x = x(s)$, $y = y(s)$, $z = z(s)$, is obtained by solving

$$\frac{\mathrm{d}x/\mathrm{d}s}{\omega_x} = \frac{\mathrm{d}y/\mathrm{d}s}{\omega_y} = \frac{\mathrm{d}z/\mathrm{d}s}{\omega_z}$$

at a particular time t.

The vortex lines which pass through some simple closed curve in space are said to form the boundary of a *vortex tube* (Fig. 5.4(*a*)).

Suppose now that we have an *inviscid, incompressible fluid of constant density moving in the presence of a conservative body force* (so that Kelvin's circulation theorem applies). Then

(1) *The fluid elements that lie on a vortex line at some instant continue to lie on a vortex line, i.e. vortex lines 'move with the fluid'.*

An immediate consequence of this is that vortex tubes move with the fluid in a like manner.

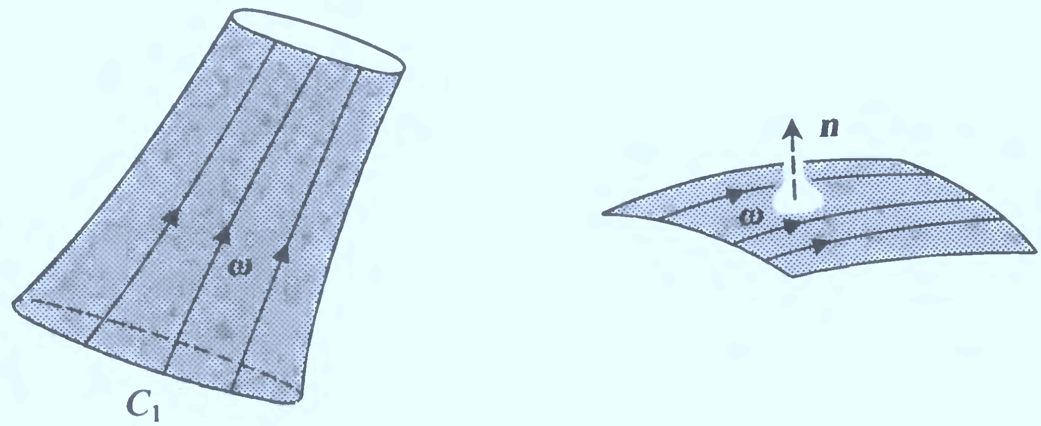

(*a*) (*b*)

Fig. 5.4. (*a*) A vortex tube. (*b*) A vortex surface.

(2) *The quantity*

$$\Gamma = \int_S \boldsymbol{\omega} \cdot \boldsymbol{n} \, \mathrm{d}S \tag{5.6}$$

is the same for all cross-sections S of a vortex tube. Furthermore, Γ is independent of time.

The quantity Γ is therefore a conserved property of the tube as a whole, called the *strength* of the tube.

Proof of (1). We first define a *vortex surface* as a surface such that $\boldsymbol{\omega}$ is tangent to the surface at every point (Fig. 5.4(b)). The proof proceeds by viewing the vortex line, in its initial configuration, as the intersection of two vortex surfaces. Mark the particles which occupy one of the vortex surfaces, at $t = 0$, with dye. Consider a closed circuit C made up of a particular set of dyed particles and spanned by a portion S_* of the vortex surface. At $t = 0$ the circulation round C is zero, for by Stokes's theorem

$$\int_C \boldsymbol{u} \cdot \mathrm{d}\boldsymbol{x} = \int_{S_*} \boldsymbol{\omega} \cdot \boldsymbol{n} \, \mathrm{d}S,$$

and $\boldsymbol{\omega} \cdot \boldsymbol{n}$ is zero on S_*. Now, as time proceeds the dyed sheet of fluid will deform, but the circulation round C will remain zero, by Kelvin's circulation theorem. This being so for all circuits such as C it follows, by using Stokes's theorem again, that $\boldsymbol{\omega} \cdot \boldsymbol{n}$ will remain zero at all points of the dyed sheet of fluid. That sheet therefore remains a vortex surface as time proceeds. The proof is completed by noting that the intersection of two such dyed sheets therefore remains the intersection of two vortex surfaces, i.e. it remains a vortex line.

Proof of (2). The statement that Γ is independent of the cross-section S has nothing to do with the equations of motion, but is simply a consequence of the fact that the vorticity $\boldsymbol{\omega} = \nabla \wedge \boldsymbol{u}$ is divergence-free (Exercise 5.5). The statement that Γ is independent of time follows on considering a circuit, such as C_1 in Fig. 5.4(a), composed of fluid particles which lie on the wall of the vortex tube and encircle it. By Stokes's theorem, Γ is the circulation round C_1, and by Kelvin's circulation theorem this remains constant as time proceeds.

It is instructive to consider the particular case of a *thin* vortex tube in which $\boldsymbol{\omega}$ is virtually constant across any particular cross-section. In that case Γ is essentially just the product $\omega\, \delta S$, where δS is the normal cross-section of the tube. But δS is also the normal cross-section of the fluid continually occupying the tube, and as the fluid must conserve its volume δS will vary inversely with the length l of a small section of the tube. Thus the vorticity ω varies in proportion to l; stretching of vortex tubes by the fluid motion intensifies the local vorticity.

In a tornado, for example, the strong thermal updraughts into the thunderclouds overhead produce intense stretching of vortex tubes, and hence the potentially devastating rotary motions observed. The funnel cloud serves, in fact, as a direct marker of the vortex tube, rather than the air occupying it, because it essentially marks regions of very low pressure (where the air rapidly expands and condenses), and these in turn are located in the core of the vortex, where all the vorticity is concentrated (see Exercise 1.3). Thus when the thunderclouds move on, and the funnel cloud tips over in the manner of Fig. 5.5, we have a vivid illustration of Helmholtz's first vortex theorem at work.

In contrast, it is the shortening of vortex tubes that is responsible for the gradual 'spin-down' of a stirred cup of tea (Fig. 5.6). The main body of the fluid is essentially inviscid and in rapid rotation, the centrifugal force being (almost) balanced by a radially inward pressure gradient. This pressure gradient also imposes itself throughout the thin viscous boundary layer on the

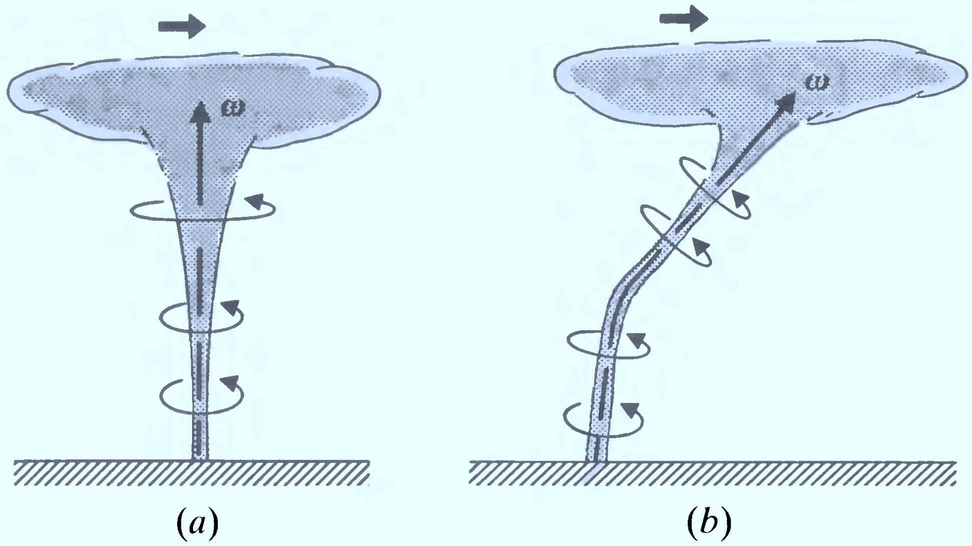

Fig. 5.5. The deformation of a tornado as the thunderclouds move overhead.

bottom of the cup, where it is stronger than required, for the fluid in the boundary layer rotates much less rapidly. That fluid therefore spirals inward (as evinced by the way in which tea leaves on the bottom of the cup congregate in the middle), and eventually turns up and out of the boundary layer, as in Fig. 5.6. In this way vortex tubes in the main body of the fluid become shorter and expand in cross-section, so that the vorticity decreases with time. It is by this subtle mixture of inviscid and viscous dynamics that the apparently innocuous spin-down of a stirred cup of tea is achieved (see §8.5).

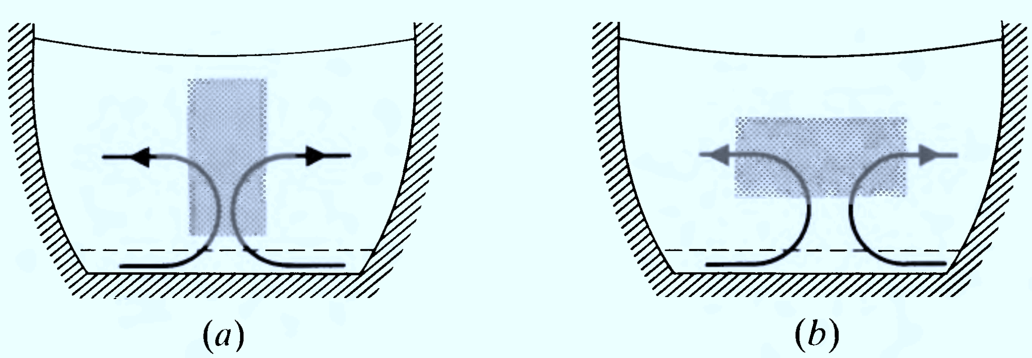

Fig. 5.6. The secondary circulation in a stirred cup of tea is driven by the bottom boundary layer (beneath the dotted line) and turns a tall, thin column of 'dyed' fluid into a short, fat one, so decreasing its angular velocity.

The Helmholtz vortex theorems and the vorticity equation

The vortex theorems above were first given by Helmholtz in 1858, but Kelvin did not obtain and publish his circulation theorem until 1867. It goes without saying, then, that Helmholtz took a different route; he appealed directly to the vorticity equation (1.25):

$$\frac{\mathrm{D}\boldsymbol{\omega}}{\mathrm{D}t} = (\boldsymbol{\omega} \cdot \nabla)\boldsymbol{u}. \tag{5.7}$$

We will not give his actual argument here,† but consider instead the relationship between eqn (5.7) and the vortex theorems in some simple specific cases.

It is possible, for instance, to see by inspection of eqn (5.7) how stretching the fluid that lies along a vortex line leads to an intensification of the local vorticity field. Suppose, for example, that the vortex lines are almost in the z-direction, as in Fig. 5.5(*a*), so that $\boldsymbol{\omega} \doteqdot \omega\boldsymbol{k}$ and

$$\frac{\mathrm{D}\boldsymbol{\omega}}{\mathrm{D}t} \doteqdot \omega\frac{\partial \boldsymbol{u}}{\partial z}. \tag{5.8}$$

The z-component of this equation gives

$$\frac{\mathrm{D}\omega}{\mathrm{D}t} \doteqdot \omega\frac{\partial w}{\partial z},$$

and the vorticity of a particular fluid element therefore increases with time if $\partial w/\partial z > 0$, i.e. if the instantaneous vertical velocity increases with z. Such is the case, of course, if fluid elements are being stretched in the vertical direction, whereas if they were being carried up or down without any vertical stretching or squashing, w would be independent of z.

A particularly simple case is that of 2-D flow. Vortex tubes are aligned with the z-axis, and $w = 0$. There is no stretching of vortex tubes, and

$$\frac{\mathrm{D}\omega}{\mathrm{D}t} = 0, \tag{5.9}$$

† It in fact contains a flaw, which may however be corrected (see, e.g. Lamb 1932, p. 206; Rosenhead 1963, pp. 122–123).

so that the vorticity ω of any particular fluid element is conserved.

A more revealing case in the present context is that of *axisymmetric* flow:

$$\boldsymbol{u} = u_R(R, z, t)\boldsymbol{e}_R + u_z(R, z, t)\boldsymbol{e}_z, \tag{5.10}$$

where (R, ϕ, z) denote cylindrical polar coordinates.† The velocity components are then independent of ϕ, the streamlines all lie in planes $\phi = \text{constant}$, and the vorticity is $\boldsymbol{\omega} = \omega\boldsymbol{e}_\phi$, where

$$\omega = \frac{\partial u_R}{\partial z} - \frac{\partial u_z}{\partial R}. \tag{5.11}$$

In axisymmetric flow the vortex tubes are therefore ring-shaped, around the symmetry axis. According to the first vortex theorem they move with the fluid. In doing so they will, in general, expand and contract about the symmetry axis, and thus change in length. As the fluid is incompressible the cross-sectional area δS of a thin tube will be in inverse proportion to the length $2\pi R$ of the tube. But the second vortex theorem implies that $\omega\,\delta S$ will be a constant, so we conclude that ω will be proportional to the length of the tube $2\pi R$. We leave it as an instructive exercise (Exercise 5.7) to show that in the case of axisymmetric flow the vorticity equation (5.7) reduces to

$$\frac{\mathrm{D}}{\mathrm{D}t}\left(\frac{\omega}{R}\right) = 0, \tag{5.12}$$

which expresses just this result, that the vorticity of any particular fluid element changes in proportion to R as time proceeds.

When, in axisymmetric flow, an isolated vortex tube is surrounded by irrotational motion, we speak of it as a *vortex ring*. The familiar 'smoke-ring' is perhaps the most common example, and provides a vivid illustration of the Helmholtz vortex theorems, though the vortex core typically occupies only a fraction of the smoke ring as a whole (see Fig. 5.7).

---

† This is not our usual notation, as we are shortly to use spherical polar coordinates (r, θ, ϕ) for axisymmetric flow. It seemed best not to have the same symbol meaning two different things in the space of a few pages. Thus ϕ has the same meaning in the two cases, and $R = r \sin\theta$.

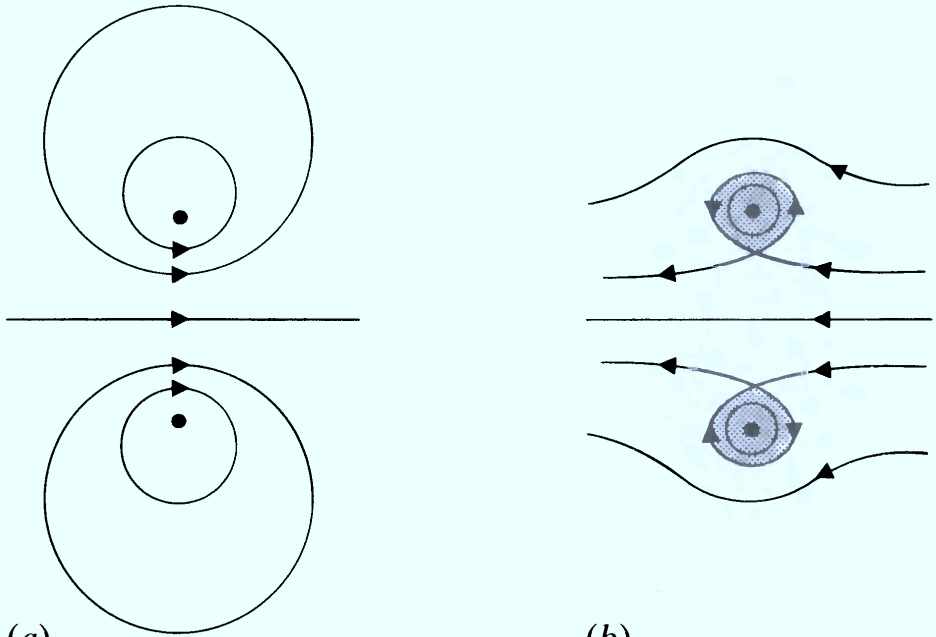

Fig. 5.7. Flow due to a vortex ring (*a*) relative to a fixed frame and (*b*) relative to a frame moving with the vortex core. Shading denotes smoke, in the case of a smoke ring, while the vortex core is indicated by the black dots.

5.4. Vortex rings

We showed in §5.1 how Kelvin's circulation theorem plays a key part in the mechanism by which an aircraft obtains lift at take-off. While this is one of the theorem's most elegant and significant applications, it is not of course what Kelvin had in mind in 1867. What he did have in mind is quite extraordinary, but clear enough from the following:

Jan. 22, 1867.

My dear Helmholtz—I have allowed too long a time to pass without thanking you for your kind letter .... Just now, ... *Wirbelbewegungen* have displaced everything else, since a few days ago Tait showed me in Edinburgh a magnificent way of producing them. Take one side (or the lid) off a box (any old packing-box will serve) and cut a large hole in the opposite side. Stop the open side loosely with a piece of cloth, and strike the middle of the cloth with your hand. If you leave anything smoking in the box, you will see a magnificent ring shot out by every blow. A piece of burning phosphorus gives very good smoke for the purpose; but I think nitric acid with pieces of zinc thrown into it, in the bottom of the box, and cloth wet with ammonia, or a large open dish of ammonia beside it, will answer better. The nitrite of ammonia makes fine white clouds in the air, which, I think, will be less pungent and disagreeable than the smoke from the phosphorus. We sometimes can make one ring shoot through another, illustrating perfectly your description; when one ring passes near another, each is much disturbed, and is seen to be in a state of violent vibration for a few seconds, till it settles again into its circular form. The accuracy of the circular form of the whole ring, and the fineness and roundness of the section, are beautifully seen. If you try it, you will easily make rings of a foot in diameter and an inch or so in section, and be able to follow them and see the constituent rotary motion. The vibrations make a beautiful subject for mathematical work. The solution for the longitudinal vibration of a straight vortex column comes out easily enough. The absolute permanence of the rotation, and the unchangeable relation you have proved between it and the portion of the fluid once acquiring such motion in a perfect fluid, shows that if there is a perfect fluid all through space, constituting the substance of all matter, a vortex-ring would be as permanent as the solid hard atoms assumed by Lucretius and his followers (and predecessors) to account for the permanent properties of bodies (as gold, lead, etc.) and the differences of their characters. Thus, if two vortex-rings were once created in a perfect fluid, passing through one another like links of a chain, they never could come into collision, or break one another, they would form an indestructible atom; every variety of combinations might exist. Thus a long chain of vortex-rings, or three rings, each running through each of the other, would give each very characteristic reactions upon other such kinetic atoms.

This atomic theory,† 40 years ahead of that of Niels Bohr, was no speculative sideline to Kelvin's hydrodynamic researches at the time; it was the main impetus behind them, and in the opening sentence of his 1867 paper he more or less says as much.

One hundred and twenty years later, vortex rings still exercise a certain fascination, although more modest and less dangerous ways of producing them are perhaps to be recommended. All that is needed is some arrangement for discharging smoke through a circular hole in a plane rigid boundary, where separation of the boundary layer can take place and be followed by the rolling up of the consequent vortex sheet (Fig. 5.9). Any simple apparatus which achieves this will suffice; I employ a syringe of the kind commonly used to squeeze icing on to cakes.

† Atiyah (1988) observes that one particular notion in this theory—that of using topology as a source of stability—may be said to have surfaced again in modern physics, albeit in a different guise.

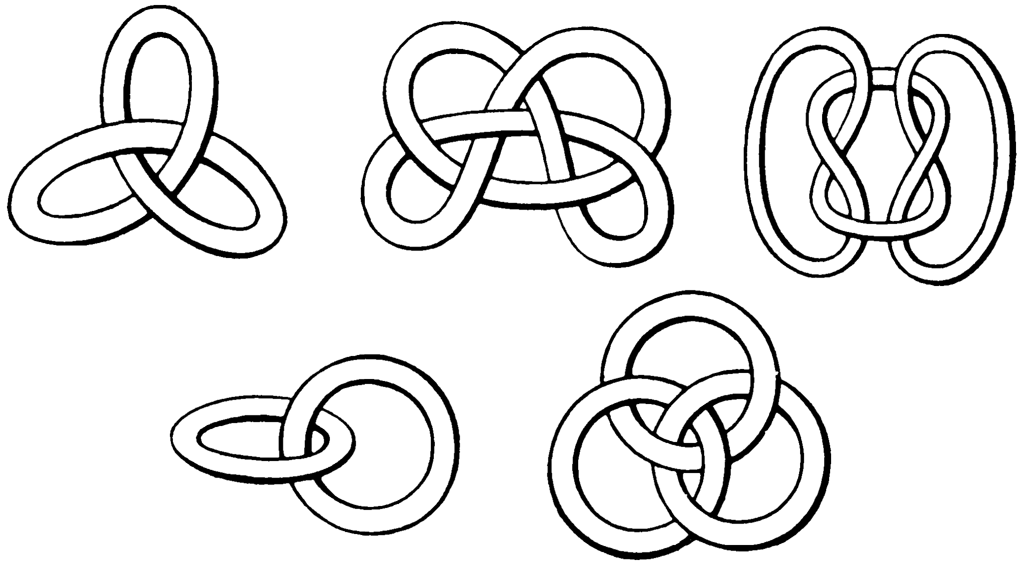

Fig. 5.8. Kelvin's sketches of knotted and linked vortex rings, the basis for his 'vortex atom' theory of matter.

A satisfactory procedure, having detached the nozzle itself, is as follows. Push the piston fully in, then puff cigar smoke through the circular hole while rapidly withdrawing the piston, so that the smoke is sucked into the syringe. As soon as the piston is fully withdrawn, put a hand over the hole to keep the smoke in. Allow a few moments for the motions inside to die down, and then generate vortex rings by holding the cylinder horizontally and giving the piston short, sharp taps. Each ring should travel a foot or so while maintaining its form, provided that the surrounding air is fairly still.

Helmholtz considered vortex rings in his 1858 paper, and after deducing that rings of smaller radius travel faster, went on:

> We can ... see how two ring-formed vortex filaments having the same axis would mutually affect each other, since each, in addition to its proper motion, has that of its elements of fluid as produced by the other . . .

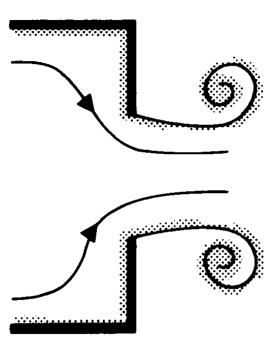

Fig. 5.9. Generation of a vortex ring by the discharge of fluid through a circular hole.

> If they have equal radii and equal and opposite angular velocities, they will approach each other and widen one another; so that finally, when they are very near each other, their velocity of approach becomes smaller and smaller, and their rate of widening faster and faster. If they are perfectly symmetrical, the velocity of fluid elements midway between them parallel to the axis is zero. Here, then, we might imagine a rigid plane to be inserted, which would not disturb the motion, and so obtain the case of a vortex-ring which encounters a fixed plane.

The last sentence is, of course, an interesting example of the method of images, while in saying earlier 'they will approach each other *and widen one another*' Helmholtz is applying his first vortex theorem.

He considers, too, the case when the vortex rings are travelling in the same direction. On the same basis he deduces:

> . . . the foremost widens and travels more slowly, the pursuer shrinks and travels faster, till finally, if their velocities are not too different, it overtakes the first and penetrates it. Then the same game goes on in the opposite order, so that the rings pass through each other alternately.

Good photographs of this 'leap-frogging' phenomenon may be found in Yamada and Matsui (1978), in Oshima (1978) and on p. 46 of van Dyke (1982). In practice, of course, viscous effects act to stop such leap-frogging from continuing indefinitely; indeed they have profound effects, more generally, on the behaviour of real vortex rings (Maxworthy 1972).

Kelvin was of course well aware that real vortex rings do not, on account of viscous effects, wholly retain their identity in the manner indicated by Helmholtz's vortex theorems. One nevertheless wonders, given his hopes for the theory of vortex atoms, what he would have made of an experiment by Oshima and Asaka (1975) in which a red vortex ring and a yellow vortex ring (in water) collide at a certain angle. The rings merge, then break up again into two separate rings, each half yellow and half red. The way in which they do this is indicated in Fig. 5.10. In (*a*) the vortex rings are coming towards us, but they are also approaching one another. In (*b*) they collide, and after a distortion (*c*) of the resulting (single) vortex ring two separate rings are formed (*d*). These come towards us but move apart in a plane at right angles to the plane of approach. Oshima and Asaka provide excellent photographs of this collision process, and further photographs and analysis may be found in Fohl and Turner (1975).

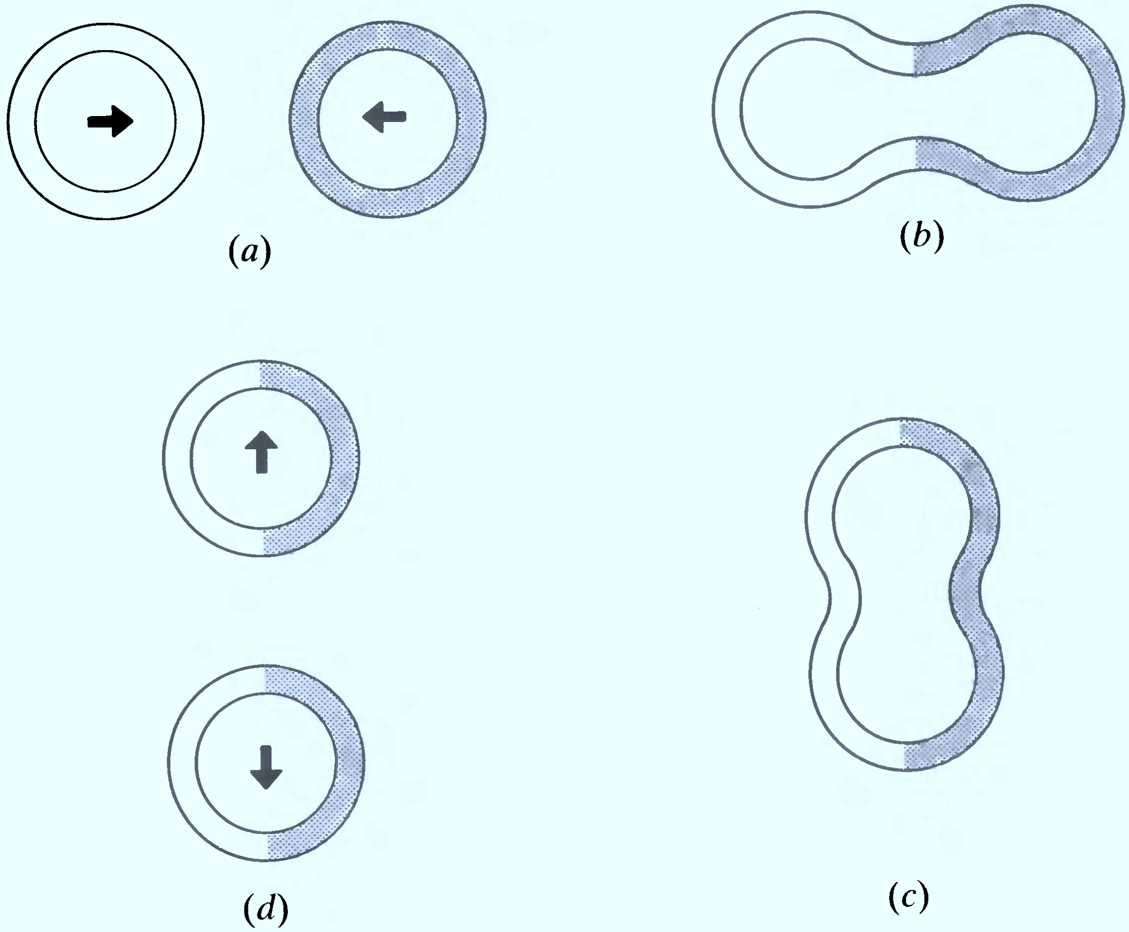

Fig. 5.10. The collision of two viscous vortex rings.

Even within the framework of strictly inviscid theory there are subtle aspects of vortex rings which have taken a long time to emerge. Kelvin himself expressed the view that 'the known phenomena of . . . smoke rings . . . convinces . . . us . . . that the steady configuration . . . is stable', and J. J. Thomson purported to demonstrate as much in his 1883 essay, *A treatise on vortex motion*. But Widnall and Tsai (1977) have carried out a more accurate calculation, and have shown that a vortex ring is in fact unstable, even according to ideal flow theory. The instability takes the form of bending waves around the perimeter, and these grow in amplitude as time proceeds (Fig. 5.11).

5.5. Axisymmetric flow

The uniform motion of a vortex ring—let alone its instability—presents theoretical difficulties, but there is one particular circumstance in which it is quite easy to calculate the self-induced motion of an isolated, axisymmetric patch of vorticity. Before doing this we introduce one or two concepts that are of more general value for axisymmetric flow.

6 The Navier–Stokes equations

6.1 Introduction

In Book II of the *Principia* (1687) Newton writes:

SECTION IX

The circular motion of fluids

HYPOTHESIS

The resistance arising from the want of lubricity in the parts of a fluid is, other things being equal, proportional to the velocity with which the parts of the fluid are separated from one another.

PROPOSITION LI. THEOREM XXXIX

If a solid cylinder infinitely long, in an uniform and infinite fluid, revolves with an uniform motion about an axis given in position, and the fluid be forced round by only this impulse of the cylinder, and every part of the fluid continues uniformly in its motion: I say, that the periodic times of the parts of the fluid are as their distances from the axis of the cylinder.

This is the essence of what Newton has to say about viscous flow. The hypothesis, of course, gets the subject off to a good start, but it is contained and applied wholly within a section on the *circular* motion of fluids, and it is immediately followed by a proposition which is false; the final statement implies that u_θ is independent of r, whereas the correct conclusion, on the basis of Newton's own hypothesis, is that u_θ is inversely proportional to r (see Exercise 2.8). This error gives one small indication of how rudimentary fluid mechanics was at the time, even in the hands of a great master.

Indeed, setting viscous effects aside for a moment, it was not until about 1743, when John Bernoulli published his *Hydraulica*, that the concept of internal pressure was used with clarity and confidence in the study of moving fluids. Furthermore, in spite of all Newton's work, the full generality of the basic principles of mechanics did not emerge until 1752, when Euler advanced

> *The principle of linear momentum*: the total force on a body is equal to the rate of change of the total momentum of the body,

with the clear understanding that the term 'body' might be applied to each and every part of a continuous medium such as a fluid or elastic solid. In 1755 Euler combined this with the concept of internal pressure to obtain his equations of motion for an inviscid fluid (1.12), the achievement being all the greater because he was having to formulate the calculus of partial derivatives as he went along. It was Euler, too, who put forward in 1775

> *The principle of moment of momentum*: the total torque on a body about some fixed point is equal to the rate of change of the moment of momentum of the body about that same point.

He recognized this at the time as an equally general, but quite independent, law of mechanics (see Truesdell 1968).

The next key steps were taken in 1822, when Cauchy introduced the concept of the *stress tensor*, and combined it with Euler's laws of mechanics to construct a general theoretical framework for the motion of any continuous medium. To study, say, a Newtonian viscous fluid it became necessary only to add the appropriate *constitutive relation* describing its physical properties. Yet it was not until 1845, a full 158 years after the *Principia*, that Stokes extended Newton's original hypothesis in a wholly rational way to obtain that constitutive relation, so deriving what we now term the Navier–Stokes equations.†

6.2. The stress tensor

In this section and the next we describe Cauchy's theory. While we use freely the term 'fluid' in what follows, the formalism applies equally well to any continuous deformable medium.

† In recognition of the fact that Navier obtained the correct equations of motion (rather earlier than Stokes), but by making assumptions about the molecular basis of viscous effects which have not stood the test of time.

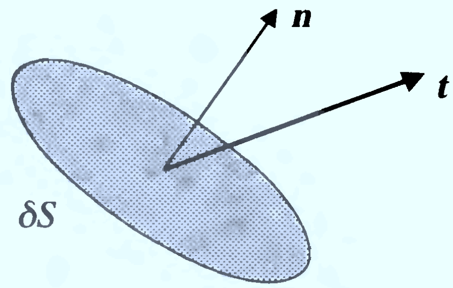

Fig. 6.1. The stress vector.

The stress vector

Let $\boldsymbol{x}$ denote the position vector of some fixed point in the fluid, and let δS be a small geometrical surface element, unit normal $\boldsymbol{n}$, drawn through $\boldsymbol{x}$. Consider the force exerted on this surface *by* the fluid *towards which* $\boldsymbol{n}$ is directed.

We assume that this force is

$$\boldsymbol{t}\,\delta S, \tag{6.1}$$

where the *stress vector* $\boldsymbol{t}$, so defined, depends on the surface element in question only through its normal $\boldsymbol{n}$. For an inviscid fluid, for example, $\boldsymbol{t} = -p(\boldsymbol{x}, t)\boldsymbol{n}$ (see eqn (1.10)), but more generally we expect $\boldsymbol{t}$ to have components both tangential and normal to δS.

Definition of nine local quantities T_{ij}

The nine elements T_{ij} of the *stress tensor* are defined at any point, relative to rectangular Cartesian coordinates, as follows:

> T_{ij} *is the i-component of stress on a surface element* δS *which has a normal* $\boldsymbol{n}$ *pointing in the j-direction* (6.2)

(see Fig. 6.2).

The stress on a small surface element of arbitrary orientation

Consider the stress $\boldsymbol{t}$ on a small surface element δS with unit normal $\boldsymbol{n}$. We wish to demonstrate that the components t_i of the stress are given in terms of the components T_{ij} of the stress tensor by

$$t_i = T_{ij}n_j, \tag{6.3}$$

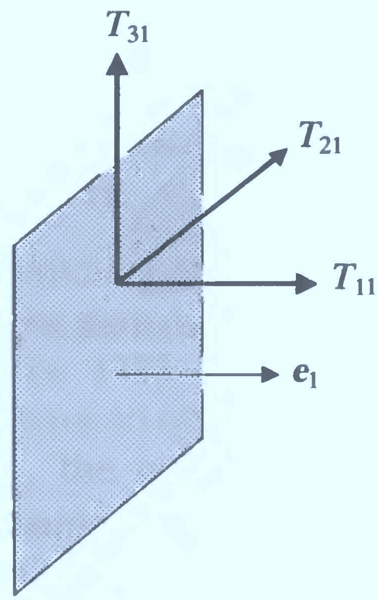

Fig. 6.2. Three components of the stress tensor T_{ij}.

where summation over $j = 1, 2, 3$ is understood by virtue of the repeated suffix.

To do this we take δS to be the large face of the tetrahedron in Fig. 6.3, and apply the principle of linear momentum to the fluid that momentarily occupies the tetrahedron. Consider the i-component of force on the fluid element. That exerted by the surrounding fluid on the main face is $t_i\,\delta S$. The i-component of stress exerted by the surrounding fluid on the face which is

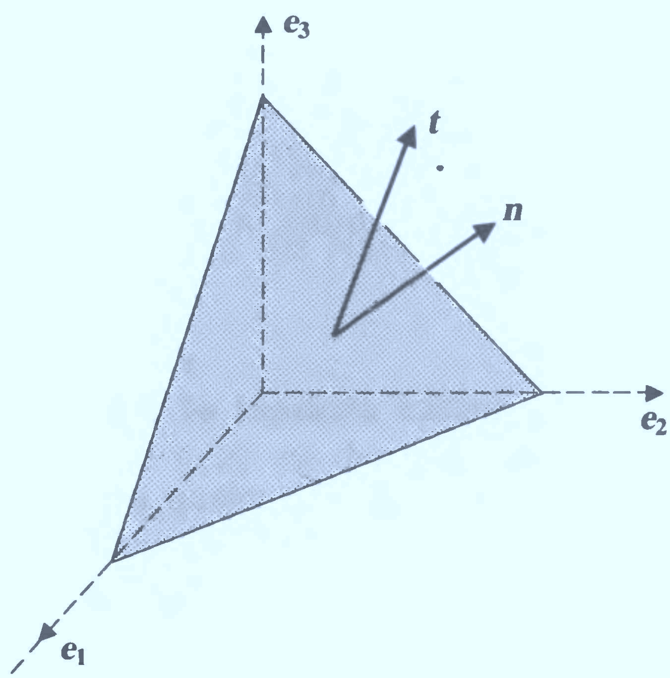

Fig. 6.3. Definition sketch for the proof of eqn (6.3).

normal to $\boldsymbol{e}_1$ is $-T_{i1}$, because the normal $\boldsymbol{n}$ to that surface is pointing in the $-\boldsymbol{e}_1$ direction, according to the conventions established above in the definition of the stress vector and stress tensor. Now, the area of the face which is normal to $\boldsymbol{e}_1$ is, by vector algebra or elementary geometry, $n_1\,\delta S$, where $\boldsymbol{n}$ denotes the unit outward normal to the large face. The i-component of force on the face which is normal to $\boldsymbol{e}_1$ is therefore $-T_{i1}n_1\,\delta S$. A similar argument holds for the remaining two faces. The i-component of the force exerted on the element by the surrounding fluid is therefore

$$(t_i - T_{ij}n_j)\,\delta S,$$

summation over j being understood.

This force, together with a body force $\rho\boldsymbol{g}\,\delta V$, will be equal to the mass $\rho\,\delta V$ of the element multiplied by its (finite) acceleration. Now let the linear dimension L of the tetrahedron tend to zero, while maintaining the orientation $\boldsymbol{n}$ of its large surface. As δV is proportional to L^3 and δS is proportional to L^2, it follows that $t_i = T_{ij}n_j$, as claimed above.

6.3. Cauchy's equation of motion

Having developed the notion of the stress tensor, Cauchy obtained the general equation of motion for any continuous medium:

$$\rho\frac{\mathrm{D}u_i}{\mathrm{D}t} = \frac{\partial T_{ij}}{\partial x_j} + \rho g_i. \tag{6.4}$$

To establish this we consider the ith component of force exerted, by the surrounding fluid, on some dyed blob of fluid with surface S. This is

$$\int_S t_i\,\mathrm{d}S = \int_S T_{ij}n_j\,\mathrm{d}S = \int_V \frac{\partial T_{ij}}{\partial x_j}\,\mathrm{d}V, \tag{6.5}$$

where we have used eqn (6.3) together with the divergence theorem. If we consider a *small* blob of fluid, then, $\partial T_{ij}/\partial x_j$ will be almost constant throughout it, and the surrounding fluid will exert on it a force having an i-component which is $\partial T_{ij}/\partial x_j$ multiplied by the volume of the blob δV. If there is also a body force $\boldsymbol{g}$ per unit mass, equating the total force on the small blob to the rate of change of its momentum gives eqn (6.4), bearing in mind that the mass $\rho\,\delta V$ of the blob is conserved.

Reynolds's transport theorem

This theorem is about rates of change of volume integrals over finite 'dyed' blobs of fluid, and it provides, in particular, a pleasing alternative derivation of eqn (6.4). The theorem states that

$$\frac{\mathrm{d}}{\mathrm{d}t}\int_{V(t)} G\,\mathrm{d}V = \int_{V(t)} \left(\frac{\mathrm{D}G}{\mathrm{D}t} + G\,\nabla\cdot\boldsymbol{u}\right)\mathrm{d}V, \tag{6.6a}$$

where $G(\boldsymbol{x}, t)$ is any scalar or vector function and $V(t)$ denotes the region of space occupied by a finite, deforming blob of fluid.

A strict proof of this result may be found in Exercise 6.13. For the present we simply cast it into a different and more obvious form by writing $G = \rho F$. Then it follows that for any function $F(\boldsymbol{x}, t)$:

$$\frac{\mathrm{d}}{\mathrm{d}t}\int_{V(t)} F\rho\,\mathrm{d}V = \int_{V(t)} \frac{\mathrm{D}F}{\mathrm{D}t}\rho\,\mathrm{d}V \tag{6.6b}$$

(see Exercise 6.5). This is no surprise; the rate of change of the quantity $F\rho\,\delta V$ following a small element δV is $\mathrm{D}F/\mathrm{D}t$ multiplied by $\rho\,\delta V$, because the mass $\rho\,\delta V$ of any particular element is conserved.

Alternative derivation of Cauchy's equation

The principle of linear momentum, applied to a finite blob of dyed fluid, gives

$$\frac{\mathrm{d}}{\mathrm{d}t}\int_{V(t)} \rho u_i\,\mathrm{d}V = \int_{S(t)} t_i\,\mathrm{d}S + \int_{V(t)} \rho g_i\,\mathrm{d}V$$

and on applying Reynolds's transport theorem (6.6b) to the left-hand side and eqn (6.5) to the right we obtain

$$\int_{V(t)} \left(\rho\frac{\mathrm{D}u_i}{\mathrm{D}t} - \frac{\partial T_{ij}}{\partial x_j} - \rho g_i\right)\mathrm{d}V = 0.$$

This being true for arbitrary $V(t)$ we deduce—provided that the integrand is continuous—that eqn (6.4) must hold, the argument being exactly the same as that leading to eqn (1.11).

Summary

The development so far is valid for *any* continuous medium, and:

(i) the stress components t_i on a surface element with normal $\boldsymbol{n}$ may be written

$$t_i = T_{ij}n_j \tag{6.7}$$

where T_{ij} are the elements of a *stress tensor*;

(ii) the principle of linear momentum takes the form

$$\rho\frac{\mathrm{D}u_i}{\mathrm{D}t} = \frac{\partial T_{ij}}{\partial x_j} + \rho g_i. \tag{6.8}$$

It is also the case, in fact, that the principle of moment of momentum (§6.1) implies

$$T_{ij} = T_{ji},$$

save in circumstances which, from a practical point of view, are most exceptional (see Exercise 6.14).

What we do not know at this stage, and what we cannot possibly know without deciding what kind of deformable medium we are working with, is how to calculate the elements T_{ij}.

6.4. A Newtonian viscous fluid: the Navier–Stokes equations

We now restrict attention to an incompressible fluid, for which

$$\nabla \cdot \boldsymbol{u} = 0,$$

and at this point it is possible to take

$$T_{ij} = -p\,\delta_{ij} + \mu\left(\frac{\partial u_j}{\partial x_i} + \frac{\partial u_i}{\partial x_j}\right) \tag{6.9}$$

as the constitutive relation *defining* an incompressible, Newtonian viscous fluid of viscosity μ. Notably, the stress tensor is symmetric, i.e. $T_{ij} = T_{ji}$. In view of this symmetry, eqn (6.9) amounts to six, rather than nine equations:

$$T_{11} = -p + 2\mu \frac{\partial u_1}{\partial x_1}, \qquad T_{22} = -p + 2\mu \frac{\partial u_2}{\partial x_2},$$

$$T_{33} = -p + 2\mu \frac{\partial u_3}{\partial x_3}, \qquad T_{23} = \mu\left(\frac{\partial u_3}{\partial x_2} + \frac{\partial u_2}{\partial x_3}\right),$$

$$T_{31} = \mu\left(\frac{\partial u_1}{\partial x_3} + \frac{\partial u_3}{\partial x_1}\right), \qquad T_{12} = \mu\left(\frac{\partial u_2}{\partial x_1} + \frac{\partial u_1}{\partial x_2}\right).$$

The physical significance of the quantity p, called the pressure, is simply that $-p$ is the mean of the three normal stresses at a point, i.e.

$$p = -\tfrac{1}{3}(T_{11} + T_{22} + T_{33})$$

(see Fig. 6.2).

On substituting eqn (6.9) into Cauchy's equation of motion we obtain, in the case of constant viscosity μ,

$$\rho \frac{\mathrm{D}u_i}{\mathrm{D}t} = -\frac{\partial p}{\partial x_i} + \mu \frac{\partial}{\partial x_j}\left(\frac{\partial u_j}{\partial x_i} + \frac{\partial u_i}{\partial x_j}\right) + \rho g_i$$

$$= -\frac{\partial p}{\partial x_i} + \mu \frac{\partial}{\partial x_i}\left(\frac{\partial u_j}{\partial x_j}\right) + \mu \frac{\partial^2 u_i}{\partial x_j^2} + \rho g_i.$$

But

$$\frac{\partial^2}{\partial x_j^2} = \frac{\partial^2}{\partial x_1^2} + \frac{\partial^2}{\partial x_2^2} + \frac{\partial^2}{\partial x_3^2},$$

and for an incompressible fluid

$$\partial u_j / \partial x_j = \nabla \cdot \boldsymbol{u} = 0,$$

whence the Navier–Stokes equations

$$\rho \frac{\mathrm{D}\boldsymbol{u}}{\mathrm{D}t} = -\nabla p + \rho \boldsymbol{g} + \mu \nabla^2 \boldsymbol{u}, \tag{6.10}$$

$$\nabla \cdot \boldsymbol{u} = 0, \tag{6.11}$$

as claimed in eqn (2.3).

Using the vector identity (A.10) we may rewrite eqn (6.10) as

$$\rho \frac{\mathrm{D}\boldsymbol{u}}{\mathrm{D}t} = -\nabla p + \rho \boldsymbol{g} - \mu \nabla \wedge (\nabla \wedge \boldsymbol{u}) \tag{6.12}$$

and this can be more convenient when working in non-Cartesian coordinate systems.

We also observe that on combining eqns (6.7) and (6.9) the stress vector may be written

$$\boldsymbol{t} = -p\boldsymbol{n} + \mu[2(\boldsymbol{n}\cdot\nabla)\boldsymbol{u} + \boldsymbol{n}\wedge(\nabla\wedge\boldsymbol{u})]. \tag{6.13}$$

We leave the proof as an exercise (Exercise 6.1).

Where does eqn (6.9) come from?

Stokes (1845) deduced eqn (6.9) from three elementary hypotheses. On writing $T_{ij} = -p\delta_{ij} + T_{ij}^D$ these amount essentially to:

(i) each T_{ij}^D should be a linear function of the velocity gradients $\partial u_1/\partial x_1$, $\partial u_1/\partial x_2$, etc.;

(ii) each T_{ij}^D should vanish if the flow involves no deformation of fluid elements;

(iii) the relationship between T_{ij}^D and the velocity gradients should be isotropic, as the physical properties of the fluid are assumed to show no preferred direction.

We do not pursue the argument in detail here (see Exercise 6.11), but try instead to indicate by example how eqn (6.9) conforms to each of the above hypotheses. With regard to (i), which is the most natural extension of Newton's original proposal, there is little to do beyond observe that in eqn (6.9) the quantities T_{ij}^D are indeed linear functions of the quantities $\partial u_i/\partial x_j$.

With regard to (ii), consider first a fluid element in 2-D flow, as in Fig. 6.4, where we have displayed the velocity components of the fluid particles at B and C relative to those of the particle at A. Plainly, the distance between the particles at A and B is momentarily increasing with time if $\partial u_1/\partial x_1 > 0$ and decreasing if $\partial u_1/\partial x_1 < 0$. Thus the terms $2\mu\,\partial u_1/\partial x_1$ and $2\mu\,\partial u_2/\partial x_2$ in the 2-D version of eqn (6.9) have a simple physical interpretation in terms of the stretching (or shrinking) of fluid elements, and they vanish if the fluid is moving without deformation. Similarly, we see that the fluid line element AB is momentarily rotating with angular velocity $\partial u_2/\partial x_1$, while the fluid line element AC is rotating with angular velocity $-\partial u_1/\partial x_2$. The angle between AB

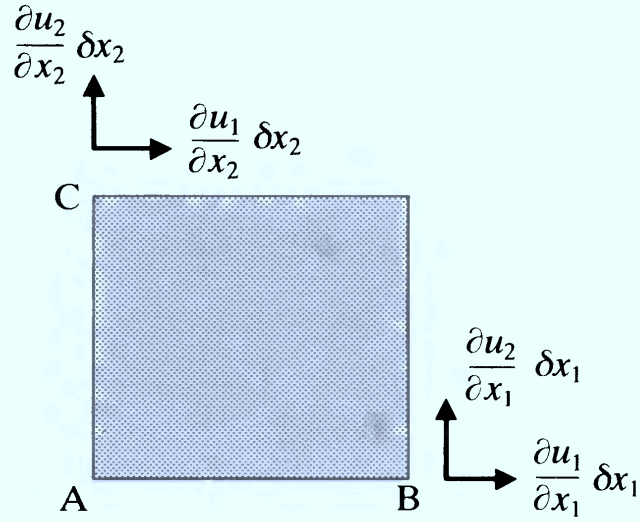

Fig. 6.4. Velocity components at two points of a fluid element, relative to those at A.

and AC is therefore momentarily decreasing with time at a rate $\partial u_2/\partial x_1 + \partial u_1/\partial x_2$. The so-called 'shear stress' term $\mu(\partial u_2/\partial x_1 + \partial u_1/\partial x_2)$ in the 2-D version of eqn (6.9) therefore also has a simple physical interpretation, and again vanishes if the fluid is moving without deformation. We say more about (ii) in the subsection which follows.

With regard to (iii) let us consider the simple example of a 2-D shear flow

$$u_1 = \beta x_2, \qquad u_2 = 0$$

over a rigid plane boundary $x_2 = 0$. In this case

$$T_{11} = -p, \qquad T_{22} = -p, \qquad T_{12} = \mu\beta.$$

The tangential stress on the boundary is

$$t_1 = T_{1j}n_j = T_{12}n_2 = T_{12} = \mu\beta. \tag{6.14}$$

Note that the terms $2\mu\, \partial u_1/\partial x_1$ and $2\mu\, \partial u_2/\partial x_2$ are zero.

But suppose that, somewhat perversely, we carry out the whole calculation of the tangential stress on the boundary not with reference to the obvious coordinate system but with reference to the coordinates x_1', x_2' shown in Fig. 6.5 instead. The velocity components relative to these coordinates are

$$u_1' = \frac{\beta}{2}(x_1' + x_2'), \qquad u_2' = -\frac{\beta}{2}(x_1' + x_2'),$$

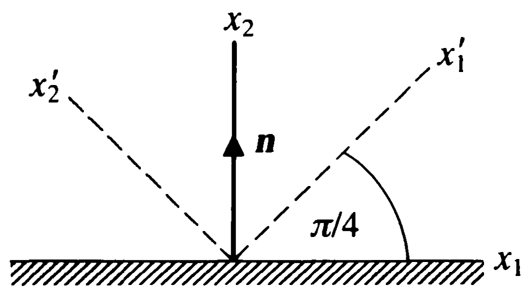

Fig. 6.5. The two coordinate systems.

and if, as is being claimed, the relationship (6.9) is isotropic, then it must take exactly the same form relative to the new axes, i.e.

$$T'_{11} = -p + 2\mu \frac{\partial u'_1}{\partial x'_1}, \qquad T'_{22} = -p + 2\mu \frac{\partial u'_2}{\partial x'_2},$$

$$T'_{12} = \mu\left(\frac{\partial u'_2}{\partial x'_1} + \frac{\partial u'_1}{\partial x'_2}\right).$$

The purpose of the present calculation is to check that this does, indeed, lead to the same expression (6.14) for the stress on the boundary. Thus

$$T'_{11} = -p + \mu\beta, \qquad T'_{22} = -p - \mu\beta, \qquad T'_{12} = 0.$$

Now

$$t'_i = T'_{ij} n'_j,$$

where n'_j are the components of the unit normal to the boundary relative to the new axes. This gives

$$t'_i = T'_{i1} n'_1 + T'_{i2} n'_2 = \frac{1}{\sqrt{2}}(T'_{i1} + T'_{i2}),$$

whence

$$t'_1 = \frac{1}{\sqrt{2}}(-p + \mu\beta), \qquad t'_2 = \frac{1}{\sqrt{2}}(-p - \mu\beta),$$

and finally

$$t_1 = \frac{1}{\sqrt{2}}(t'_1 - t'_2) = \mu\beta \tag{6.15}$$

as before. As it happens, in this (crazy) formulation of the problem the 'shear stress' T'_{12} is actually zero, and eqn (6.15) originates wholly from the terms $2\mu\,\partial u'_1/\partial x'_1$ and $2\mu\,\partial u'_2/\partial x'_2$.

The general deformation of a fluid element

We now look more deeply at (ii), and at this point it is useful to define the rate-of-strain tensor

$$e_{ij} = \tfrac{1}{2}\left(\frac{\partial u_i}{\partial x_j} + \frac{\partial u_j}{\partial x_i}\right), \tag{6.16}$$

in which case the constitutive relation for an incompressible Newtonian viscous fluid is

$$T_{ij} = -p\delta_{ij} + 2\mu e_{ij}. \tag{6.17}$$

In the foregoing discussion we have provided some evidence that e_{ij} vanishes if there is no deformation of fluid elements. We now explore this notion further.

Let the fluid velocity at some fixed point be $\boldsymbol{u}_\mathrm{P}$. By Taylor's theorem the velocity at a point Q a small distance $\boldsymbol{s}$ from P is, to first order in $\boldsymbol{s}$,

$$\boldsymbol{u}_\mathrm{Q} = \boldsymbol{u}_\mathrm{P} + (\boldsymbol{s}\cdot\nabla)\boldsymbol{u}, \tag{6.18}$$

the derivatives in this expression being evaluated at P. We are interested in how $\boldsymbol{u}_\mathrm{Q}$ depends, locally, on $\boldsymbol{s}$, and the key to this lies in rewriting eqn (6.18) as

$$\boldsymbol{u}_\mathrm{Q} = \boldsymbol{u}_\mathrm{P} + \tfrac{1}{2}(\nabla\wedge\mathbf{u})\wedge\boldsymbol{s} + \tfrac{1}{2}\nabla_{\boldsymbol{s}}(e_{ij}s_is_j), \tag{6.19}$$

where $\nabla\wedge\boldsymbol{u}$ and e_{ij} are evaluated at P (Exercise 6.7). Here $\nabla_{\boldsymbol{s}}$ denotes the operator $\boldsymbol{e}_k\,\partial/\partial s_k$, i.e. the ∇ operator with respect to the variable $\boldsymbol{s}$.

Now, the term $\tfrac{1}{2}(\nabla\wedge\boldsymbol{u})\wedge\boldsymbol{s}$ is of the form '$\boldsymbol{\Omega}\wedge\boldsymbol{x}$' and

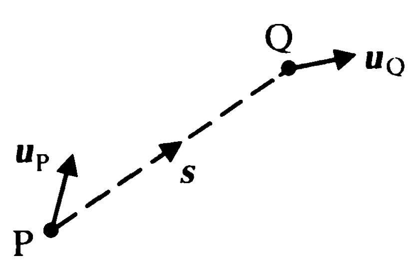

Fig. 6.6. Definition sketch for eqn (6.18).

represents a local rigid-body rotation with angular velocity $\frac{1}{2}(\nabla \wedge \boldsymbol{u})$. Thus the vorticity $\nabla \wedge \boldsymbol{u}$ (or, more precisely, one half of it) acts as a measure of the extent to which a fluid element is spinning, just as we observed in §1.4 in a strictly 2-D context.

To see that the term $\frac{1}{2}\nabla_s(e_{ij}s_is_j)$ represents a pure straining motion, i.e. one involving stretching/squashing in mutually perpendicular directions but no overall rotation, note first that it denotes a vector field which is everywhere normal to surfaces of constant $e_{ij}s_is_j$. To picture these surfaces consider first a simple 2-D example in which

$$\boldsymbol{u} = (\alpha x_1, -\alpha x_2, 0). \tag{6.20}$$

In this case

$$e_{ij} = \begin{pmatrix} \alpha & 0 & 0 \\ 0 & -\alpha & 0 \\ 0 & 0 & 0 \end{pmatrix}$$

(which is untypical, in that e_{ij} is the same, no matter which $\boldsymbol{x}_P$ we choose), and

$$\begin{aligned} e_{ij}s_is_j &= (s_1 \quad s_2 \quad s_3)\begin{pmatrix} \alpha & 0 & 0 \\ 0 & -\alpha & 0 \\ 0 & 0 & 0 \end{pmatrix}\begin{pmatrix} s_1 \\ s_2 \\ s_3 \end{pmatrix} \\ &= \alpha(s_1^2 - s_2^2). \end{aligned}$$

Thus the cross-sections of surfaces of constant $e_{ij}s_is_j$ are, in this case, as in Fig. 6.7. More generally, we note that as e_{ij} is

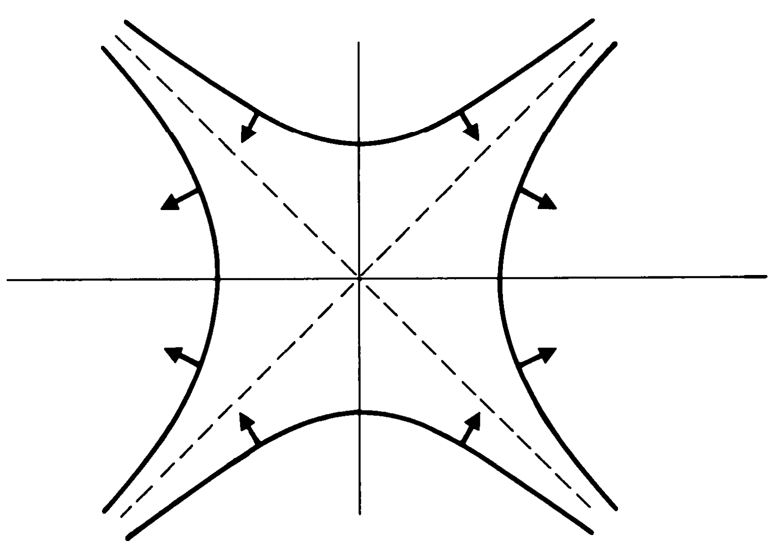

Fig. 6.7. Surfaces of constant $e_{ij}s_is_j$ in a pure straining motion.

symmetric principal axes can always be found with respect to which it is diagonal, and with respect to those axes the quantity $e_{ij}s_is_j$ is

$$e'_{11}s_1'^2 + e'_{22}s_2'^2 + e'_{33}s_3'^2.$$

Together with the incompressibility condition ($e'_{11} + e'_{22} + e'_{33} = 0$) this implies that surfaces of constant $e_{ij}s_is_j$ are hyperboloids, and the associated motions are accordingly simple 3-D equivalents of the kind shown in Fig. 6.7.

Thus eqn (6.19) does indeed decompose the flow in the neighbourhood of any point P into a pure translation (first term), a rotary flow involving no deformation (second term) and a flow involving deformation but no rotation (third term).

Finding the components of the stress vector $\boldsymbol{t}$ in cylindrical or spherical polar coordinates

If we are solving a flow problem in cylindrical or spherical polar coordinates we need a quick and effective way of calculating the stress vector $\boldsymbol{t}$.

Consider, for example, the flow

$$\boldsymbol{u} = u_\theta(r)\boldsymbol{e}_\theta$$

between two rotating cylinders, as in eqn (2.31). One way of obtaining the stress $\boldsymbol{t}$ at any point on the inner cylinder is to use the expression (6.13), as in Exercise 6.4. This method is quite effective, although the calculation of $(\boldsymbol{n} \cdot \nabla)\boldsymbol{u}$ requires careful attention to how the unit base vectors change with position, as Exercise 6.9 shows.

An alternative way of obtaining t_θ, say, is to pick some particular point of the inner cylinder and set up Cartesian axes coincident with the unit vectors $\boldsymbol{e}_r$, $\boldsymbol{e}_\theta$, and $\boldsymbol{e}_z$ at that point. Then we want t_2, i.e.

$$t_2 = T_{2j}n_j = T_{21}n_1 + T_{22}n_2 + T_{23}n_3,$$

for which

$$t_\theta = T_{\theta r}n_r + T_{\theta\theta}n_\theta + T_{\theta z}n_z \qquad (6.21)$$

is no more than an alternative notation. In the present instance

$\boldsymbol{n} = \boldsymbol{e}_r$, and on using eqn (6.17):

$$t_\theta = T_{\theta r} = T_{r\theta} = 2\mu e_{r\theta}.$$

To find $e_{r\theta}$ we may turn to eqn (A.36), and as $u_r = 0$ on the cylinder we obtain

$$t_\theta = \mu r \frac{\mathrm{d}}{\mathrm{d}r}\left(\frac{u_\theta}{r}\right),$$

as in Exercise 6.4.

This is effective, but it requires some understanding of where expressions such as eqn (A.36) come from. To this end, note that

$$\begin{aligned} 2e_{r\theta} = 2e_{12} = \frac{\partial u_2}{\partial x_1} + \frac{\partial u_1}{\partial x_2} &= (\boldsymbol{e}_1 \cdot \nabla)(\boldsymbol{u} \cdot \boldsymbol{e}_2) + (\boldsymbol{e}_2 \cdot \nabla)(\boldsymbol{u} \cdot \boldsymbol{e}_1) \\ &= [(\boldsymbol{e}_1 \cdot \nabla)\boldsymbol{u}] \cdot \boldsymbol{e}_2 + [(\boldsymbol{e}_2 \cdot \nabla)\boldsymbol{u}] \cdot \boldsymbol{e}_1, \end{aligned} \tag{6.22}$$

the final step following because (in marked contrast to $\boldsymbol{e}_r$, $\boldsymbol{e}_\theta$, $\boldsymbol{e}_z$) the unit vectors $\boldsymbol{e}_1$, $\boldsymbol{e}_2$, and $\boldsymbol{e}_3$ are all constant. Thus

$$\begin{aligned} 2e_{r\theta} &= [(\boldsymbol{e}_r \cdot \nabla)\boldsymbol{u}] \cdot \boldsymbol{e}_\theta + [(\boldsymbol{e}_\theta \cdot \nabla)\boldsymbol{u}] \cdot \boldsymbol{e}_r \\ &= \left[\frac{\partial}{\partial r}(u_r \boldsymbol{e}_r + u_\theta \boldsymbol{e}_\theta + u_z \boldsymbol{e}_z)\right] \cdot \boldsymbol{e}_\theta \\ &\quad + \left[\frac{1}{r}\frac{\partial}{\partial \theta}(u_r \boldsymbol{e}_r + u_\theta \boldsymbol{e}_\theta + u_z \boldsymbol{e}_z)\right] \cdot \boldsymbol{e}_r. \end{aligned} \tag{6.23}$$

Now, the unit vectors $\boldsymbol{e}_r$ and $\boldsymbol{e}_\theta$ change with θ according to eqn (A.29), so

$$\begin{aligned} 2e_{r\theta} &= \frac{\partial u_\theta}{\partial r} + \frac{1}{r}\left[\frac{\partial u_r}{\partial \theta}\boldsymbol{e}_r + u_r \boldsymbol{e}_\theta + \frac{\partial u_\theta}{\partial \theta}\boldsymbol{e}_\theta - u_\theta \boldsymbol{e}_r + \frac{\partial u_z}{\partial \theta}\boldsymbol{e}_z\right] \cdot \boldsymbol{e}_r \\ &= \frac{\partial u_\theta}{\partial r} + \frac{1}{r}\frac{\partial u_r}{\partial \theta} - \frac{u_\theta}{r} \\ &= r\frac{\partial}{\partial r}\left(\frac{u_\theta}{r}\right) + \frac{1}{r}\frac{\partial u_r}{\partial \theta}, \end{aligned}$$

which is the last of the expressions (A.36).

6.5. Viscous dissipation of energy

Consider the kinetic energy

$$T = \tfrac{1}{2}\int_V \rho u_i^2 \,\mathrm{d}V \tag{6.24}$$

of a dyed blob of fluid V with surface S. The rate of change of T is

$$\frac{\mathrm{d}T}{\mathrm{d}t} = \int_V u_i \frac{\mathrm{D}u_i}{\mathrm{D}t}\rho \,\mathrm{d}V,$$

(see eqn (6.6b)), and by virtue of Cauchy's equation (6.4) we may rewrite this as

$$\frac{\mathrm{d}T}{\mathrm{d}t} = \int_V \rho u_i g_i \,\mathrm{d}V + \int_V u_i \frac{\partial T_{ij}}{\partial x_j}\,\mathrm{d}V. \tag{6.25}$$

Now,

$$\int_V u_i \frac{\partial T_{ij}}{\partial x_j}\,\mathrm{d}V = \int_V \frac{\partial}{\partial x_j}(u_i T_{ij})\,\mathrm{d}V - \int_V T_{ij}\frac{\partial u_i}{\partial x_j}\,\mathrm{d}V,$$

and

$$\int_V \frac{\partial}{\partial x_j}(u_i T_{ij})\,\mathrm{d}V = \int_S u_i T_{ij} n_j \,\mathrm{d}S = \int_S u_i t_i \,\mathrm{d}S,$$

where we have used eqn (6.3) and the divergence theorem (A.13). Furthermore,

$$T_{ij}\frac{\partial u_i}{\partial x_j} = \tfrac{1}{2}\left(T_{ij}\frac{\partial u_i}{\partial x_j} + T_{ji}\frac{\partial u_j}{\partial x_i}\right) = \tfrac{1}{2}T_{ij}\left(\frac{\partial u_i}{\partial x_j} + \frac{\partial u_j}{\partial x_i}\right)$$

as (i) summation over $i = 1, 2, 3$ and $j = 1, 2, 3$ is understood, and (ii) T_{ij} is symmetric. Using the relation (6.9) for an incompressible Newtonian viscous fluid, together with $\nabla \cdot \boldsymbol{u} = 0$, we see that

$$T_{ij}\frac{\partial u_i}{\partial x_j} = \tfrac{1}{2}\mu\left(\frac{\partial u_i}{\partial x_j} + \frac{\partial u_j}{\partial x_i}\right)^2 = 2\mu e_{ij}^2$$

(see eqn (6.16)). Thus

$$\frac{\mathrm{d}T}{\mathrm{d}t} = \int_V \rho \boldsymbol{u} \cdot \boldsymbol{g}\,\mathrm{d}V + \int_S \boldsymbol{t} \cdot \boldsymbol{u}\,\mathrm{d}S - 2\mu \int_V e_{ij}^2 \,\mathrm{d}V. \tag{6.26}$$

The first term on the right-hand side represents the rate of decrease of potential energy of the 'dyed' fluid, while the second term represents the rate at which the surrounding fluid is doing work on the dyed fluid via the surface stresses $\boldsymbol{t}$. Not all this goes into increasing the kinetic energy of the dyed fluid; viscous stresses within the blob are evidently dissipating energy at a rate

$$2\mu e_{ij}^2 \tag{6.27}$$

per unit volume which, written out in full, is

$$2\mu(e_{11}^2 + e_{22}^2 + e_{33}^2 + 2e_{23}^2 + 2e_{31}^2 + 2e_{12}^2).$$

This viscous dissipation of energy is zero only if $e_{ij} = 0$ for all i and j, i.e. if there is no deformation of fluid elements.

Exercises

6.1. We may deduce from eqns (6.7) and (6.9) that

$$t_i = -pn_i + \mu n_j\left(\frac{\partial u_i}{\partial x_j} + \frac{\partial u_j}{\partial x_i}\right).$$

Show that this identical to

$$\boldsymbol{t} = -p\boldsymbol{n} + \mu[2(\boldsymbol{n} \cdot \nabla)\boldsymbol{u} + \boldsymbol{n} \wedge (\nabla \wedge \boldsymbol{u})],$$

by expanding this expression using the suffix notation and the summation convention.

6.2. Use eqn (6.13) and various vector identities to show that the net force exerted on a finite blob of fluid by the surrounding fluid is

$$\int_S \boldsymbol{t}\, \mathrm{d}S = \int_V (-\nabla p + \mu\, \nabla^2 \boldsymbol{u})\, \mathrm{d}V,$$

where S is the surface of the blob and V the region occupied by the blob. Deduce that if the blob is small the net force on it, excluding gravity, is $-\nabla p + \mu\, \nabla^2 \boldsymbol{u}$ per unit volume, in agreement with eqn (6.10).

6.3. Verify that in the case of a simple shear flow

$$\boldsymbol{u} = [u(y), 0, 0]$$

eqn (6.13) reduces, when $\boldsymbol{n} = (0, 1, 0)$, to

$$\boldsymbol{t} = \left[\mu\frac{\mathrm{d}u}{\mathrm{d}y}, -p, 0\right].$$

6.4. Show that in the case of a purely rotary flow

$$\boldsymbol{u} = u_\theta(r)\boldsymbol{e}_\theta$$

eqn (6.13) reduces, when $\boldsymbol{n} = \boldsymbol{e}_r$, to

$$\boldsymbol{t} = -p\boldsymbol{e}_r + \mu r \frac{\mathrm{d}}{\mathrm{d}r}\left(\frac{u_\theta}{r}\right)\boldsymbol{e}_\theta,$$

and note that the second term vanishes in the case of uniform rotation, $u_\theta \propto r$, for there is then no deformation of fluid elements.

Use this result to calculate the torque exerted on the inner cylinder by the flow (2.31) and (2.32).

6.5. Use Reynolds's transport theorem (6.6a) to provide an alternative derivation of the conservation of mass equation

$$\frac{\mathrm{D}\rho}{\mathrm{D}t} + \rho\nabla\cdot\boldsymbol{u} = 0$$

(cf. Exercise 1.1). Then use this equation to deduce eqn (6.6b) from eqn (6.6a).

6.6. Show that the terms $\mu(\partial u_j/\partial x_i + \partial u_i/\partial x_j)$ of the stress tensor (6.9) are zero for the uniformly rotating flow $\boldsymbol{u} = \boldsymbol{\Omega} \wedge \boldsymbol{x}$, $\boldsymbol{\Omega}$ being a constant vector.

6.7. Expand eqn (6.19) using the suffix notation and summation convention:

$$\boldsymbol{u}_{\mathrm{Q}} = \boldsymbol{u}_{\mathrm{P}} + \tfrac{1}{2}\left[\left(\boldsymbol{e}_i \wedge \frac{\partial \boldsymbol{u}}{\partial x_i}\right) \wedge \boldsymbol{s} + \boldsymbol{e}_k \frac{\partial}{\partial s_k}(e_{ij}s_i s_j)\right]$$

etc., to show that eqn (6.19) is equivalent to eqn (6.18).

6.8. Separate the shear flow $\boldsymbol{u} = (\beta x_2, 0, 0)$ of Fig. 1.4 into its local (i) translation, (ii) rotation, and (iii) pure straining parts, using eqn (6.19). Find the directions of the principal axes of e_{ij}, and verify that this decomposition of the flow can be represented schematically as in Fig. 6.8.

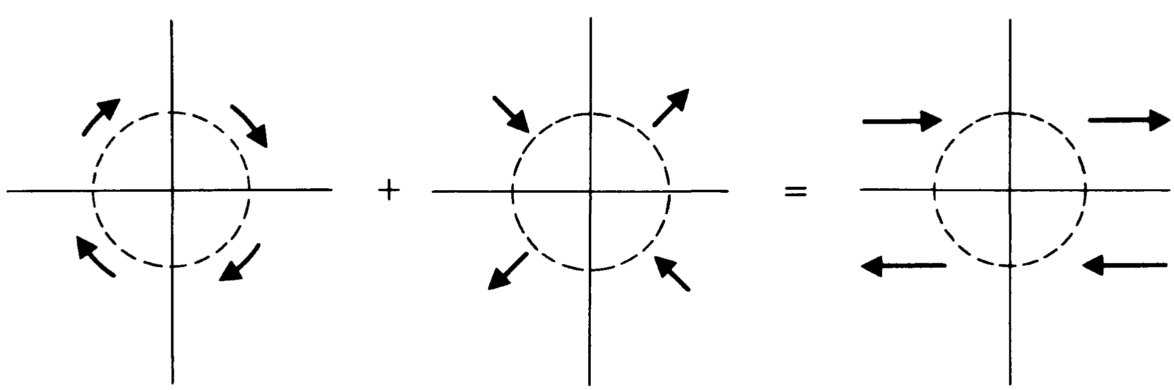

Fig. 6.8. The decomposition of a uniform shear flow.

6.9. Consider a 2-D viscous flow

$$\boldsymbol{u} = u_r(r, \theta)\boldsymbol{e}_r,$$

as might occur in a converging or diverging channel (see, e.g. Exercise 7.6). Use both methods described at the end of §6.4 to show that the stress exerted by the fluid in $\theta > 0$ on that in $\theta < 0$ is

$$\boldsymbol{t} = \frac{\mu}{r}\frac{\partial u_r}{\partial \theta}\boldsymbol{e}_r + \left(-p + \frac{2\mu u_r}{r}\right)\boldsymbol{e}_\theta.$$

[Note that the normal component of stress is not due to the pressure p alone.]

6.10. Verify by direct calculation the expression for $e_{\theta\phi}$ in the spherical polar formulae (A.44).

6.11. If T_{ij}^D is a linear function of e_{11}, e_{12}, etc., then we may write

$$T_{ij}^D = c_{ijkl}e_{kl}.$$

It is shown in books on tensor analysis (e.g. Bourne and Kendall 1977, §8.3) that the most general fourth-order *isotropic* tensor is of the form

$$c_{ijkl} = A\delta_{ij}\delta_{kl} + B\delta_{ik}\delta_{jl} + C\delta_{il}\delta_{jk},$$

where A, B, and C are scalars. Use this to show that

$$T_{ij}^D = \lambda e_{kk}\delta_{ij} + 2\mu e_{ij},$$

where λ and μ are scalars.

Show that if p is defined, as in §6.4, so that

$$p = -\tfrac{1}{3}T_{ii},$$

then

$$T_{ij} = -(p + \tfrac{2}{3}\mu\nabla\cdot\boldsymbol{u})\delta_{ij} + \mu\left(\frac{\partial u_i}{\partial x_j} + \frac{\partial u_j}{\partial x_i}\right),$$

which reduces to eqn (6.9) when the fluid is incompressible.

[With a compressible fluid some care is needed in distinguishing between the mechanical pressure, defined above, and the thermodynamic pressure (see Batchelor 1967, p. 154).]

6.12. Observe that if a flow $\boldsymbol{u}$ is irrotational, the viscous term is zero in the equation of motion (6.12).

Consider now the flow

$$\boldsymbol{u} = \frac{\Omega a^2}{r}\boldsymbol{e}_\theta, \qquad r \geqslant a,$$

driven by a rotating cylinder at $r = a$, as in Exercise 2.8. 'The flow is irrotational in $r \geqslant a$; therefore the viscous term is zero; therefore the viscous forces are zero; and so the torque on the cylinder is zero.' But it is not. What is wrong with the argument?

6.13. Let $\boldsymbol{x} = \boldsymbol{x}(\boldsymbol{X}, t)$ denote some fluid motion, as in Exercises 1.7, 5.18, and 5.21, and let J denote the determinant

$$J = \begin{vmatrix} \dfrac{\partial x_1}{\partial X_1} & \dfrac{\partial x_1}{\partial X_2} & \dfrac{\partial x_1}{\partial X_3} \\[2ex] \dfrac{\partial x_2}{\partial X_1} & \dfrac{\partial x_2}{\partial X_2} & \dfrac{\partial x_2}{\partial X_3} \\[2ex] \dfrac{\partial x_3}{\partial X_1} & \dfrac{\partial x_3}{\partial X_2} & \dfrac{\partial x_3}{\partial X_3} \end{vmatrix}.$$

Establish *Euler's identity*

$$\mathrm{D}J/\mathrm{D}t = J\,\nabla \cdot \boldsymbol{u},$$

and use this to give a proof of Reynolds's transport theorem (6.6a).

6.14. If we apply the principle of moment of momentum (§6.1) to a finite 'dyed' blob of some continuous medium occupying a region $V(t)$ we obtain†

$$\frac{\mathrm{d}}{\mathrm{d}t}\int_{V(t)} \boldsymbol{x} \wedge \rho \boldsymbol{u}\,\mathrm{d}V = \int_{S(t)} \boldsymbol{x} \wedge \boldsymbol{t}\,\mathrm{d}S + \int_{V(t)} \boldsymbol{x} \wedge \rho \boldsymbol{g}\,\mathrm{d}V.$$

Use Reynolds's transport theorem, together with eqns (6.7) and (6.8), to write this in the form

$$\int_{V(t)} x_k \boldsymbol{e}_k \wedge \frac{\partial T_{ij}}{\partial x_j}\boldsymbol{e}_i\,\mathrm{d}V = \int_{S(t)} x_k \boldsymbol{e}_k \wedge T_{ij} n_j \boldsymbol{e}_i\,\mathrm{d}S$$

where summation over 1, 2, 3 is implied for i, j, and k. Re-cast this equation into the form

$$\boldsymbol{e}_k \wedge \boldsymbol{e}_i \int_{V(t)} T_{ik}\,\mathrm{d}V = 0,$$

and hence deduce that, *subject to the proviso in the footnote,*

$$T_{ij} = T_{ji},$$

i.e. the stress tensor must be symmetric, *whatever the nature of the deformable medium in question.* (This famous requirement, to which eqn (6.9) conforms, is due to Cauchy.)

† There is a proviso here, namely that the net torque on the blob is due simply to the moment of the stresses $\boldsymbol{t}$ on its surface and the moment of the body force $\boldsymbol{g}$ per unit mass. This is very generally the case, but there are exotic exceptions, as when the medium consists of a suspension of ferromagnetic particles, each being subject to the torque of an applied magnetic field (see Chap. 8 of Rosensweig 1985).

Appendix

A.1. Vector identities

$$(\boldsymbol{a} \wedge \boldsymbol{b}) \wedge \boldsymbol{c} = (\boldsymbol{a} \cdot \boldsymbol{c})\boldsymbol{b} - (\boldsymbol{b} \cdot \boldsymbol{c})\boldsymbol{a}, \tag{A.1}$$

$$\nabla \wedge \nabla\phi = 0, \qquad \nabla \cdot (\nabla \wedge \boldsymbol{F}) = 0, \tag{A.2, A.3}$$

$$\nabla \cdot (\phi\boldsymbol{F}) = \phi\nabla \cdot \boldsymbol{F} + \boldsymbol{F} \cdot \nabla\phi, \tag{A.4}$$

$$\nabla \wedge (\phi\boldsymbol{F}) = \phi\nabla \wedge \boldsymbol{F} + (\nabla\phi) \wedge \boldsymbol{F}, \tag{A.5}$$

$$\nabla \wedge (\boldsymbol{F} \wedge \boldsymbol{G}) = (\boldsymbol{G} \cdot \nabla)\boldsymbol{F} - (\boldsymbol{F} \cdot \nabla)\boldsymbol{G} + \boldsymbol{F}(\nabla \cdot \boldsymbol{G}) - \boldsymbol{G}(\nabla \cdot \boldsymbol{F}), \tag{A.6}$$

$$\nabla \cdot (\boldsymbol{F} \wedge \boldsymbol{G}) = \boldsymbol{G} \cdot (\nabla \wedge \boldsymbol{F}) - \boldsymbol{F} \cdot (\nabla \wedge \boldsymbol{G}), \tag{A.7}$$

$$\nabla(\boldsymbol{F} \cdot \boldsymbol{G}) = \boldsymbol{F} \wedge (\nabla \wedge \boldsymbol{G}) + \boldsymbol{G} \wedge (\nabla \wedge \boldsymbol{F}) + (\boldsymbol{F} \cdot \nabla)\boldsymbol{G} + (\boldsymbol{G} \cdot \nabla)\boldsymbol{F}, \tag{A.8}$$

$$(\boldsymbol{F} \cdot \nabla)\boldsymbol{F} = (\nabla \wedge \boldsymbol{F}) \wedge \boldsymbol{F} + \nabla(\tfrac{1}{2}\boldsymbol{F}^2), \tag{A.9}$$

$$\nabla^2\boldsymbol{F} = \nabla(\nabla \cdot \boldsymbol{F}) - \nabla \wedge (\nabla \wedge \boldsymbol{F}). \tag{A.10}$$

A.2. Two properties of the gradient operator ∇

Let $\phi(\boldsymbol{x})$ be some scalar function of $\boldsymbol{x}$, and let $\mathrm{d}\phi/\mathrm{d}s$ be its rate of change, with distance s, in the direction of some unit vector $\boldsymbol{t}$. Then

$$\mathrm{d}\phi/\mathrm{d}s = \boldsymbol{t} \cdot \nabla\phi. \tag{A.11}$$

For this very reason, the line integral of $\nabla\phi$ along some curve C is equal to the difference in ϕ between the two end-points of the curve:

$$\int_C \nabla\phi \cdot \mathrm{d}\boldsymbol{x} = [\phi]_C. \tag{A.12}$$

A.3. The divergence theorem

Let the region V be bounded by a simple closed surface S with unit outward normal $\boldsymbol{n}$. Then

$$\int_S \boldsymbol{F}\cdot\boldsymbol{n}\,\mathrm{d}S = \int_V \nabla\cdot\boldsymbol{F}\,\mathrm{d}V. \tag{A.13}$$

In suffix notation, and using the summation convention, this takes the form

$$\int_S F_j n_j\,\mathrm{d}S = \int_V \frac{\partial F_j}{\partial x_j}\,\mathrm{d}V.$$

There are many identities which may be derived from the divergence theorem. The identity

$$\int_S \phi\boldsymbol{n}\,\mathrm{d}S = \int_V \nabla\phi\,\mathrm{d}V \tag{A.14}$$

is particularly valuable, and may be written

$$\int_S \phi n_j\,\mathrm{d}S = \int_V \frac{\partial\phi}{\partial x_j}\,\mathrm{d}V. \tag{A.15}$$

The following are immediate consequences:

$$\int_S F_i n_j\,\mathrm{d}S = \int_V \frac{\partial F_i}{\partial x_j}\,\mathrm{d}V, \qquad \int_S T_{ij} n_j\,\mathrm{d}S = \int_V \frac{\partial T_{ij}}{\partial x_j}\,\mathrm{d}V, \tag{A.16, A.17}$$

$$\int_S u_i v_j n_j\,\mathrm{d}S = \int_V \frac{\partial}{\partial x_j}(u_i v_j)\,\mathrm{d}V. \tag{A.18}$$

Other identities derivable from the divergence theorem include:

$$\int_S \boldsymbol{F}\wedge\boldsymbol{n}\,\mathrm{d}S = -\int_V \nabla\wedge\boldsymbol{F}\,\mathrm{d}V, \qquad \int_S \boldsymbol{n}\cdot\nabla\phi\,\mathrm{d}S = \int_V \nabla^2\phi\,\mathrm{d}V, \tag{A.19, A.20}$$

$$\int_S \phi\frac{\partial\psi}{\partial n}\,\mathrm{d}S = \int_V (\phi\nabla^2\psi + \nabla\phi\cdot\nabla\psi)\,\mathrm{d}V, \tag{A.21}$$

$$\int_S \left(\phi\frac{\partial\psi}{\partial n} - \psi\frac{\partial\phi}{\partial n}\right)\mathrm{d}S = \int_V (\phi\nabla^2\psi - \psi\nabla^2\phi)\,\mathrm{d}V. \tag{A.22}$$

A.4. Stokes's theorem

Let C be a simple closed curve spanned by a surface S with unit normal $\boldsymbol{n}$. Then

$$\int_C \boldsymbol{F} \cdot d\boldsymbol{x} = \int_S (\nabla \wedge \boldsymbol{F}) \cdot \boldsymbol{n} \, dS, \tag{A.23}$$

where the line integral is taken in an appropriate sense, according to that of $\boldsymbol{n}$ (see Fig. A.1).

Green's theorem in the plane may be viewed as a special case of Stokes's theorem, with $\boldsymbol{F} = [u(x, y), v(x, y), 0]$. If C is a simple closed curve in the x–y plane, and S denotes the region enclosed by C, then

$$\int_C u \, dx + v \, dy = \int_S \left(\frac{\partial v}{\partial x} - \frac{\partial u}{\partial y} \right) dx \, dy. \tag{A.24}$$

A useful identity derivable from Stokes's theorem is

$$\int_C \phi \, d\boldsymbol{x} = -\int_S (\nabla \phi) \wedge \boldsymbol{n} \, dS. \tag{A.25}$$

A.5. Orthogonal curvilinear coordinates

Let u, v, and w denote a set of orthogonal curvilinear coordinates, and let $\boldsymbol{e}_u$, $\boldsymbol{e}_v$ and $\boldsymbol{e}_w$ denote unit vectors parallel to the coordinate lines and in the directions of increase of u, v, and w respectively. Then

$$\boldsymbol{e}_u = \boldsymbol{e}_v \wedge \boldsymbol{e}_w, \qquad \text{etc.},$$

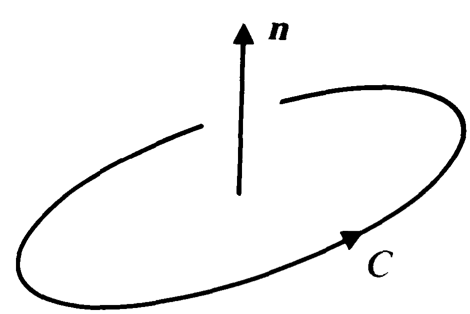

Fig. A.1.

and

$$\delta \boldsymbol{x} = h_1\, \delta u \boldsymbol{e}_u + h_2\, \delta v \boldsymbol{e}_v + h_3\, \delta w \boldsymbol{e}_w,$$

where

$$h_1 = |\partial \boldsymbol{x}/\partial u|, \qquad \text{etc.}$$

Furthermore,

$$\nabla\phi = \frac{1}{h_1}\frac{\partial\phi}{\partial u}\boldsymbol{e}_u + \frac{1}{h_2}\frac{\partial\phi}{\partial v}\boldsymbol{e}_v + \frac{1}{h_3}\frac{\partial\phi}{\partial w}\boldsymbol{e}_w, \tag{A.26}$$

$$\nabla\cdot\boldsymbol{F} = \frac{1}{h_1h_2h_3}\left[\frac{\partial}{\partial u}(h_2h_3F_u) + \frac{\partial}{\partial v}(h_3h_1F_v) + \frac{\partial}{\partial w}(h_1h_2F_w)\right], \tag{A.27}$$

$$\nabla\wedge\boldsymbol{F} = \frac{1}{h_1h_2h_3}\begin{vmatrix} h_1\boldsymbol{e}_u & h_2\boldsymbol{e}_v & h_3\boldsymbol{e}_w \\ \dfrac{\partial}{\partial u} & \dfrac{\partial}{\partial v} & \dfrac{\partial}{\partial w} \\ h_1F_u & h_2F_v & h_3F_w \end{vmatrix}. \tag{A.28}$$

For *cylindrical polar coordinates* (Fig. A.2)

$$u = r, \qquad v = \theta, \qquad w = z,$$

$$h_1 = 1. \qquad h_2 = r, \qquad h_3 = 1.$$

For *spherical polar coordinates* (Fig. A.3)

$$u = r, \qquad v = \theta, \qquad w = \phi,$$

$$h_1 = 1, \qquad h_2 = r, \qquad h_3 = r\sin\theta.$$

A.6. Cylindrical polar coordinates

Cylindrical polar coordinates (r, θ, z) are such that

$$x_1 = r\cos\theta, \qquad x_2 = r\sin\theta, \qquad x_3 = z,$$

as in Fig. A.2. Clearly,

$$\delta\boldsymbol{x} = \delta r\boldsymbol{e}_r + r\,\delta\theta\boldsymbol{e}_\theta + \delta z\boldsymbol{e}_z$$

and

$$\boldsymbol{e}_r = \cos\theta\,\boldsymbol{e}_1 + \sin\theta\,\boldsymbol{e}_2, \qquad \boldsymbol{e}_\theta = -\sin\theta\,\boldsymbol{e}_1 + \cos\theta\,\boldsymbol{e}_2, \qquad \boldsymbol{e}_z = \boldsymbol{e}_3.$$

The unit vectors do not change with r or z, but

$$\frac{\partial\boldsymbol{e}_r}{\partial\theta} = \boldsymbol{e}_\theta, \qquad \frac{\partial\boldsymbol{e}_\theta}{\partial\theta} = -\boldsymbol{e}_r, \qquad \frac{\partial\boldsymbol{e}_z}{\partial\theta} = 0. \tag{A.29}$$

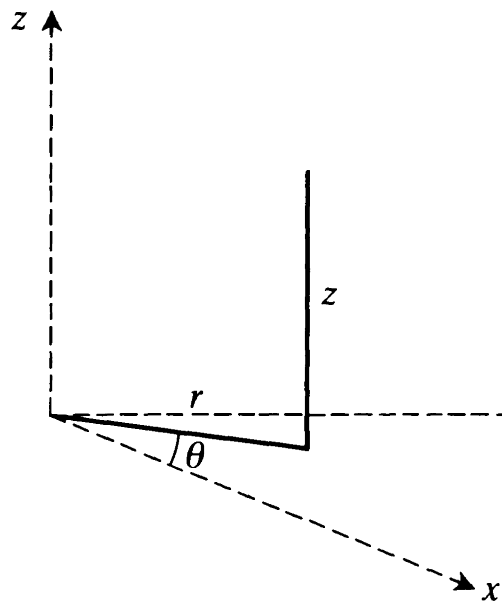

Fig. A.2 Cylindrical polar coordinates.

Also,

$$\nabla\phi = \frac{\partial\phi}{\partial r}\boldsymbol{e}_r + \frac{1}{r}\frac{\partial\phi}{\partial\theta}\boldsymbol{e}_\theta + \frac{\partial\phi}{\partial z}\boldsymbol{e}_z, \tag{A.30}$$

$$\nabla\cdot\boldsymbol{F} = \frac{1}{r}\frac{\partial}{\partial r}(rF_r) + \frac{1}{r}\frac{\partial F_\theta}{\partial\theta} + \frac{\partial F_z}{\partial z}, \tag{A.31}$$

$$\nabla\wedge\boldsymbol{F} = \frac{1}{r}\begin{vmatrix} \boldsymbol{e}_r & r\boldsymbol{e}_\theta & \boldsymbol{e}_z \\ \dfrac{\partial}{\partial r} & \dfrac{\partial}{\partial\theta} & \dfrac{\partial}{\partial z} \\ F_r & rF_\theta & F_z \end{vmatrix}, \tag{A.32}$$

$$\nabla^2 = \frac{1}{r}\frac{\partial}{\partial r}\left(r\frac{\partial}{\partial r}\right) + \frac{1}{r^2}\frac{\partial^2}{\partial\theta^2} + \frac{\partial^2}{\partial z^2}, \tag{A.33}$$

$$\boldsymbol{u}\cdot\nabla = u_r\frac{\partial}{\partial r} + \frac{u_\theta}{r}\frac{\partial}{\partial\theta} + u_z\frac{\partial}{\partial z}. \tag{A.34}$$

The Navier–Stokes equations in cylindrical polar coordinates are:

$$\frac{\partial u_r}{\partial t} + (\boldsymbol{u} \cdot \nabla)u_r - \frac{u_\theta^2}{r} = -\frac{1}{\rho}\frac{\partial p}{\partial r} + \nu\left(\nabla^2 u_r - \frac{u_r}{r^2} - \frac{2}{r^2}\frac{\partial u_\theta}{\partial \theta}\right),$$

$$\frac{\partial u_\theta}{\partial t} + (\boldsymbol{u} \cdot \nabla)u_\theta + \frac{u_r u_\theta}{r} = -\frac{1}{\rho r}\frac{\partial p}{\partial \theta} + \nu\left(\nabla^2 u_\theta + \frac{2}{r^2}\frac{\partial u_r}{\partial \theta} - \frac{u_\theta}{r^2}\right),$$

(A.35)

$$\frac{\partial u_z}{\partial t} + (\boldsymbol{u} \cdot \nabla)u_z = -\frac{1}{\rho}\frac{\partial p}{\partial z} + \nu\, \nabla^2 u_z,$$

$$\frac{1}{r}\frac{\partial}{\partial r}(r u_r) + \frac{1}{r}\frac{\partial u_\theta}{\partial \theta} + \frac{\partial u_z}{\partial z} = 0.$$

The components of the rate-of-strain tensor are given by:

$$e_{rr} = \frac{\partial u_r}{\partial r}, \qquad e_{\theta\theta} = \frac{1}{r}\frac{\partial u_\theta}{\partial \theta} + \frac{u_r}{r}, \qquad e_{zz} = \frac{\partial u_z}{\partial z},$$

$$2e_{\theta z} = \frac{1}{r}\frac{\partial u_z}{\partial \theta} + \frac{\partial u_\theta}{\partial z}, \qquad 2e_{zr} = \frac{\partial u_r}{\partial z} + \frac{\partial u_z}{\partial r}, \qquad \text{(A.36)}$$

$$2e_{r\theta} = r\frac{\partial}{\partial r}\left(\frac{u_\theta}{r}\right) + \frac{1}{r}\frac{\partial u_r}{\partial \theta}.$$

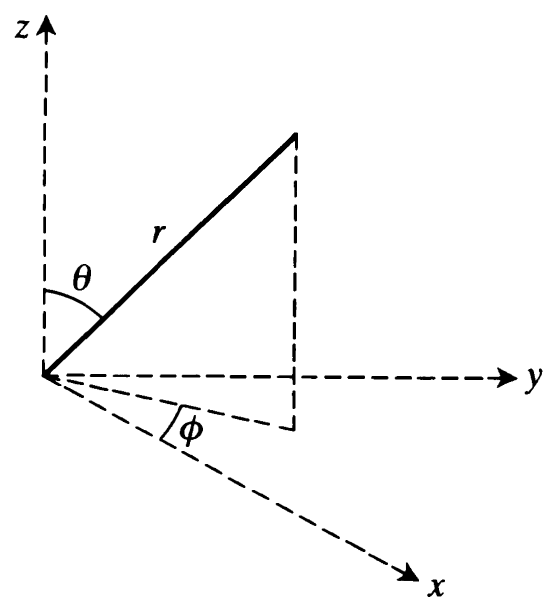

Fig. A.3. Spherical polar coordinates.

A.7. Spherical polar coordinates

Spherical polar coordinates (r, θ, ϕ) are such that

$$x_1 = r\sin\theta\cos\phi, \qquad x_2 = r\sin\theta\sin\phi, \qquad x_3 = r\cos\theta,$$

as in Fig. A.3. Clearly,

$$\delta\boldsymbol{x} = \delta r\boldsymbol{e}_r + r\delta\theta\boldsymbol{e}_\theta + r\sin\theta\,\delta\phi\boldsymbol{e}_\phi$$

and

$$\boldsymbol{e}_r = \sin\theta\cos\phi\,\boldsymbol{e}_1 + \sin\theta\sin\phi\,\boldsymbol{e}_2 + \cos\theta\,\boldsymbol{e}_3,$$

$$\boldsymbol{e}_\theta = \cos\theta\cos\phi\,\boldsymbol{e}_1 + \cos\theta\sin\phi\,\boldsymbol{e}_2 - \sin\theta\,\boldsymbol{e}_3,$$

$$\boldsymbol{e}_\phi = -\sin\phi\,\boldsymbol{e}_1 + \cos\phi\,\boldsymbol{e}_2.$$

The unit vectors do not change with r, but

$$\partial\boldsymbol{e}_r/\partial\theta = \boldsymbol{e}_\theta, \qquad \partial\boldsymbol{e}_\theta/\partial\theta = -\boldsymbol{e}_r, \qquad \partial\boldsymbol{e}_\phi/\partial\theta = 0,$$

$$\partial\boldsymbol{e}_r/\partial\phi = \sin\theta\,\boldsymbol{e}_\phi, \qquad \partial\boldsymbol{e}_\theta/\partial\phi = \cos\theta\,\boldsymbol{e}_\phi, \tag{A.37}$$

$$\partial\boldsymbol{e}_\phi/\partial\phi = -\sin\theta\,\boldsymbol{e}_r - \cos\theta\,\boldsymbol{e}_\theta.$$

Also,

$$\nabla\Phi = \frac{\partial\Phi}{\partial r}\boldsymbol{e}_r + \frac{1}{r}\frac{\partial\Phi}{\partial\theta}\boldsymbol{e}_\theta + \frac{1}{r\sin\theta}\frac{\partial\Phi}{\partial\phi}\boldsymbol{e}_\phi, \tag{A.38}$$

$$\nabla\cdot\boldsymbol{F} = \frac{1}{r^2}\frac{\partial}{\partial r}(r^2F_r) + \frac{1}{r\sin\theta}\frac{\partial}{\partial\theta}(F_\theta\sin\theta) + \frac{1}{r\sin\theta}\frac{\partial F_\phi}{\partial\phi}, \tag{A.39}$$

$$\nabla\wedge\boldsymbol{F} = \frac{1}{r^2\sin\theta}\begin{vmatrix} \boldsymbol{e}_r & r\boldsymbol{e}_\theta & r\sin\theta\boldsymbol{e}_\phi \\ \dfrac{\partial}{\partial r} & \dfrac{\partial}{\partial\theta} & \dfrac{\partial}{\partial\phi} \\ F_r & rF_\theta & r\sin\theta F_\phi \end{vmatrix}, \tag{A40}$$

$$\nabla^2 = \frac{1}{r^2}\frac{\partial}{\partial r}\left(r^2\frac{\partial}{\partial r}\right) + \frac{1}{r^2\sin\theta}\frac{\partial}{\partial\theta}\left(\sin\theta\frac{\partial}{\partial\theta}\right) + \frac{1}{r^2\sin^2\theta}\frac{\partial^2}{\partial\phi^2}, \tag{A.41}$$

$$\boldsymbol{u}\cdot\nabla = u_r\frac{\partial}{\partial r} + \frac{u_\theta}{r}\frac{\partial}{\partial\theta} + \frac{u_\phi}{r\sin\theta}\frac{\partial}{\partial\phi}. \tag{A.42}$$

The Navier–Stokes equations in spherical polar coordinates are:

$$\frac{\partial u_r}{\partial t}+(\boldsymbol{u}\cdot\nabla)u_r-\frac{u_\theta^2}{r}-\frac{u_\phi^2}{r}$$

$$=-\frac{1}{\rho}\frac{\partial p}{\partial r}+\nu\left[\nabla^2u_r-\frac{2u_r}{r^2}-\frac{2}{r^2\sin\theta}\frac{\partial}{\partial\theta}(u_\theta\sin\theta)-\frac{2}{r^2\sin\theta}\frac{\partial u_\phi}{\partial\phi}\right],$$

$$\frac{\partial u_\theta}{\partial t}+(\boldsymbol{u}\cdot\nabla)u_\theta+\frac{u_ru_\theta}{r}-\frac{u_\phi^2\cot\theta}{r}$$

$$=-\frac{1}{\rho r}\frac{\partial p}{\partial\theta}+\nu\left[\nabla^2u_\theta+\frac{2}{r^2}\frac{\partial u_r}{\partial\theta}-\frac{u_\theta}{r^2\sin^2\theta}-\frac{2\cos\theta}{r^2\sin^2\theta}\frac{\partial u_\phi}{\partial\phi}\right],$$

$$\frac{\partial u_\phi}{\partial t}+(\boldsymbol{u}\cdot\nabla)u_\phi+\frac{u_\phi u_r}{r}+\frac{u_\theta u_\phi\cot\theta}{r}$$

$$=-\frac{1}{\rho r\sin\theta}\frac{\partial p}{\partial\phi}+\nu\left[\nabla^2u_\phi+\frac{2}{r^2\sin\theta}\frac{\partial u_r}{\partial\phi}+\frac{2\cos\theta}{r^2\sin^2\theta}\frac{\partial u_\theta}{\partial\phi}-\frac{u_\phi}{r^2\sin^2\theta}\right],$$

$$\frac{1}{r^2}\frac{\partial}{\partial r}(r^2u_r)+\frac{1}{r\sin\theta}\frac{\partial}{\partial\theta}(u_\theta\sin\theta)+\frac{1}{r\sin\theta}\frac{\partial u_\phi}{\partial\phi}=0. \quad \text{(A.43)}$$

The components of the rate-of-strain tensor are given by:

$$e_{rr}=\frac{\partial u_r}{\partial r},\qquad e_{\theta\theta}=\frac{1}{r}\frac{\partial u_\theta}{\partial\theta}+\frac{u_r}{r},$$

$$e_{\phi\phi}=\frac{1}{r\sin\theta}\frac{\partial u_\phi}{\partial\phi}+\frac{u_r}{r}+\frac{u_\theta\cot\theta}{r},$$

$$2e_{\theta\phi}=\frac{\sin\theta}{r}\frac{\partial}{\partial\theta}\left(\frac{u_\phi}{\sin\theta}\right)+\frac{1}{r\sin\theta}\frac{\partial u_\theta}{\partial\phi}, \quad \text{(A.44)}$$

$$2e_{\phi r}=\frac{1}{r\sin\theta}\frac{\partial u_r}{\partial\phi}+r\frac{\partial}{\partial r}\left(\frac{u_\phi}{r}\right),$$

$$2e_{r\theta}=r\frac{\partial}{\partial r}\left(\frac{u_\theta}{r}\right)+\frac{1}{r}\frac{\partial u_r}{\partial\theta}.$$

Hints and answers for exercises

Chapter 1

1.1 The rate of flow of mass out of S is $\int_S \rho \boldsymbol{u} \cdot \boldsymbol{n} \, \mathrm{d}S$, and this must be equal to $-\int_V (\partial \rho / \partial t) \, \mathrm{d}V$, the rate at which mass is decreasing in the region enclosed by S.

Use (A.4).

$\mathrm{D}\rho/\mathrm{D}t = 0$ does *not* mean that ρ is a constant; it means that ρ is conserved by each individual fluid element, and this makes sense, as each element conserves both its mass and (if $\nabla \cdot \boldsymbol{u} = 0$) its volume.

1.2. The flow is not irrotational, as $\nabla \wedge \boldsymbol{u} = (0, 0, 2\Omega)$, so the theorem following eqn (1.17) does not apply. The flow *is* steady, so the Bernoulli streamline theorem applies, but there is then no telling how p might vary from one streamline to another.

Free surface: $z = (\Omega^2/2g)(x^2 + y^2) + \text{constant}$.

1.3. The preceding exercise implies

$$p/\rho = \tfrac{1}{2}\Omega^2 r^2 - gz + c_1 \qquad \text{for } r < a.$$

For $r > a$ the flow is irrotational, so the Bernoulli theorem following eqn (1.17) gives

$$\frac{p}{\rho} = -\frac{1}{2}\frac{\Omega^2 a^4}{r^2} - gz + c_2 \qquad \text{for } r > a.$$

Continuity of p at $r = a$ implies that $c_2 - c_1 = \Omega^2 a^2$ etc.

1.4. Take the Euler equation in the form (1.14), multiply by ρ, take the dot product of both sides with $\boldsymbol{u}$, and then use eqn (A.4) to obtain

$$\frac{\partial}{\partial t}(\tfrac{1}{2}\rho \boldsymbol{u}^2) = -\nabla \cdot [(p' + \tfrac{1}{2}\rho \boldsymbol{u}^2)\boldsymbol{u}].$$

Then integrate both sides over V and use the divergence theorem.

1.5. Much as in §1.5, but use eqn (A.5) in dealing with

$$\nabla \wedge \left(\frac{1}{\rho} \nabla p\right).$$

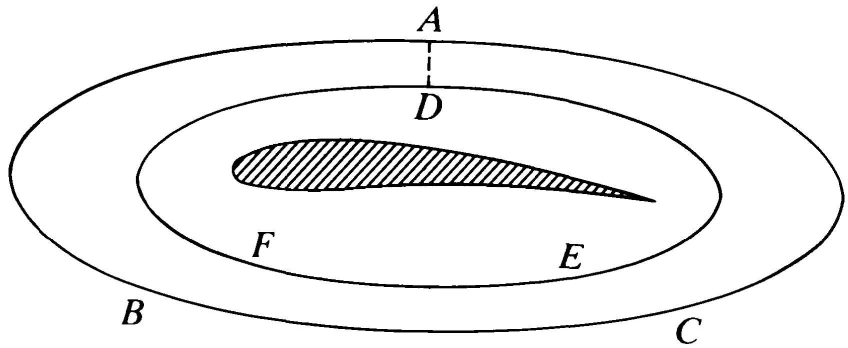

Fig. H.1.

Use conservation of mass to replace $\nabla \cdot \boldsymbol{u}$, when it appears, by

$$-\frac{1}{\rho}\frac{\mathrm{D}\rho}{\mathrm{D}t}.$$

If $p = p(\rho)$, then $\nabla p = p'(\rho)\,\nabla\rho$, so $\nabla p \wedge \nabla \rho = 0$.

1.6. Consider the circulation round the closed circuit ABCADEFDA in Fig. H.1, which does not enclose the wing, and thereby show that

$$\int_{\text{ABCA}} \boldsymbol{u} \cdot \mathrm{d}\boldsymbol{x} = \int_{\text{DFED}} \boldsymbol{u} \cdot \mathrm{d}\boldsymbol{x}.$$

1.7. See Fig. 4.1 for the streamlines.

No, because $\mathrm{D}c/\mathrm{D}t = 0$.

The results are true in general because holding $\boldsymbol{X}$ (as opposed to $\boldsymbol{x}$) constant corresponds to restricting attention to a particular fluid element.

$c(X, Y, t) = \beta X^2 Y$, and this gives a slightly different perspective on why it is that c does not change with time for a particular fluid element.

1.8 The streamlines are

$$y = \frac{kt}{u_0}x + \text{constant}, \qquad z = \text{constant},$$

obtained by integrating eqn (1.5) at fixed time t.

A particle path is obtained by integrating

$$(\partial x/\partial t)_{\boldsymbol{X}} = u_0, \qquad (\partial y/\partial t)_{\boldsymbol{X}} = kt, \qquad (\partial z/\partial t)_{\boldsymbol{X}} = 0$$

(see Exercise 1.7), so

$$x = u_0 t + F_1(\boldsymbol{X}), \qquad y = \tfrac{1}{2}kt^2 + F_2(\boldsymbol{X}), \qquad z = F_3(\boldsymbol{X}).$$

The arbitrary functions of X, Y, and Z are determined by the condition that $\boldsymbol{x} = \boldsymbol{X}$ when $t = 0$, so

$$x = u_0 t + X, \qquad y = \tfrac{1}{2}kt^2 + Y, \qquad z = Z.$$

Eliminating t gives the particle paths.

Chapter 2

2.1. (i) 4×10^7; (ii) 10^3; (iii) 0.003; (iv) 10^{-3}.
The boundary layer thickness is of order 1 mm.

2.2.

$$(\boldsymbol{u}' \cdot \nabla')\boldsymbol{u}' = -\nabla' p' + \frac{1}{R}\nabla'^2 \boldsymbol{u}', \qquad \nabla' \cdot \boldsymbol{u}' = 0,$$

subject to

$$\boldsymbol{u}' = 0 \quad \text{on } x'^2 + y'^2 = 1; \qquad \boldsymbol{u}' \to (1, 0, 0) \quad \text{as } x'^2 + y'^2 \to \infty.$$

Solving this will give $\boldsymbol{u}'$ as some specific function (or functions—the solution may not be unique) of $\boldsymbol{x}'$ and R. Thus, in particular, the *direction* of $\boldsymbol{u}'$ depends, at a given $\boldsymbol{x}' = \boldsymbol{x}/a$, not on ν, a, or U individually but only on $R = Ua/\nu$.

(The same argument may evidently be used for flow past a body of any shape.)

2.3. (i) Seek a solution to the Navier–Stokes equations of the form $\boldsymbol{u} = [u(y), 0, 0]$, taking care that: (1) $\nabla \cdot \boldsymbol{u} = 0$; (2) all three components of the momentum equation (2.3) are satisfied; and (3) $u(y)$ satisfies the no-slip condition on $y = \pm h$.

(ii) Likewise, assuming $\boldsymbol{u} = [0, 0, u_z(r)]$, and using eqn (2.22). The condition that u_z is finite at $r = 0$ is needed.

2.4. Extend the single-layer analysis in the text to show that $\partial p/\partial x = 0$ in both layers. The interface conditions are

$$u_1 = u_2, \qquad \mu_1 \frac{du_1}{dy} = \mu_2 \frac{du_2}{dy} \quad \text{at } y = h_1,$$

because the tangential stress exerted on the lower layer by the upper layer is $\mu_2\, du_2/dy$, that exerted on the upper layer by the lower layer is $-\mu_1\, du_1/dy$, and the two must be equal and opposite.

The upper layer is not accelerating, and there is no tangential stress on it from above, so the tangential stress on it from below must exactly cancel the net gravitational force on it in the x-direction, which is proportional to its mass. The (equal and opposite) tangential stress on the lower layer thus depends on h_2, but not on ν_2.

2.5. The boundary conditions are homogeneous, but the equation is not, so write $u = u_0(y) + u_1(y, t)$, where

$$u_0(y) = (P/2\mu)(h^2 - y^2)$$

is the steady solution satisfying the boundary conditions (but not the initial conditions), as in Exercise 2.3. Then solve the resulting problem for $u_1(y, t)$ as in the text.

$$u = \frac{P}{2\mu}\left[h^2 - y^2 - h^2 \sum_{N=0}^{\infty} \frac{4(-1)^N}{(N+\frac{1}{2})^3\pi^3} e^{-(N+\frac{1}{2})^2\pi^2\nu t/h^2} \cos(N+\tfrac{1}{2})\frac{\pi y}{h}\right].$$

2.6. When $v_0 h/\nu \ll 1$, $e^{-v_0 y/\nu} \doteqdot 1 - v_0 y/\nu$ etc., so

$$u \doteqdot U\left(1 - \frac{y}{h}\right).$$

When $v_0 h/\nu \gg 1$, $e^{-v_0 h/\nu}$ is extremely small, and so too is $e^{-v_0 y/\nu}$ throughout most of the range $0 < y < h$, though *not* within a distance of order ν/v_0 of the lower boundary $y = 0$. In this boundary layer

$$u \doteqdot U e^{-v_0 y/\nu}.$$

2.8. There will at first be a thin boundary layer of negative vorticity on $r = a$, and this will gradually diffuse outwards until, as $t \to \infty$, the vorticity tends to zero at any finite r, however large.

On the outer cylinder $r = b$ there will at first be a boundary layer with positive vorticity. This vorticity will diffuse inwards, gradually cancelling the outward-diffusing negative vorticity, so that $\omega \to 0$ as $t \to \infty$.

2.9. The result for u_r comes directly from $\nabla \cdot \boldsymbol{u} = 0$. The general solution of the equation is

$$u_\theta = \frac{A}{r} + \frac{B}{r^{R-1}},$$

provided that $R \neq 2$. When $R > 2$ a free parameter is left in the solution, so there are in fact infinitely many flows satisfying the conditions.

2.10. We have

$$f'' + \left(\tfrac{1}{2}\eta - \frac{1}{\eta}\right)f' = 0,$$

which is a first-order equation for f'.

The vorticity is concentrated in the (expanding) region $r < O(\nu t)^{\frac{1}{2}}$, and it decreases with time (as t^{-1}) at $r = 0$.

2.11. If $\boldsymbol{u} = u_\theta(r, z)\boldsymbol{e}_\theta$, the r- and z-components of the Navier–Stokes equations (2.22) together imply that $u_\theta(r, z)$ is independent of z, but this is incompatible with the no-slip boundary conditions on $z = 0$ and $z = h$.

2.12 Multiply both sides by $r u_\theta$, integrate both sides between $r = 0$ and

$r = a$, and then use integration by parts to obtain

$$\frac{d}{dt}\int_0^a \tfrac{1}{2}u_\theta^2 r \, dr = -\nu \int_0^a r\left(\frac{\partial u_\theta}{\partial r}\right)^2 dr - \nu \int_0^a \frac{u_\theta^2}{r} dr.$$

The second term is less than or equal to zero; the third term needs to be compared with

$$-\nu \int_0^a \frac{r u_\theta^2}{a^2} dr.$$

$E \to 0$ as $t \to \infty$ because $E e^{2\nu t/a^2}$ is a decreasing function of t.

2.14. Substitute into the Navier–Stokes equations, integrate the y-component with respect to y, and deduce that $\partial p/\partial x$ is a function of x only. Turn to the x-component, deduce that $x^{-1}\,\partial p/\partial x$ is a constant, because the rest of the equation is a function of y alone, etc.

$$p = -\tfrac{1}{2}\rho\alpha^2 x^2 - \rho\nu\alpha(f' + \tfrac{1}{2}f^2) + \text{constant}.$$

2.15. The supposition that the main, inviscid flow is not much disturbed requires the existence of a thin boundary layer on the plate in order to satisfy the no-slip condition. But the mainstream flow speed αy at the edge of such a boundary layer would decrease rapidly with distance along the plate from the leading edge. By Bernoulli's theorem there would therefore be a substantial *increase* in pressure p along the plate in the flow direction (as is evident from Fig. 2.13), and, as explained in §2.1, this is exactly the circumstance in which boundary-layer separation occurs.

Chapter 3

3.1. The new boundary condition is $\partial\phi/\partial y = 0$ on $y = -h$. The analysis is valid only if $\eta \ll \lambda$ *and* $\eta \ll h$. The particle paths are ellipses that become flatter with depth.

3.2. The condition that $p_1 = p_2$ at the interface gives, on using eqn (3.19) in each layer and linearizing:

$$\rho_1 \frac{\partial\phi_1}{\partial t} + \rho_1 g\eta = \rho_2 \frac{\partial\phi_2}{\partial t} + \rho_2 g\eta \qquad \text{on } y = 0.$$

Seek suitable solutions of $\partial^2\phi/\partial x^2 + \partial^2\phi/\partial y^2 = 0$ in each layer, ensuring that $\phi_1 \to 0$ as $y \to -\infty$ and $\phi_2 \to 0$ as $y \to \infty$ (at which stage $|k|$ enters the analysis).

3.3. By the argument of §3.4, $p_2 - p_1 = T\,\partial^2\eta/\partial x^2$ at $y = \eta(x, t)$. In each layer, seek solutions of Laplace's equation of the form $\phi = f(x)g(y)\sin(\omega t + \varepsilon)$; the conditions $\partial\phi/\partial x = 0$ at $x = 0$ and at $x = a$ help to determine $f(x)$.

At the time t at which two characteristics from x_0 and $x_0 + \delta x_0$ cross, the value of x is the same, so the relevant time t is that at which $(\partial x/\partial x_0)_t = 0$.

3.20 The first term represents the rate of working by pressure forces on the cross-section; the second and third represent the rates at which kinetic and potential energy are being swept through the cross-section.

To obtain the first result use the fact that the pressure is hydrostatic, i.e. $p = -\rho g(y - h_1)$, because the flow is uniform. To obtain the second result, consider the difference in energy fluxes and use eqns (3.124) and (3.125).

3.21. Write down the Euler momentum equation (1.12) with $\boldsymbol{g} = 0$, use eqn (A.9) to rewrite the $(\boldsymbol{u} \cdot \nabla)\boldsymbol{u}$ term, and then write $p = c\rho^\gamma$, where c is a constant, etc.

3.22. Write $p = c\rho^\gamma$, where c is a constant, and eliminate p. It can then be helpful to establish the relationship

$$\frac{2}{a}\frac{\partial a}{\partial x} = \frac{\gamma - 1}{\rho}\frac{\partial \rho}{\partial x},$$

which also holds if $\partial/\partial x$ is replaced by $\partial/\partial t$.

The final part involves adding and subtracting the equations for u and a.

3.23. Use eqn (3.136), writing $u = F(\xi)$, where $\xi = x - [\frac{1}{2}(\gamma + 1)u + a_0]t$. Therefore

$$\frac{\partial u}{\partial x} = \frac{F'(\xi)}{1 + \frac{1}{2}(\gamma + 1)tF'(\xi)} \qquad \text{(cf. eqn (3.115))},$$

and, of course, $F(\xi) = \frac{1}{2}U[1 - \tanh(\xi/L)]$, by virtue of the initial conditions.

3.24. After one integration

$$(a_0 - V)f + \tfrac{1}{4}(\gamma + 1)f^2 = \tfrac{2}{3}\nu f' + c,$$

where c is a constant. Now $f \to 0$ as $\xi \to \infty$, so $\frac{2}{3}\nu f' \to -c$ as $\xi \to \infty$, and the only way this is compatible with $f \to 0$ as $\xi \to \infty$ is by c being zero. Similar considerations as $\xi \to -\infty$ give the shock speed V.

Chapter 4

4.1. (i) Use Stokes's theorem (A.23).

(ii) Use Green's theorem in the plane (A.24), with u in place of v and $-v$ in place of u.

4.2. Treat similarly to the line vortex flow (4.18).

No contradiction: does $\partial u/\partial x + \partial v/\partial y = 0$—on which Exercise 4.1(ii) depends—hold *everywhere* for a line source flow?

$$w = \frac{Q}{2\pi}\log(z-d) + \frac{Q}{2\pi}\log(z+d).$$

On wall $x = 0$, $v = Qy/\pi(y^2 + d^2)$ and $p + \frac{1}{2}\rho v^2 = \text{constant}$.

4.3. Use eqn (4.11) to obtain ϕ, and then eqn (4.12) to obtain the complex potential of the flow when the cylinder is absent, $w = \frac{1}{2}A(z-c)^2$. Then use the circle theorem (4.29).

$$\psi = Ay\left[x\left\{1 + \frac{a^2}{x^2+y^2}\right\} - c\right]\left(1 - \frac{a^2}{x^2+y^2}\right)$$

(so $\psi = 0$ on $x^2 + y^2 = a^2$, as desired).

$$F_x = -2\pi\rho A^2 c a^2, \qquad F_y = 0.$$

4.5. $$\delta\mathcal{N} = x\delta F_y - y\delta F_x = \mathcal{R}[(x+\mathrm{i}y)(\delta F_y + \mathrm{i}\delta F_x)].$$

4.7. Note that $Z = X + \mathrm{i}Y = 2a\cos\theta$ on the plate.

$\int_{-1}^{1}[(1-s)/(1+s)]^{\frac{1}{2}}\,\mathrm{d}s$ can be evaluated by putting $s = \cos 2\gamma$.

For the torque, re-work the calculation for the ellipse in §4.10, but with

$$w = U\left(z\mathrm{e}^{-\mathrm{i}\alpha} + \frac{a^2}{z}\mathrm{e}^{\mathrm{i}\alpha}\right) - \frac{\mathrm{i}\Gamma}{2\pi}\log z.$$

The terms involving Γ do give a contribution to the integral, but this disappears when the real part is taken.

4.8. Note as a check, or as part of the argument in obtaining Fig. 4.16, that $\mathrm{d}Z/\mathrm{d}z = 0$ (but $\mathrm{d}^2Z/\mathrm{d}z^2 \neq 0$) at $z = a$, so that angles between two line elements through $z = a$ are doubled by the mapping, as in Fig. H.3 (see §4.6).

$$W(Z) = U\left[z - \mathrm{i}a\cot\beta + \frac{a^2\operatorname{cosec}^2\beta}{z - \mathrm{i}a\cot\beta}\right] - \frac{\mathrm{i}\Gamma}{2\pi}\log(z - \mathrm{i}a\cot\beta),$$

where

$$z = \tfrac{1}{2}Z + (\tfrac{1}{4}Z^2 - a^2)^{\frac{1}{2}}.$$

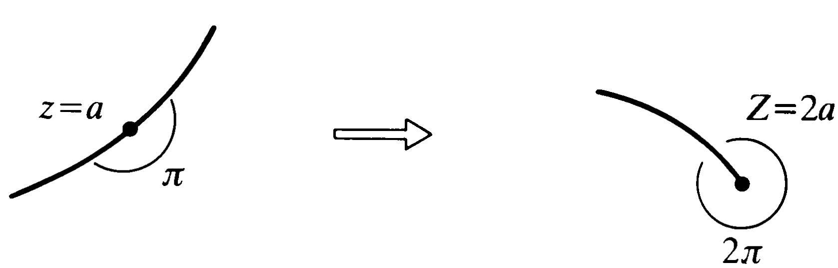

Fig. H.3.

4.9. (i) The image sources are at $z = \pm 2nib$, $n = 1, 2, 3 \ldots$. To sum, use the argument leading to eqn (5.29), and the identity quoted there.

$$w = \frac{Q}{2\pi}\log(e^{\pi z/2b} - e^{-\pi z/2b}).$$

(ii) Write $Z = R^{i\Theta} = e^{\alpha(x+iy)}$ to find the corresponding fluid region in the Z-plane. The choice $\alpha = \pi/b$ opens that region up so that there is just a barrier along the negative real Z-axis, which does not affect the flow caused by the line source at $Z = 1$. But there is a subtlety. In the z-plane there is a volume flux $Q/2$ in both positive and negative x-directions. As $x \to \pm\infty$, then, the flow becomes uniform with velocity $(\pm Q/4b, 0)$. What happens, under the given mapping, to the uniform flow at large negative x?

4.10. Apply the x-component of eqn (4.70) to the region ABCDA in Fig. 4.10, showing that the right-hand side is zero, while the left-hand side is $(p_1 - p_2)d - F_x$, where p_1 is the pressure far upstream and p_2 the pressure far downstream. Then apply Bernoulli's streamline theorem and use eqn (4.73).

No: the Kutta–Joukowski theorem is for a single aerofoil, and in any case $F_x \to 0$ as $d \to \infty$ (and $v_2 \to 0$) for fixed Γ.

Chapter 5

5.1. $\boldsymbol{u} = (\partial \boldsymbol{x}/\partial t)_s = (a\alpha \sin s, 0, 0)$. (Note that holding s constant is exactly like holding $\boldsymbol{X}$ constant in Exercise 1.7.)

The integrand $\boldsymbol{u} \cdot \partial \boldsymbol{x}/\partial s$ is time-dependent, as expected, but $\Gamma = -\pi a^2 \alpha$.

5.2.

$$\frac{\partial}{\partial t}\left(\boldsymbol{u} \cdot \frac{\partial \boldsymbol{x}}{\partial s}\right) = \left(\frac{\partial \boldsymbol{u}}{\partial t}\right)_s \cdot \left(\frac{\partial \boldsymbol{x}}{\partial s}\right)_t + \boldsymbol{u} \cdot \left(\frac{\partial}{\partial t}\right)_s \left(\frac{\partial \boldsymbol{x}}{\partial s}\right)_t.$$

Now, $(\partial \boldsymbol{u}/\partial t)_s$ is the acceleration of a fluid element, otherwise written $\mathrm{D}\boldsymbol{u}/\mathrm{D}t$ (cf. Exercise 1.7). Also,

$$\left(\frac{\partial}{\partial t}\right)_s \left(\frac{\partial \boldsymbol{x}}{\partial s}\right)_t = \left(\frac{\partial}{\partial s}\right)_t \left(\frac{\partial \boldsymbol{x}}{\partial t}\right)_s = \left(\frac{\partial \boldsymbol{u}}{\partial s}\right)_t,$$

and

$$\boldsymbol{u} \cdot \frac{\partial \boldsymbol{u}}{\partial s} = \frac{\partial}{\partial s}\left(\tfrac{1}{2}\boldsymbol{u}^2\right),$$

which integrates to zero, as $\boldsymbol{u}$ is a single-valued function of position.

[Note that the partial derivatives commute only because $\boldsymbol{x}$ is viewed consistently as a function of s and t. Suppose the original $\partial/\partial t$ had been the 'normal' one in this text, namely $\partial/\partial t$ *holding* $\boldsymbol{x}$ *constant.* Then, typically,

$$\left(\frac{\partial}{\partial t}\right)_{\boldsymbol{x}}\left(\frac{\partial \boldsymbol{x}}{\partial s}\right)_t \neq \left(\frac{\partial}{\partial s}\right)_t\left(\frac{\partial \boldsymbol{x}}{\partial t}\right)_{\boldsymbol{x}},$$

because the right-hand side is zero, because $(\partial \boldsymbol{x}/\partial t)_{\boldsymbol{x}}$ is trivially zero, but the left-hand side is typically not zero. The reason that these differential operators do not commute is that in each case the dependent variable is being viewed as a function of $\boldsymbol{x}$ and t during one differentiation but as a function of s and t during the other.]

5.3. See note (c) following the proof of the theorem in §5.1.

5.4. After Stokes's theorem use (A.5), and note that if $p = f(\rho)$ then $\nabla p = f'(\rho)\nabla\rho$. The unnecessary assumption is the same as that in Exercise 5.3. Alternative:

$$-\frac{1}{\rho}f'(\rho)\,\nabla\rho = \nabla h,$$

where

$$h(\rho) = -\int_0^{\rho}\frac{1}{\alpha}f'(\alpha)\,\mathrm{d}\alpha.$$

Then $\mathrm{d}\Gamma/\mathrm{d}t = [h]_C = 0$, as ρ is a single-valued function of position.

In the thin vortex tube argument replace conservation of volume by (the more generally valid) conservation of mass.

5.5. Apply the divergence theorem to $\boldsymbol{\omega} = \nabla \wedge \boldsymbol{u}$, the region V being a portion of the vortex tube of finite length.

5.6. Proceed as in Exercise 5.2 until

$$\frac{\mathrm{d}\mathscr{C}}{\mathrm{d}t} = \int_0^1\left[\left(\frac{\partial \boldsymbol{a}}{\partial t}\right)_s\cdot\frac{\partial \boldsymbol{x}}{\partial s} + \boldsymbol{a}\cdot\frac{\partial \boldsymbol{u}}{\partial s}\right]\mathrm{d}s.$$

Then take the right-hand side of the desired result, recognizing that $\partial \boldsymbol{a}/\partial t$ *there* means $(\partial \boldsymbol{a}/\partial t)_{\boldsymbol{x}}$, and write it using the suffix notation and the summation convention as

$$\int_{C(t)}\left[\left(\frac{\partial \boldsymbol{a}}{\partial t}\right)_{\boldsymbol{x}} + \left(\boldsymbol{e}_i \wedge \frac{\partial \boldsymbol{a}}{\partial x_i}\right)\wedge \boldsymbol{u}\right]\cdot \mathrm{d}\boldsymbol{x}.$$

Expand the triple vector product, and note that

$$(\partial \boldsymbol{a}/\partial t)_s = (\partial \boldsymbol{a}/\partial t)_{\boldsymbol{x}} + (\boldsymbol{u}\cdot\nabla)\boldsymbol{a},$$

because both sides of this expression denote the rate of change of $\boldsymbol{a}$ following a particular fluid particle (cf. Exercise 5.2).

5.7. Note that $\boldsymbol{\omega} = \omega(R, z, t)\boldsymbol{e}_\phi$, so that

$$(\boldsymbol{\omega} \cdot \nabla)\boldsymbol{u} = \frac{\omega}{R}\frac{\partial}{\partial \phi}[u_R(R, z, t)\boldsymbol{e}_R + u_z(R, z, t)\boldsymbol{e}_z] = \frac{\omega u_R}{R}\boldsymbol{e}_\phi,$$

by virtue of eqn (A.29), allowing for the difference in notation.

5.8. Let the vortex be at $z_1 = x_1 + \mathrm{i}y_1$. The image system consists of *three* vortices at $\bar{z}_1$, $-\bar{z}_1$, and $-z_1$. Proceed as with eqn (5.27) to obtain

$$\frac{\mathrm{d}x_1}{\mathrm{d}t} - \mathrm{i}\frac{\mathrm{d}y_1}{\mathrm{d}t} = -\frac{\mathrm{i}\Gamma}{2\pi}\left[-\frac{1}{z_1 - \bar{z}_1} - \frac{1}{z_1 + \bar{z}_1} + \frac{1}{2z_1}\right];$$

hence

$$\mathrm{d}y_1/\mathrm{d}x_1 = -(y_1/x_1)^3 \qquad \text{etc.}$$

To understand the behaviour of the trailing vortices, view the whole of $y \geqslant 0$ in the above problem as occupied by fluid, with a single boundary at $y = 0$.

5.9. See eqn (3.19).

5.10. The net force on the wall is zero.

If the vortex were somehow fixed at $(d, 0)$, the $\partial\phi/\partial t$ term would be absent and there would be a net force $\rho\Gamma^2/4\pi d$ on the wall, directed towards the vortex.

5.12.

$$w(z) = -\frac{\mathrm{i}\Gamma}{2\pi}[\log(z - z_2) - \log(z - \bar{z}_2) - \log(z - z_1) + \log(z - \bar{z}_1)] - \tfrac{1}{2}\alpha z^2.$$

5.13. Let $P = \bar{\varepsilon}_2 + \varepsilon_1$ and $Q = \bar{\varepsilon}_2 - \varepsilon_1$, and deduce that

$$\dot{P} = -\tfrac{1}{4}\bar{P}, \qquad \dot{Q} = -\tfrac{1}{2}\mathrm{i}Q.$$

Then write $P = P_R + \mathrm{i}P_I$ and solve for P_R and P_I.

5.14. Let the n vortices be at

$$z_m = a\mathrm{e}^{\mathrm{i}2\pi m/n}, \qquad m = 0, 1, \ldots, n - 1.$$

The complex potential due to all these vortices is

$$w = -\frac{\mathrm{i}\Gamma}{2\pi}\log(z^n - a^n),$$

and that due to all except the one at $z = a$ can be written

$$w = -\frac{\mathrm{i}\Gamma}{2\pi}\log\left[1 + \frac{z}{a} + \left(\frac{z}{a}\right)^2 + \ldots + \left(\frac{z}{a}\right)^{n-1}\right].$$

5.15. For last part, multiply the equation by Γ_s and sum from 1 to n.

5.16.

$$\frac{\mathrm{D}}{\mathrm{D}t}(\boldsymbol{u}\cdot\boldsymbol{\omega})=\frac{\mathrm{D}\boldsymbol{u}}{\mathrm{D}t}\cdot\boldsymbol{\omega}+\boldsymbol{u}\cdot\frac{\mathrm{D}\boldsymbol{\omega}}{\mathrm{D}t}.$$

Then use Euler's equation (1.12), the vorticity equation (5.7), and the fact that $\nabla\cdot(\nabla\wedge\boldsymbol{u})=0$ to show that

$$\frac{\mathrm{D}}{\mathrm{D}t}(\boldsymbol{u}\cdot\boldsymbol{\omega})=\nabla\cdot\left[\left(-\frac{p}{\rho}-\chi+\tfrac{1}{2}\boldsymbol{u}^2\right)\boldsymbol{\omega}\right].$$

Then use the divergence theorem.

5.17. Bring $\nabla\cdot[(\boldsymbol{\omega}\wedge\boldsymbol{u})\wedge\nabla\lambda]$ into play using eqn (A.7), expand the triple vector product using eqn (A.1), then use eqn (A.4).

Having said this, the problem lends itself to a much more straightforward approach using suffix notation and the summation convention:

$$\begin{aligned}\frac{\mathrm{D}}{\mathrm{D}t}\left(\omega_i\frac{\partial\lambda}{\partial x_i}\right)&=\frac{\mathrm{D}\omega_i}{\mathrm{D}t}\frac{\partial\lambda}{\partial x_i}+\omega_i\left(\frac{\partial}{\partial t}+u_k\frac{\partial}{\partial x_k}\right)\frac{\partial\lambda}{\partial x_i}\\&=\omega_j\frac{\partial u_i}{\partial x_j}\frac{\partial\lambda}{\partial x_i}+\omega_i\frac{\partial}{\partial x_i}\left(\frac{\partial\lambda}{\partial t}\right)+\omega_iu_k\frac{\partial^2\lambda}{\partial x_k\,\partial x_i},\end{aligned}$$

where we have used the vorticity equation in its form (5.7). By reversing the order of partial differentiation in the final term, and then changing the dummy suffices, it may be written $\omega_ju_i\,\partial^2\lambda/\partial x_j\,\partial x_i$, with summation understood, of course, over $i=1,2,3$ and $j=1,2,3$. Thus

$$\frac{\mathrm{D}}{\mathrm{D}t}\left(\omega_i\frac{\partial\lambda}{\partial x_i}\right)=\omega_i\frac{\partial}{\partial x_i}\left(\frac{\partial\lambda}{\partial t}\right)+\omega_j\frac{\partial}{\partial x_j}\left(u_i\frac{\partial\lambda}{\partial x_i}\right),$$

which is the result.

5.18. The flow has two elements: a *uniform rotation,* angular velocity $\Omega e^{\alpha t}$, which steadily increases with time as a result of a *secondary flow* of the kind in Fig. 5.17 which keeps stretching the vortex lines (if $\alpha>0$).

5.19. The condition that u_θ be finite at $r=0$ is needed.

5.20. The suitable vector identities are eqns (A.9) and (A.10).

5.21. X_1, X_2, and X_3 are three scalar quantities that are (rather trivially) conserved by an individual fluid element, and $X_i=x_i$ at $t=0$, so Ertel's theorem gives

$$\omega_j\frac{\partial X_i}{\partial x_j}=\omega_{0i}.$$

These are three linear algebraic equations for ω_1, ω_2, and ω_3. They can be solved by writing

$$\omega_{0i}\frac{\partial x_k}{\partial X_i}=\omega_j\frac{\partial X_i}{\partial x_j}\frac{\partial x_k}{\partial X_i}=\omega_j\frac{\partial x_k}{\partial x_j}=\omega_j\delta_{jk}=\omega_k,$$

where we have used the chain rule in the second step (note that summation over $i=1, 2, 3$ is understood).

5.22. Let $x_i=x_i\{X(s), t\}$ denote the current position of the particle that was, at $t=0$, a distance s along the initial curve. Then

$$\left(\frac{\partial x_i}{\partial s}\right)_t=\left(\frac{\partial x_i}{\partial X_j}\right)_t\frac{\mathrm{d}X_j}{\mathrm{d}s}=\frac{\partial x_i}{\partial X_j}\frac{\omega_{0j}}{|\boldsymbol{\omega}_0|}=\frac{\omega_i}{|\boldsymbol{\omega}_0|}.$$

5.23.

$$T=\tfrac{1}{2}\rho\int(\nabla\phi)\cdot(\nabla\phi)\,\mathrm{d}V=\tfrac{1}{2}\rho\int[\nabla\cdot(\phi\,\nabla\phi)-\phi\nabla\cdot(\nabla\phi)]\,\mathrm{d}V,$$

by eqn (A.4), and then use the divergence theorem.

5.24. Suppose there are two different irrotational flows, i.e. $\boldsymbol{u}_1=\nabla\phi_1$ and $\boldsymbol{u}_2=\nabla\phi_2$, where

$$\nabla^2\phi_1=0 \quad \text{in } V, \qquad \partial\phi_1/\partial n=f \quad \text{on } S;$$

$$\nabla^2\phi_2=0 \quad \text{in } V, \qquad \partial\phi_2/\partial n=f \quad \text{on } S.$$

Consider the problem for $\phi'=\phi_2-\phi_1$, and use Exercise 5.23 to show that $\nabla\phi'$ must be zero, whereupon $\boldsymbol{u}_1=\boldsymbol{u}_2$, contradicting the original supposition.

5.25. Let $\nabla\phi$ be the unique irrotational flow satisfying the boundary condition, and write any other incompressible flow doing so as $\boldsymbol{u}=\nabla\phi+\boldsymbol{u}'$, where, consequently,

$$\nabla\cdot\boldsymbol{u}'=0 \quad \text{in } V, \qquad \text{and} \qquad \boldsymbol{u}'\cdot\boldsymbol{n}=0 \quad \text{on } S.$$

Then expand $T=\frac{1}{2}\rho\int(\nabla\phi+\boldsymbol{u}')^2\,\mathrm{d}V$, and use eqn (A.4) and the divergence theorem.

5.26. If z denotes distance downstream from the centre of the sphere, then $\phi\sim Uz$ as $r\to\infty$, i.e. $\phi\sim Ur\cos\theta$ as $r\to\infty$. The other boundary condition is $\partial\phi/\partial r=0$ on $r=a$. By trying $\phi=f(r)\cos\theta$—or by a more formal application of the method of separation of variables—obtain

$$\phi=U\left(r+\frac{a^3}{2r^2}\right)\cos\theta.$$

To find the pressure distribution on the sphere, use Bernoulli's theorem.

5.27. Use Exercise 5.23 to find the kinetic energy, $T = \frac{1}{4}MU^2$, where $M = \frac{4}{3}\pi a^3 \rho$ is the mass of fluid displaced by the sphere. Then use the argument leading to eqn (4.77).

5.28. The boundary conditions are

$$\frac{1}{r}\frac{\partial \phi}{\partial \theta} = \pm \Omega r \qquad \text{at } \theta = \pm \Omega t,$$

and trying an appropriate separable solution gives

$$\phi = -(\Omega r^2 \cos 2\theta)/(2 \sin 2\Omega t).$$

The streamlines are $xy = \text{constant}$. At $\theta = \pm \Omega t$ use Exercise 5.9 to obtain

$$\frac{p}{\rho} = \text{constant} - \tfrac{1}{2}\Omega^2 r^2 \left[\frac{3}{\sin^2 2\Omega t} - 2\right].$$

5.29. The last result in Exercise 5.23 assumes that ϕ is a single-valued function of position, which is guaranteed only in a simply connected region. Here, $\phi = \Gamma\theta/2\pi$. Remedy: make the region simply connected by a *cut* (Fig. H.4), and apply the last result of Exercise 5.23 to the surface ABCDEFA, which encloses a simply connected region V. Check your answer by using the second result in Exercise 5.23, which is a more straightforward method.

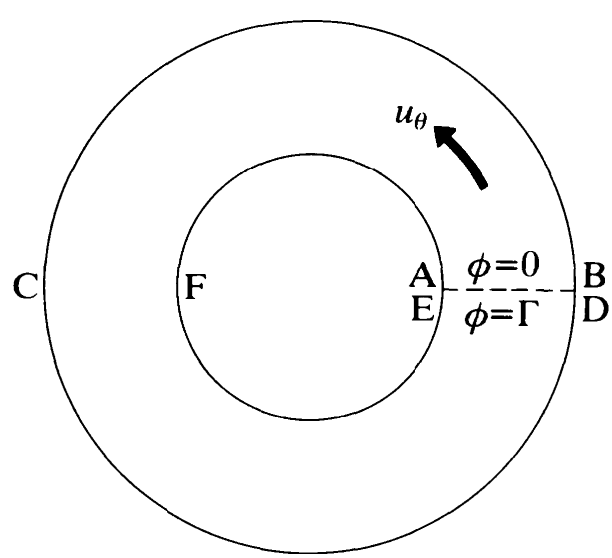

Fig. H.4.

Chapter 6

6.1.

$$\begin{aligned}\boldsymbol{n} \wedge (\nabla \wedge \boldsymbol{u}) &= \boldsymbol{n} \wedge \left(\boldsymbol{e}_i \wedge \frac{\partial \boldsymbol{u}}{\partial x_i}\right) \\ &= \left(\boldsymbol{n} \cdot \frac{\partial \boldsymbol{u}}{\partial x_i}\right)\boldsymbol{e}_i - (\boldsymbol{n} \cdot \boldsymbol{e}_i)\frac{\partial \boldsymbol{u}}{\partial x_i} \\ &= n_j \frac{\partial u_j}{\partial x_i}\boldsymbol{e}_i - n_i \frac{\partial}{\partial x_i}(u_j \boldsymbol{e}_j) \\ &= n_j \frac{\partial u_j}{\partial x_i}\boldsymbol{e}_i - n_j \frac{\partial u_i}{\partial x_j}\boldsymbol{e}_i \qquad \text{etc.,}\end{aligned}$$

where in the last term we have switched the dummy suffices i and j, summation being understood over both $i = 1, 2, 3$ and $j = 1, 2, 3$.

6.2. The vector identities needed are eqns (A.14), (A.19), (A.20), and (A.10).

6.4. The torque is

$$\int_0^{2\pi} r_1 t_\theta r_1 \, \mathrm{d}\theta = \frac{4\pi\mu(\Omega_2 - \Omega_1) r_1^2 r_2^2}{r_2^2 - r_1^2}$$

per unit length in the z-direction. It is positive if $\Omega_2 > \Omega_1$, as we would expect.

6.5. Put $G = \rho$ in eqn (6.6a).

6.7.

$$\begin{aligned}\frac{\partial}{\partial s_k}(e_{ij} s_i s_j) &= e_{ij}(\delta_{ik} s_j + s_i \delta_{jk}) \\ &= e_{kj} s_j + e_{ik} s_i.\end{aligned}$$

But $e_{ik} = e_{ki}$, so this is equal to $2e_{kj}s_j$ etc.

6.8.

$$\boldsymbol{u}_Q = \boldsymbol{u}_P + \tfrac{1}{2}(\beta s_2, -\beta s_1, 0) + \tfrac{1}{2}(\beta s_2, \beta s_1, 0).$$

The principal axes of e_{ij} are (everywhere) at an angle of $\pi/4$ to the coordinate axes, which is why T'_{12} turned out to be zero in the analysis leading to eqn (6.15). (More usually, the principal axes will vary with the position of the point P.)

6.10.

$$2e_{\theta\phi} = [(\boldsymbol{e}_\theta \cdot \nabla)\boldsymbol{u}] \cdot \boldsymbol{e}_\phi + [(\boldsymbol{e}_\phi \cdot \nabla)\boldsymbol{u}] \cdot \boldsymbol{e}_\theta \qquad \text{etc.,}$$

using eqns (A.37) and (A.38).

6.11. Direct substitution gives $T_{ij}^{\mathrm{D}} = A\delta_{ij}e_{kk} + Be_{ij} + Ce_{ji}$, and $e_{ij} = e_{ji}$ by eqn (6.16). In the second part, note that $e_{ii} = \nabla \cdot \boldsymbol{u}$ and $\delta_{ii} = 3$.

6.12. In the momentum equation, the term $\mu \nabla^2 \boldsymbol{u}$ or $-\mu \nabla \wedge (\nabla \wedge \boldsymbol{u})$ represents the *net* viscous force on a small fluid element (cf. eqn (2.11)). While this is zero for an irrotational flow, it does not follow at all that 'the viscous forces are zero'. There will typically be viscous stresses all around a fluid element, even if the *resultant* force is zero; these stresses will be zero all around the element only if it is not being *deformed*, and that is certainly not the case here (see Fig. 1.5).

6.13. $\mathrm{D}J/\mathrm{D}t = (\partial J/\partial t)_{\boldsymbol{X}}$, and differentiating the determinant gives the sum of three determinants, in each of which only one row is differentiated. The top row of the first of these is

$$\left(\frac{\partial}{\partial t}\right)_{\boldsymbol{X}} \frac{\partial x_1}{\partial X_1} \quad \left(\frac{\partial}{\partial t}\right)_{\boldsymbol{X}} \frac{\partial x_1}{\partial X_2} \quad \left(\frac{\partial}{\partial t}\right)_{\boldsymbol{X}} \frac{\partial x_1}{\partial X_3},$$

and on changing the order of partial differentiation this is

$$\frac{\partial u_1}{\partial X_1} \quad \frac{\partial u_1}{\partial X_2} \quad \frac{\partial u_1}{\partial X_3}.$$

On using the chain rule this can be written

$$\frac{\partial u_1}{\partial x_i}\frac{\partial x_i}{\partial X_1} \quad \frac{\partial u_1}{\partial x_i}\frac{\partial x_i}{\partial X_2} \quad \frac{\partial u_1}{\partial x_i}\frac{\partial x_i}{\partial X_3},$$

where summation over $i = 1, 2, 3$ is understood in each case. The $i = 1$ terms give a contribution $J\, \partial u_1/\partial x_1$ to this first determinant. The terms $i = 2, 3$ give no contribution to it, because in each case two rows of the resulting determinant are multiples of one another.

To prove Reynolds's transport theorem,

$$\begin{aligned}\frac{\mathrm{d}}{\mathrm{d}t}\int_{V(t)} G\,\mathrm{d}V &= \frac{\mathrm{d}}{\mathrm{d}t}\int_{V(t)} G\,\mathrm{d}x_1\,\mathrm{d}x_2\,\mathrm{d}x_3 \\ &= \frac{\mathrm{d}}{\mathrm{d}t}\int_{V(0)} GJ\,\mathrm{d}X_1\,\mathrm{d}X_2\,\mathrm{d}X_3 \\ &= \int_{V(0)} \left[\left(\frac{\partial G}{\partial t}\right)_{\boldsymbol{X}} J + G\left(\frac{\partial J}{\partial t}\right)_{\boldsymbol{X}}\right] \mathrm{d}X_1\,\mathrm{d}X_2\,\mathrm{d}X_3 \qquad \text{etc.,}\end{aligned}$$

the Jacobian determinant J entering when we make a change of variables, $V(0)$ denoting the region *initially* occupied by the 'dyed' blob.

Bibliography

Aref, H. (1983). *Ann. Rev. Fluid Mech.* **15,** 345–89.

Aref, H. (1986). *J. Fluid Mech.* **173,** 15–41.

Atiyah, M. F. (1988). *Q. J. R. Astron. Soc.* **29,** 287–99.

Batchelor, G. K. (1956). *J. Fluid Mech.* **1,** 177–90.

Batchelor, G. K. (1967). *An introduction to fluid dynamics.* Cambridge University Press.

Benjamin, T. B. (1978). *Proc. R. Soc. Lond.* A **359,** 27–43.

Benjamin, T. B. and Mullin, T. (1982). *J. Fluid Mech.* **121,** 219–30.

Bouard, R. and Coutanceau, M. (1980). *J. Fluid Mech.* **101,** 583–607.

Bourne, D. E. and Kendall, P. C. (1977). *Vector analysis and Cartesian tensors.* Nelson, London.

Busse, F. H. (1985). In Swinney and Gollub (1985), pp. 97–137.

Campbell, L. J. and Ziff, R. M. (1979). *Phys. Rev.* B **20**, 1886–902.

Carrier, G. F., Krook, M., and Pearson, C. E. (1966). *Functions of a complex variable.* McGraw-Hill, New York.

Cattaneo, F. and Hughes, D. W. (1988). *J. Fluid Mech.* **196,** 323–44.

Chaiken, J., Chevray, R., Tabor, M., and Tan, Q. M. (1986). *Proc. R. Soc. Lond.* A **408,** 165–74.

Chen, J.-D. (1989). *J. Fluid Mech.* **201,** 223–42.

Childress, S. (1981). *Mechanics of swimming and flying.* Cambridge University Press.

Coles, D. (1965). *J. Fluid Mech.* **21,** 385–425.

Couder, Y. and Basdevant, C. (1986). *J. Fluid Mech.* **173,** 225–51.

Coutanceau, M. and Bouard, R. (1977). *J. Fluid Mech.* **79,** 231–56.

Craik, A. D. D. (1985). *Wave interactions and fluid flows.* Cambridge University Press.

Crapper, G. D. (1984). *Introduction to water waves.* Ellis Horwood, Chichester.

Cruickshank, J. O. (1988). *J. Fluid Mech.* **193,** 111–27.

Cvitanović, P. (1986). *Universality in chaos.* Adam Hilger, Bristol.

Dalton, S. (1977). *The miracle of flight.* McGraw-Hill, New York.

Di Prima, R. C. and Swinney, H. L. (1985). In Swinney and Gollub (1985), pp. 139–80.

Donnelly, R. J. (1988). *Scient. Am.* **259**(5), 66–74.

Drazin, P. G. and Johnson, R. S. (1989). *Solitons: an introduction.* Cambridge University Press.

Drazin, P. G. and Reid, W. H. (1981). *Hydrodynamic stability.* Cambridge University Press.

Dritschel, D. G. (1985). *J. Fluid Mech.* **157,** 95–134.
Dritschel, D. G. (1986), *J. Fluid Mech.* **172,** 157–82.
Euler, L. (1755). See the translation and commentary in Truesdell (1954), especially pp. LXXXIV–XCI.
Feigenbaum, M. J. (1980). *Los Alamos Science* **1,** 4–27. (Also in Cvitanović (1986), pp. 49–84.)
Fenstermacher, P. R., Swinney, H. L., and Gollub, J. P. (1979), *J. Fluid Mech.* **94,** 103–29.
Fohl, T. and Turner, J. S. (1975). *Phys. Fluids* **18,** 433–6.
Fornberg, B. (1985). *J. Comput. Phys.* **61,** 297–320.
Gleick, J. (1988). *Chaos.* Heinemann, London.
Goldstein, S. (1938). *Modern developments in fluid dynamics.* Clarendon Press, Oxford. (Paperback edn: Dover, New York, 1965.)
Goldstein, S. (1969). *Ann. Rev. Fluid Mech.* **1,** 1–28.
Gollub, J. P. and Benson, S. V. (1980). *J. Fluid Mech.* **100,** 449–70.
Greenspan, H. P. (1968). *The theory of rotating fluids.* Cambridge University Press.
Greenspan, H. P. and Howard, L. N. (1963). *J. Fluid Mech.* **17,** 385–404.
Hall, P. and Walton, I. C. (1977). *Proc. R. Soc. Lond.* A **358,** 199–221.
Hasimoto, H. and Sano, O. (1980). *Ann. Rev. Fluid Mech.* **12,** 335–63.
Hele-Shaw, H. J. S. (1898). *Nature* **58,** 34–6.
Helmholtz, H. von (1858). See translation in *Phil. Mag.* (4) **33,** 485–512 (1867).
Hide, R. (1977), *Q. J. R. Met. Soc.* **103,** 1–28.
Higdon, J. J. L. (1985). *J. Fluid Mech.* **159,** 195–226.
Homsy, G. M. (1987). *Ann. Rev. Fluid Mech.* **19,** 271–311.
Huppert, H. E. (1982). *J. Fluid Mech.* **121,** 43–58.
Huppert, H. E. (1986). *J. Fluid Mech.* **173,** 557–94.
Jimenez, J. (1987). *J. Fluid Mech.* **178,** 177–94.
Joseph, D. D. (1976). *Stability of fluid motions.* Springer-Verlag, New York.
Joseph, D. D. (1985). In Swinney and Gollub (1985), pp. 27–76.
Kelvin, Lord (1869). *Trans. R. Soc. Edinb.* **25,** 217–260. (*Math. Phys. Papers* **4,** 13–66.)
Korteweg, D. J. and de Vries, G. (1895). *Phil. Mag.* **39,** 422–43.
Kutta, W. M. (1902). *Illust. Aeronaut. Mitt.* **6,** 133–5.
Lamb, H. (1932). *Hydrodynamics* (6th edn). Cambridge University Press.
Lanchester, F. W. (1907). *Aerodynamics.* Constable, London.
Landau, L. D. and Lifshitz, E. M. (1987). *Fluid mechanics* (2nd edn). Pergamon, Oxford.
Lanford, O. E. (1985). In Swinney and Gollub (1985), pp. 7–26.

Libchaber, A., Laroche, C., and Fauve, S. (1982). *J. Phys. Lett.* **43,** L211–16. (Also in Cvitanović (1986), pp. 137–42.)

Lighthill, J. (1973). *J. Fluid Mech.* **60,** 1–17.

Lighthill, J. (1978). *Waves in fluids*. Cambridge University Press.

Lighthill, J. (1986). *An informal introduction to theoretical fluid mechanics*. Clarendon Press, Oxford.

Loc, T. P. and Bouard, R. (1985). *J. Fluid Mech.* **160,** 93–117.

Lorenz, E. N. (1963). *J. Atmos. Sci.* **20,** 130–41.

Maxworthy, T. (1972). *J. Fluid Mech.* **51,** 15–32.

May, R. M. (1976). *Nature* **261,** 459–67.

Meiron, D. I., Saffman, P. G., and Schatzman, J. C. (1984). *J. Fluid Mech.* **147,** 187–212.

Mellor, G. L., Chapple, P. J., and Stokes, V. K. (1968). *J. Fluid Mech.* **31,** 95–112.

Miles, J. (1984). *Adv. Appl. Mech.* **24,** 189–214.

Moffatt, H. K. (1964). *J. Fluid Mech.* **18,** 1–18.

Moffatt, H. K. (1969). *J. Fluid Mech.* **35,** 117–29.

Moffatt, H. K. (1977a). *J. Mécanique* **16,** 651–73.

Moffatt, H. K. (1977b). Six lectures on fluid dynamics. In *Fluid dynamics,* Proc. Summer School Theor. Phys., Les Houches, France, July 1973. pp. 149–234. Gordon & Breach, London.

Moffatt, H. K. and Duffy, B. R. (1980). *J. Fluid Mech.* **96,** 299–313.

Moon, F. C. (1987). *Chaotic vibrations*. Wiley, Chichester.

Moore, D. R., Toomre, J., Knobloch, E., and Weiss, N. O. (1983). *Nature* **303,** 348–52.

Nakayama, Y. (ed.) (1988). *Visualized flow*. Pergamon, Oxford.

Newton, I. (1687). *Principia*. Translated into English by Andrew Motte in 1729. The translation revised, and supplied with an historical and explanatory appendix, by Florian Cajori. University of California Press, Berkeley (1934).

Nishioka, M., Iida, S. and Ichikawa, Y. (1975). *J. Fluid Mech.* **72,** 731–51.

Ockendon, H. and Tayler, A. B. (1983). *Inviscid fluid flows*. Springer-Verlag, New York.

Oshima, Y. (1978). *J. Phys. Soc. Japan* **45,** 660–64.

Oshima, Y. and Asaka, S. (1975). *Nat. Sci. Rep. Ochanomizu Univ.* **26,** 31–7.

Ottino, J. M. (1989a). *Scient. Am.* **260**(1), 40–9.

Ottino, J. M. (1989b). *The kinematics of mixing: stretching, chaos and transport*. Cambridge University Press.

Perry, A. E., Chong, M. S., and Lim, T. T. (1982). *J. Fluid Mech.* **116,** 77–90.

Pippard, A. B. (1985). *Response and stability*. Cambridge University Press.

Prandtl, L. (1905). *Verhandlungen des III Internationalen Mathematiker-Kongresses* (Heidelberg 1904), Leipzig, pp. 484–91. (Also in Prandtl, L. (1961). *Gesammelte Abhandlungen* **2,** 575–84. Springer-Verlag, Berlin.)

Prandtl, L. (1952). *The essentials of fluid dynamics.* Blackie, London.

Prandtl, L. and Tietjens, O. G. (1934). *Applied hydro- and aeromechanics.* McGraw-Hill, New York. (Paperback edn: Dover, New York, 1957.)

Priestley, H. A. (1985). *Introduction to complex analysis.* Clarendon Press, Oxford.

Proudman, I. and Pearson, J. R. A. (1957). *J. Fluid Mech.* **2,** 237–62.

Rayleigh, Lord (1880). *Proc. Lond. Math. Soc.* **11,** 57–70. (Also *Scientific Papers* **1,** 474–87 (1899). Cambridge University Press.)

Rayleigh, Lord (1910). *Proc. R. Soc. Lond.* A **84,** 247–84. (Also *Scientific Papers* **5,** 573–610 (1912). Cambridge University Press.)

Rayleigh, Lord (1916a). *Phil. Mag.* **32,** 529–46. (Also *Scientific Papers* **6,** 432–46 (1920). Cambridge University Press.)

Rayleigh, Lord (1916b). *Proc. R. Soc. Lond.* A **93,** 148–54. (Also *Scientific Papers* **6,** 447–53 (1920). Cambridge University Press.)

Reed, H. L. (1987). *Phys. Fluids* **30,** 2597–606.

Reichenbach, H. (1983). *Ann. Rev. Fluid Mech.* **15,** 1–28.

Reynolds, O. (1883). *Phil. Trans. R. Soc. Lond.* **174,** 935–82. (Also *Scientific Papers* **2,** 51–105 (1901). Cambridge University Press.)

Roberts, P. H. and Donnelly, R. J. (1974). *Ann. Rev. Fluid Mech.* **6,** 179–225.

Rosenhead, L. (ed.) (1963). *Laminar boundary layers.* Clarendon Press, Oxford. (Paperback edn: Dover, New York, 1988.)

Rosensweig, R. E. (1985). *Ferrohydrodynamics.* Cambridge University Press.

Rouse, H. (1946). *Elementary mechanics of fluids.* Wiley, New York. (Paperback edn: Dover, New York, 1978.)

Ruelle, D. (1980). *Math. Intellig.* **2,** 126–37. (Also in Cvitanović (1986), pp. 37–48.)

Russell, J. S. (1845). *Rep. 14th Meet. Br. Assoc. Adv. Sci., York,* pp. 311–90. John Murray, London.

Schlichting, H. (1979). *Boundary-layer theory* (7th edn). McGraw-Hill, New York.

Schneider, W. (1981). *J. Fluid Mech.* **108,** 55–65.

Schneider, W. (1985). *J. Fluid Mech.* **154,** 91–110.

Scorer, R. S. (1972). *Clouds of the world: a colour encyclopaedia.* Lothian, David & Charles, Melbourne.

Serrin, J. (1959). Mathematical principles of classical fluid mechanics. In *Handbuch der Physik* VIII/1, pp. 125–263. Springer-Verlag, Berlin.

Smith, F. T. (1977). *Proc. R. Soc. Lond.* A **356,** 443–63.

Smith, F. T. (1979). *J. Fluid Mech.* **92,** 171–205.

Smith, R. C. and Smith, P. (1968). *Mechanics.* Wiley, Chichester.

Sobey, I. J. and Drazin, P. G. (1986). *J. Fluid Mech.* **171,** 263–87.

Spedding, G. R. and Maxworthy, T. (1986). *J. Fluid Mech.* **165,** 247–72.

Stewartson, K. (1981). *SIAM Rev.* **23,** 308–43.

Stokes, G. G. (1845). *Trans. Camb. Phil. Soc.* **8,** 287–305. (Also *Math. Phys. Papers* **1,** 75–129. Cambridge University Press.)

Stokes, G. G. (1848). *Phil. Mag.* **33,** 349–56. (Also *Math. Phys. Papers* **2,** 51–8. Cambridge University Press.)

Stokes, G. G. (1851). *Trans. Camb. Phil. Soc.* **9,** 8–106. (Also *Math. Phys. Papers* **3,** 1–141. Cambridge University Press.)

Stuart, J. T. (1986). *SIAM Rev.* **28,** 315–42.

Swinney, H. L. and Gollub, J. P. (eds) (1985). *Hydrodynamic instabilities and the transition to turbulence.* Springer-Verlag, New York.

Taneda, S. (1965). *J. Phys. Soc. Japan* **20,** 1714–21.

Taneda, S. (1979). *J. Phys. Soc. Japan* **46,** 1935–42.

Tanner, R. I. (1988). *Engineering rheology.* Clarendon Press, Oxford.

Tayler, A. B. (1986). *Mathematical models in applied mechanics.* Clarendon Press, Oxford.

Taylor, G. I. (1910). *Proc. R. Soc. Lond.* A **84,** 371–7.

Taylor, G. I. (1923). *Phil. Trans. R. Soc. Lond.* A **223,** 289–343.

Thompson, J. M. T. (1982). *Instabilities and catastrophes in science and engineering.* Wiley, Chichester.

Thompson, S. P. (1910). *The life of William Thomson, Baron Kelvin of Largs.* Macmillan, London.

Thomson, J. J. (1883). *A treatise on the motion of vortex rings.* Macmillan, London.

Thorpe, S. A. (1969). *J. Fluid Mech.* **39,** 25–48.

Thorpe, S. A. (1971). *J. Fluid Mech.* **46,** 299–319.

Tritton, D. J. (1988). *Physical fluid dynamics* (2nd edn). Clarendon Press, Oxford.

Truesdell, C. A. (1954). Rational fluid mechanics (1687–1765). Editor's introduction to *Euleri Opera Omnia,* Series II, Vol. 12. Orell Füssli, Zurich.

Truesdell, C. A. (1968). *Essays in the history of mechanics.* Springer-Verlag, New York.

Turner, J. S. (1973). *Buoyancy effects in fluids.* Cambridge University Press.

van Dyke, M. (1982). *An album of fluid motion.* Parabolic Press, Stanford, California.

von Kármán, T. (1954). *Aerodynamics: selected topics in the light of their historical development.* Cornell University Press, Ithaca, New York.

Walker, J. (1987). *Scient. Am.* **257**(5), 114–7.

Weis-Fogh, T. (1973). *J. Exp. Biol.* **59,** 169–230.
Weis-Fogh, T. (1975). *Scient. Am.* **233**(5), 80–7.
Widnall, S. E. and Tsai, C.-Y. (1977). *Phil. Trans. R. Soc. Lond.* A **287,** 273–305.
Yamada, H. and Matsui, T. (1978). *Phys. Fluids* **21,** 292–4.
Yarmchuk, E. J., Gordon, M. J. V. and Packard, R. E. (1979). *Phys. Rev. Lett.* **43,** 214–17.
Zandbergen, P. J. and Dijkstra, D. (1987). *Ann. Rev. Fluid Mech.* **19,** 465–91.
Zauner, E. (1985). *J. Fluid Mech.* **154,** 111–19.

Index